ADVANCING PHOSPHORUS REDOX CATALYSIS: INNOVATIVE ORGANOCATALYTIC STRATEGIES FOR ORGANIC SYNTHESIS

Dissertation

in kumulativer Form

zur Erlangung des akademischen Grades

Doctor rerum naturalium (Dr. rer. nat.)

an der Fakultät für Naturwissenschaften, Department Chemie

der Universität Paderborn

vorgelegt von

Viktorija Medvarić

Geboren am 05. Juni 1994 in Koprivnica (Kroatien)

Paderborn, den 17. November 2025

Acknowledgment

I want to express my gratitude to my supervisor Prof. Thomas Werner for giving me the opportunity to join his research group. I am thankful for his guidance and support during my PhD, for all the scientific discussions and advice, especially for the scientific freedom he encouraged, and also for creating a relaxed and fun working atmosphere.

I am also very grateful to Prof. Jan Paradies for “adopting” me into his group for a short while and giving me the chance to work on the “Lachgas” project. I really appreciate the opportunity to attend his Retrosynthesis seminars which were definitely a highlight during my PhD, where I always learned something new and enjoyed the atmosphere and the discussions about the reaction mechanisms.

I would also like to thank our incredibly fast and reliable Analytical Department - PD Dr. Hans Egold and Karin Stolte, for their support with NMR measurements, their patience in explaining details, and their willingness to go above and beyond. My gratitude also goes to Dr. Adam Neuba and Christiane Gloger for the prompt MS analyses and for giving us unlimited access to their lab for our N_2O project.

A special thanks goes to Dr. Jan Günther Tönjes, my former lab partner at LIKAT, for our fun lab times and mental support when things in the lab didn’t work out. I am very grateful for his endless patience, for tolerating and correcting many of my mistakes and for always being ready to help.

Lots of gratitude goes to my lab colleagues and friends - Rundong, Lisa, Axel, Sebastian, Nacho, Nicole, Sascha, Pariksha, Niklas, Deepak, Athul, Maksim, Katta, Sabith - thank you for all the great memories and fun times together, both in and out of the lab. I couldn't have wished for better people to be surrounded with during my PhD.

I want to thank my family for their support and for always encouraging me to do my best.

Die vorliegende Arbeit entstand in der Zeit von 1. April 2021 bis 31. October 2025 am Leibniz Institut für Katalyse e.V. (LIKAT) und im Department Chemie der Fakultät für Naturwissenschaften der Universität Paderborn unter der Betreuung von Prof. Dr. Thomas Werner.

1. Gutachter: Prof. Dr. Thomas Werner

2. Gutachter: Prof. Dr. Jan Paradies

Kurzfassung

Diese Arbeit berichtet über neuartige, phosphankatalysierte Methoden im Bereich der P^{III}/P^{V}-Redoxkatalyse für vielfältige synthetische Anwendungen. Ein mildes, effizientes Verfahren mit geringer Katalysatormenge wurde für die Aktivierung von Amiden entwickelt. Die Methode ermöglicht eine Eintopf-Synthese von Amidinen durch die Bildung von Imidoylchloriden *in situ* und vermeidet dabei den Einsatz herkömmlicher, toxischer Chlorierungsmittel. Diese Strategie wurde auf elektrophile aromatische Substitutionen an heteroaromatischen Substraten ausgeweitet und führte zur Synthese neuer Indol- und Pyrrolimin-Derivate. Zudem wurden katalytische Verfahren zur Herstellung substituierter Furane etabliert, bei denen reaktive Zwischenstufen basenfreier Wittig-Reaktionen eingefangen werden, wodurch tri- und tetrasubstituierte Produkte mit selektiver Katalysatorkontrolle zugänglich sind. Abschließend wurde erstmals eine phosphinkatalysierte Reduktion von Distickstoffmonoxid unter milden Bedingungen demonstriert. Detaillierte kinetische Untersuchungen identifizierten hierbei den Sauerstofftransfer als geschwindigkeitsbestimmenden Schritt. Diese Fortschritte unterstreichen die Vielseitigkeit und Nachhaltigkeit der Phosphor-Redoxkatalyse in der organischen Synthese und umweltrelevanten Anwendungen.

Abstract

This work reports novel phosphine-catalyzed methods within P^{III}/P^{V} redox catalysis for diverse synthetic applications. A catalytic protocol with low catalyst loading was developed for amide activation, enabling one-pot synthesis of amidines via *in situ* imidoyl chloride formation, avoiding toxic chlorinating agents. This strategy was extended to electrophilic aromatic substitution on heteroaromatic substrates, yielding new indole and pyrrole imine derivatives. Additionally, catalytic routes to substituted furans were established in base-free Wittig reactions, accessing both tri- and tetrasubstituted products with selective catalyst control. Finally, the first phosphine-catalyzed reduction of nitrous oxide under mild conditions was demonstrated, supported by detailed kinetic studies that identified oxygen transfer as the rate-determining step. These advances highlight the versatility and sustainability of P^{III}/P^{V} redox catalysis in organic synthesis and environmentally relevant applications.

1. Introduction

1.1 Formation and impact of phosphine oxide byproducts in organic chemistry

Phosphines are key reagents in numerous classical organic transformations, including the Wittig, Appel, Mitsunobu, and Cadogan reactions.[1] Key mechanistic feature among these processes is the oxidation of P^{III} reagents to P^{V} oxide species. The formation of a strong P=O double bond (bond dissociation energy ≈ 537 $kJ \cdot mol^{-1}$) provides a significant thermodynamic driving force for these reactions.[2,3] Phosphine oxides are often challenging to separate from the desired products, which complicates purification. Their formation as a byproduct in stoichiometric yields also reduces the atom economy of the overall transformation, especially in industrial large-scale reactions.[4] Several strategies have been developed to address this issue, including the immobilization of phosphine reagents on solid supports,[5] the use of water-soluble phosphines[6] to facilitate separation, and the precipitation of phosphine oxides via complexation with metal salts such as $ZnCl_2$.[7] In an industrial process, triphenylphosphine oxide is extracted from the reaction mixture and reduced to corresponding phosphine by chlorination with phosgene or oxalyl chloride, followed by the reduction of the resulting chlorophosphonium chloride with Al or H_2.[8] While this methodology represents a significant advancement in addressing phosphine oxide waste, reagent toxicity (e.g., phosgene) makes it impractical to conduct on a smaller scale. Therefore, the development of efficient and selective strategies for the reduction of phosphine oxides, or alternative methodologies that prevent their formation, is essential. The strong P=O requires harsh conditions for reduction, however, when reagents such as $LiAlH_4$[9] and DIBAL-H[10] are used in a catalytic, *in situ* process, the chemoselectivity becomes an issue. The first catalytic reduction of phosphine oxides by silanes was reported in 1994 in the presence of titanium alkoxides.[11] A lot of effort was put into the research of hydrosilane or siloxane based reduction methods. They have gained prominence due to their chemoselectivity, compatibility with a range of functional groups, low toxicity, and ease of handling.[3,12] To this date, these reduction methods have been integrated into a variety of synthetic transformations. Catalytic applications of phosphorus involving P^{V} can be categorized into strategies

that enable recycling through different mechanistic pathways. One approach involves reduction, where phosphine oxides formed during the reaction are converted back into P^{III} species by using silanes as a reducing agent (Scheme 1A).

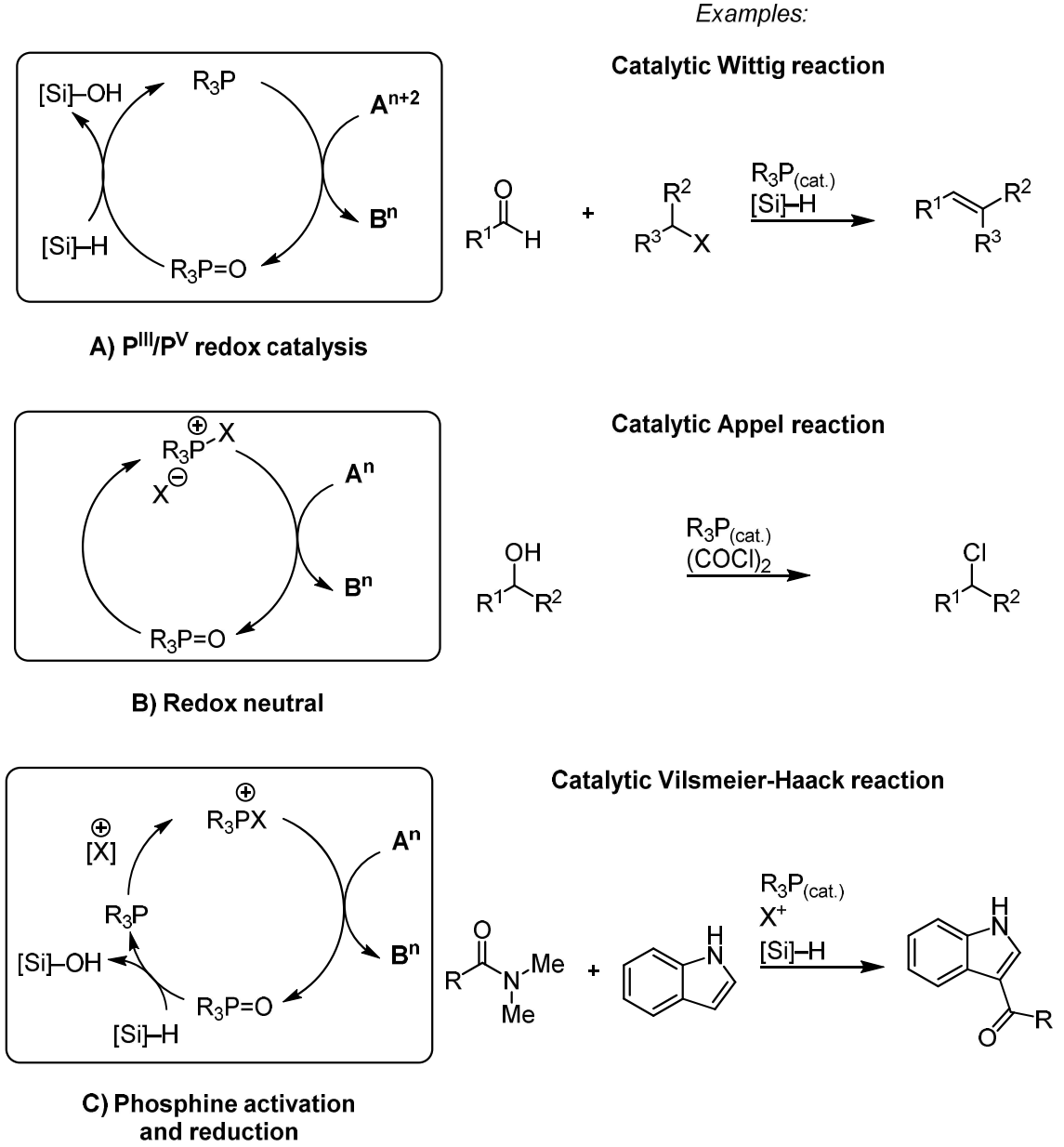

Scheme 1. Three different modes of phosphine catalysis.

This approach is used in Wittig and Cadogan reactions.[13] Another approach is redox-neutral activation of the phosphine (Scheme 1B), where its oxidation state remains unchanged throughout the catalytic cycle.[14,15–17] A third approach combines activation and reduction (Scheme 1C).[18] Here, the catalytically active species is not a free phosphine but a phosphonium cation and after participating in the reaction, the resulting phosphine oxide is subsequently reduced to regenerate

the P^{III} species. Both of the later approaches are used in the catalytic Appel reactions, as well as in amide synthesis and amide activation reactions.[16–19] Continued efforts in designing novel phosphine-based catalysts and silane-based reagents highlight the ongoing advancement and significance of redox-driven phosphorus chemistry.

1.2 Development and application of P^{III}/P^{V} redox catalysis

1.2.1 Wittig reaction

Since its discovery in 1953, the Wittig reaction has become a fundamental transformation in organic synthesis for the conversion of aldehydes or ketones into alkenes via reaction with a phosphonium ylide.[20] Despite its broad applicability, the classical Wittig reaction is limited by several drawbacks. Most significantly, phosphine oxide is generated as co-product, complicating purification due to its polarity. The development of a catalytic Wittig reaction was challenging, due to need for the selective reduction of phosphine oxides in the presence of reactive functional groups such as aldehydes, ketones and alkenes. Since triphenylphosphine was conventionally used in phosphorus-mediated processes forming highly stable triphenylphosphine oxide, regeneration of the active phosphine requires reducing agents such as $LiAlH_4$, which are typically too harsh and lack chemoselectivity. Initial attempts to avoid these issues explored the substitution of phosphorus with other group 15 elements such as arsenic or antimony, whose corresponding oxides are more readily reduced.[21] However, toxicity is a major concern, particularly in large-scale processes.[22] In 2009, O'Brien and coworkers reported a catalytic Wittig reaction using phenylsilane and diphenylsilane as reductants.[23] These silanes were selected for their functional group tolerance and mild reactivity, as hydrosilylation of carbonyl compounds typically requires transition metal catalysts.[24] A cyclic phosphine, 3-methyl-1-phenylphospholane-1-oxide (**1a**) was used as the catalyst instead of a conventional triphenylphosphine, as the ring strain in cyclic phosphine oxides significatly eases the reduction (Scheme 2).[25] The proposed catalytic cycle proceeds through four key stages. Phosphine oxide **1a** is reduced *in situ* by an organosilane to generate the active phosphine **2a**, which then undergoes the nucleophilic substitution with an alkyl bromide **3**, forming a phosphonium bromide **4**, followed by deprotonation to yield the phosphonium ylide **5**. Lastly, olefination with

the aldehyde **6** takes place, regenerating the phosphine oxide **1a** and releasing the product **7**.

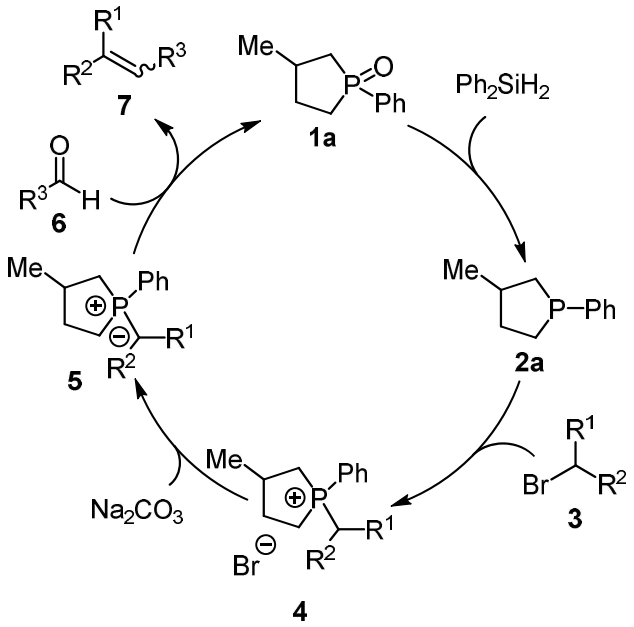

Scheme 2. Proposed mechanism for the catalytic Wittig reaction.

1.2.2 Further development of the catalytic Wittig reaction

Having established the first catalytic Wittig reaction by using phosphine based catalysts, further efforts were focused on optimizing the reaction and addressing its limitations. A key step involved the formation of the phosphonium ylide via deprotonation of the formed phosphonium salt, making the choice of base a critical parameter. The base must have a sufficient conjugate acid pK_a value, to abstract a proton forming the ylide, while maintaining compatibility with other reaction components, such as the silane reductant, organohalide, and the olefin product. Initial attempts using Na_2CO_3 were dependent on the particle size and vigorous stirring to achieve acceptable yields, due to its limited solubility in the employed organic solvents. To address this, in 2013 the O'Brien group screened for alternative bases.[26] Among the evaluated ones, only *N*,*N*-diisopropylethylamine (DIPEA) proved effective. Its base strenght is ideal for the deprotonation of the phosphonium salt, and its steric bulk and low nucleophilicity minimized undesired side reactions. The incorporation of DIPEA not only simplified reaction handling but also expanded the substrate scope and allowed a lower catalyst loading. A further advancement in the development of the catalytic Wittig reaction was achieved through the

incorporation of 2.5–10 mol% of 4-nitrobenzoic acid.[27] This additive aided in the reduction of the catalysts, allowing the reaction to proceed efficiently at room temperature. These conditions also facilitated the use of acyclic phosphine oxides as catalysts. Notably, this marked the first demonstration of triphenylphosphine oxide (**8a**) acting as a viable catalyst in catalytic Wittig reaction (Scheme 3).

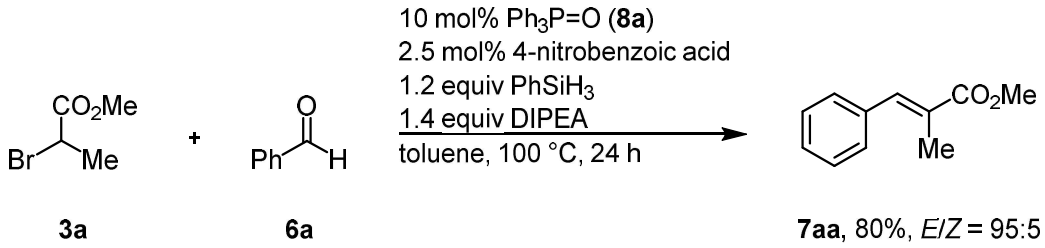

Scheme 3. Catalytic Wittig reaction with triphenylphosphine oxide (**8a**) as catalyst.

In a subsequent study reported by O'Brien in 2014,[28] the scope of the catalytic Wittig reaction was further expanded to include semistabilized and non-stabilized ylides. This was enabled by the use of a masked base, sodium 2-(carboxylatooxy)-2-methylpropane ($NaOCO_2{}^tBu$) and further catalyst optimization. Modifying the electron density at the phosphorus center through incorporation of electron-withdrawing groups, allowed effective deprotonation under relatively mild basic conditions. Additionally, steric modifications to the precatalyst significantly improved *E*/*Z* selectivity up to >95:5. The same year, Werner *et al.* introduced a first enantioselective microwave-assisted (MWI) catalytic Wittig reaction by employing **10** as the catalyst in combination with phenylsilane as a reducing agent and butylene oxide as a masked base to avoid side reactions (Scheme 4).[29] Prochiral diketone **9** was converted to bicyclic compound **11** in 39% yield and 62% enantiomeric access. This method was later also used in a key step in the natural product synthesis of dichrocephone A.[30]

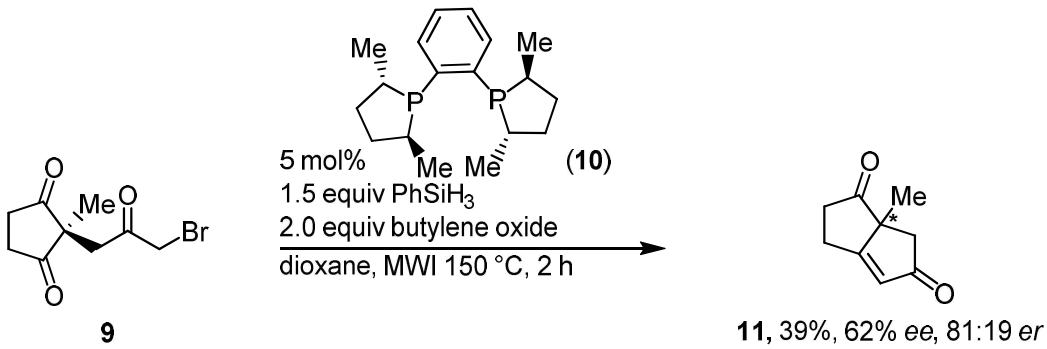

Scheme 4. First enantioselective microwave-assisted catalytic Wittig reaction.

1.2.3 Base-free Wittig reaction

After O'Brien demonstrated the catalytic Wittig reaction via P^{III}/P^{V} redox cycling, new ways of avoiding the base use in this process were developed. The first catalytic base-free Wittig (BFW) reaction was reported in 2015. by Werner *et al.* (Scheme 5).[31]

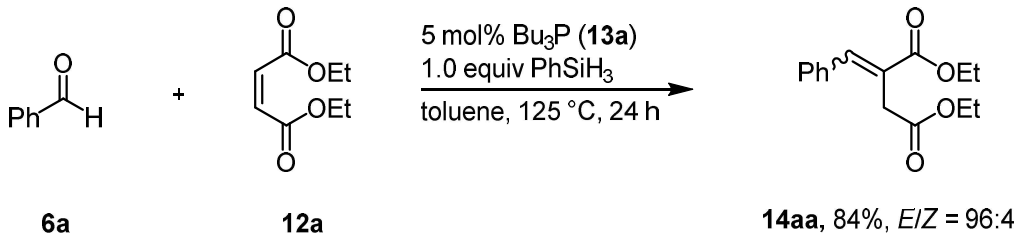

Scheme 5. First base-free catalytic Wittig reaction.

In this process, after the Michael addition of the catalyst **13a** to an olefin **12** and a protonation-deprotonation sequence of the intermediate **15**, the corresponding ylide **16** is formed (Scheme 6). Various aromatic, aliphatic and heterocyclic aldehydes **6** were converted with various maleates and fumarates in yields up to 95% and *E*/*Z* selectivities up to 99:1.

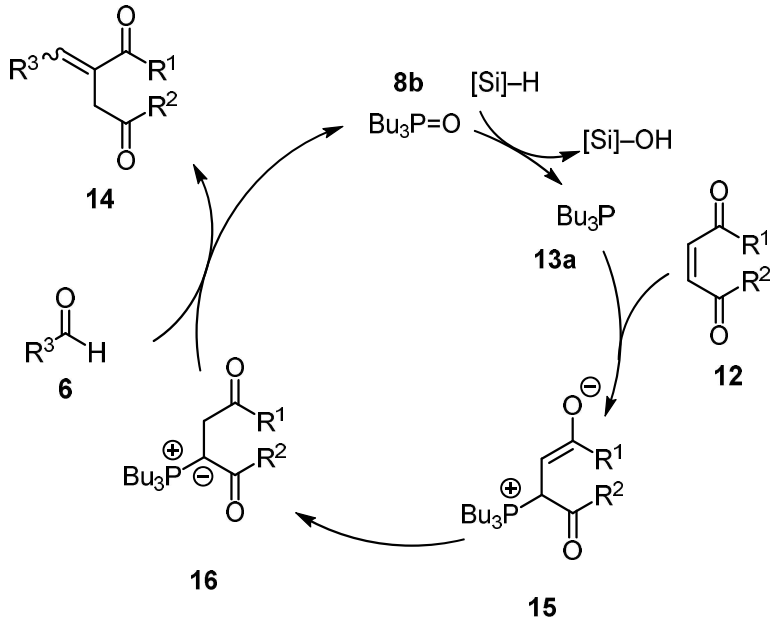

Scheme 6. Proposed reaction mechanism for the catalytic BFW reaction.

Much milder conditions for the catalytic BFW reactions were achieved by using an Brønsted acid additive (Scheme 7).[32] In this case, 5 mol% of the catalyst **1b** was used in combination with the 5 mol% benzoic acid.

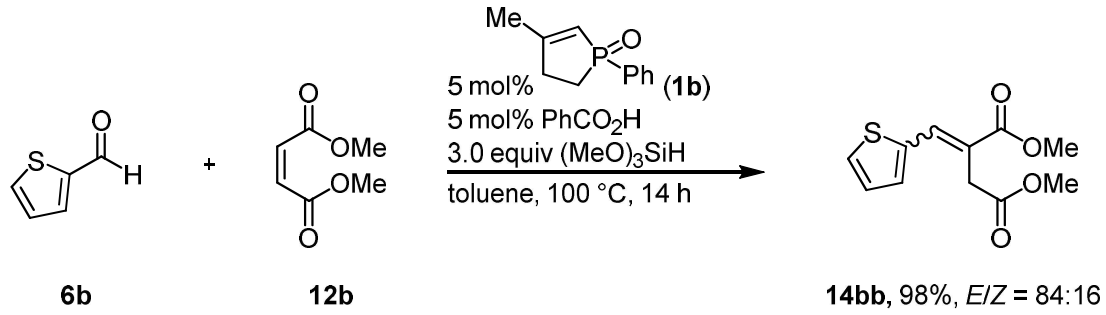

Scheme 7. Catalytic BFW reaction under milder conditions.

Catalytic amount of the Brønsted acid promotes the *in situ* reduction of the phospholene oxide to phospholene, so that the reaction can take place at lower temperature, in this case at 100 °C for 14 h, and by using $(MeO)_3SiH$. In 2019, intramolecular BFW reaction was reported for the synthesis of benzoxepinones **18** using similar conditions (Scheme 8).[33]

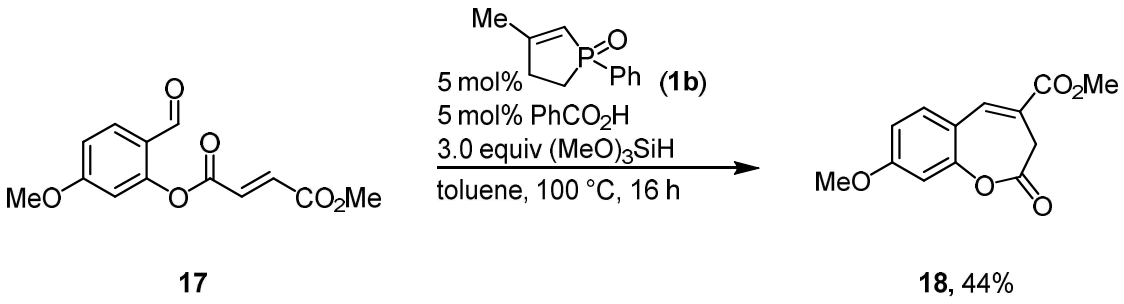

Scheme 8. Intramolecular catalytic BFW reaction.

In 2021, a more environmentally benign approach for the intermolecular BFW reaction was demonstrated by Tönjes *et al.*[34] For catalyst reduction, polymethylhydrosiloxane (PMHS) was employed as a cost-effective and environmentally safe reducing agent, in contrast to previously reported reductants such as $PhSiH_3$ and $(MeO)_3SiH$ (Scheme 9). The cyclic phosphetane oxide catalyst **19a** was identified as the most effective in terms of both product yield and *E*/*Z* selectivity. Transformations were conducted in the green solvent BuOAc at 120 °C for 24 h.[35] During the reaction optimization, a persistent side reaction yielded diethyl succinate. This undesired reduction of olefin was attributed to the presence of water.

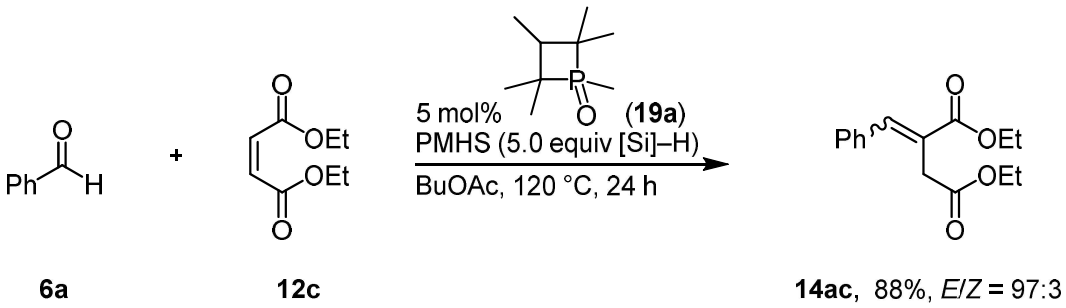

Scheme 9. PMHS as a reductant in the catalytic BFW reaction.

The authors suggested water may form via silanol condensation to siloxanes, and it was concluded that water or hydrogen formation during silane-mediated reduction of phosphine oxides is strongly dependent on reaction conditions. A reduction strategy for alkenes and alkynes, utilizing water as the hydrogen source was reported (Scheme 10).[36] Activated alkene **12** and the catalyst **19a** in the presence of water formed the ylide **22**. Its subsequent hydrolysis led to the alkane **23** and the regeneration of the phosphetane oxide **19a.**

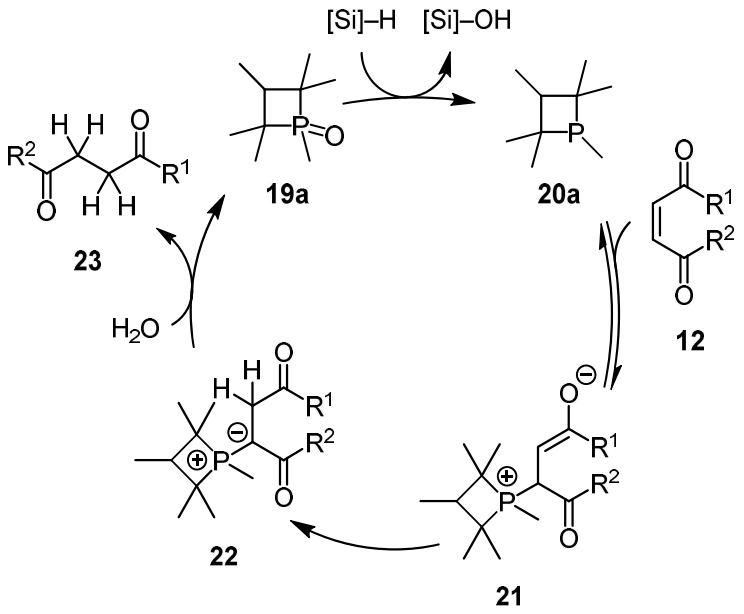

Scheme 10. Proposed mechanism for the reduction of activated alkenes by P^{III}/P^{V} redox catalysis with water.

This method demonstrates high chemoselectivity, allowing the reduction of activated carbon–carbon double or triple bonds while leaving carbonyl functionalities and non-activated double bonds intact. It has been effectively applied to the reduction of various substrates, including derivatives of formic, maleic and malonic acid, acrylates and alkynes. Also, an additional advancement was shown by employing

PMHS as a terminal reductant, with the reaction conducted in the environmentally friendly solvent BuOAc.

1.2.4 Synthesis of furanes and benzofuranes

In a transformation related to the BFW reaction, an alternative reaction pathway can take place (Scheme 11). Following the Michael addition of catalyst **13a** to substrate **12**, enolate **15** is generated. Subsequent nucleophilic attack on an acyl chloride **24** and a subsequent deprotonation, resulted in a formation of ylide **25**, which then undergoes an intramolecular Wittig reaction to yield the furan **26**.

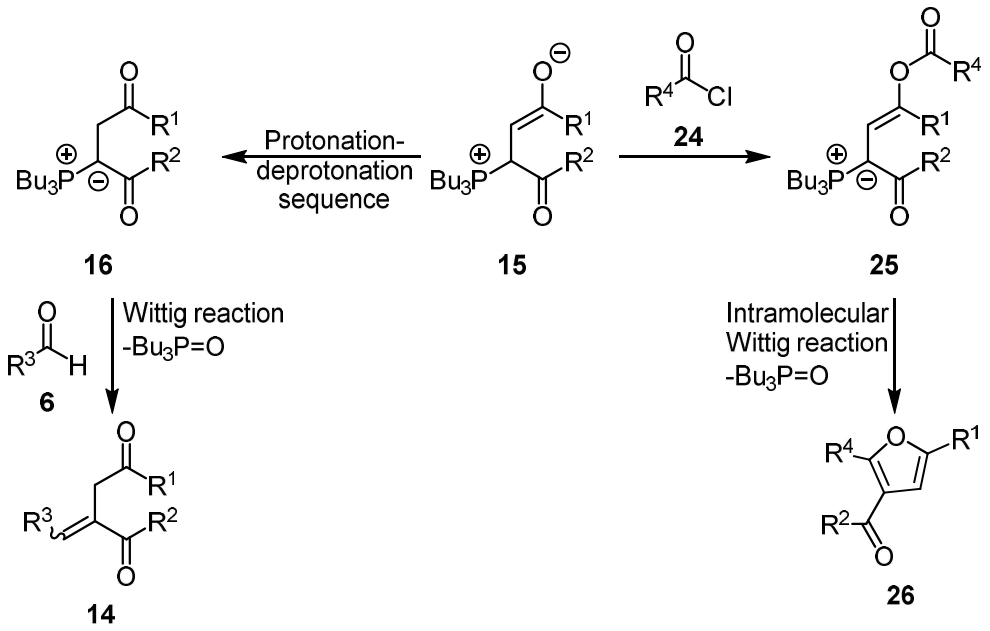

Scheme 11. BFW reaction and the formation of furan **26** from enolate **15**.

In 2016, Lee reported the synthesis of highly functionalized furans **28** via an intramolecular catalytic Wittig reaction sequence (Scheme 12).[37] The transformation required only catalytic amounts Et_3N. The *in situ* generated $Et_3N{\cdot}HCl$ catalyzes reduction of phosphine oxide **1a**, while its decomposition resulted in regeneration of base, which mediated the formation of phosphorus ylide. Additionally, a catalytic amount of Et_3SiCl was employed to activate the phosphorus oxide, also facilitating its reduction. A similar strategy for furan synthesis was developed by Fan, utilizing terminal activated olefins **29** or **31** in combination with either two or three equivalents of acyl chloride **24b** (Scheme 13).[38]

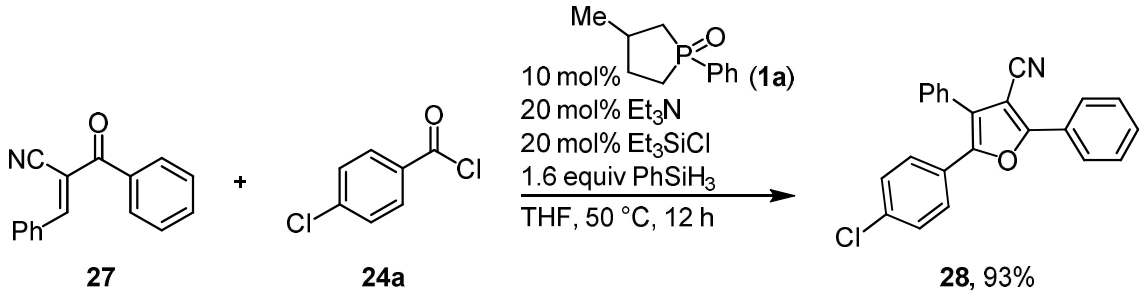

Scheme 12. Synthesis of furan derivatives **28** via intramolecular catalytic Wittig reaction.

When the olefin **29** was functionalized with an electron-withdrawing group such as an ester or a cyano group, the reaction afforded tetra-substituted furan derivatives **30**, whereas the use of methyl vinyl ketone **31** led to the formation of tri-substituted furan **32**.

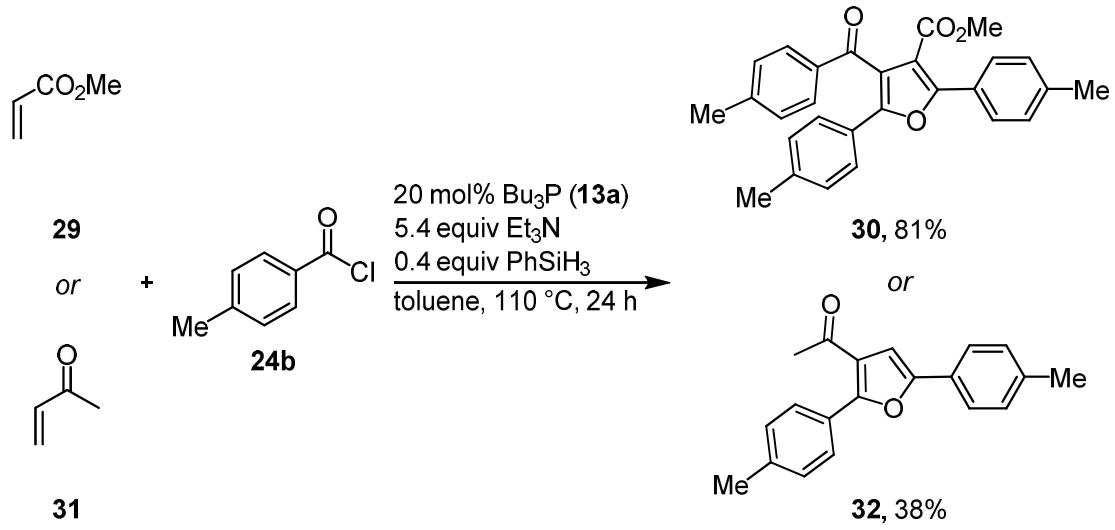

Scheme 13. Synthesis of tri- and tetra-substituted furan derivatives **32** and **30**.

A protocol for the construction of functionalized 3-alkenyl benzofurans **34** via intramolecular Wittig reaction was demonstrated by Liou *et al.* (Scheme 14).[39] This one-pot transformation proceeds via initial *O*-acylation of the nitrostyrene **33**, followed by a Michael addition of a phosphine to the resulting *O*-acylated intermediate. After the elimination of nitrous acid, phosphorus ylide is generated. The ylide undergoes an intramolecular Wittig reaction, leading to the formation of benzofuran **33**. Additional experiments with the intermediate, formed after the reaction with the acyl chloride, indicated that the Wittig reaction proceeds without the need for a base, and the 1.2 equivalents of Et_3N are required for the *O*-acylation step, characterizing the overall transformation as BFW reaction.

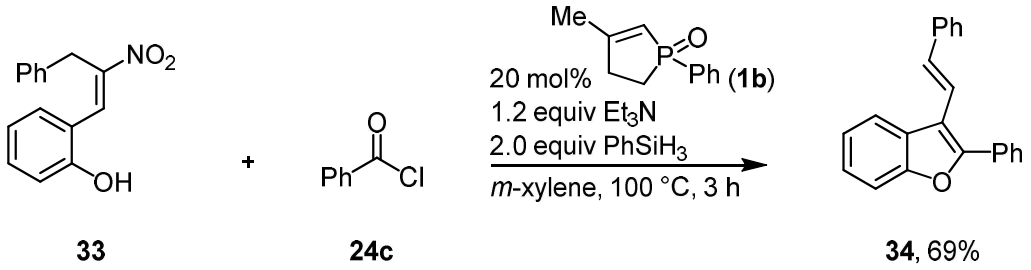

Scheme 14. Synthesis of the fuctionalized benzofuran **34** via intramolecular BFW reaction.

1.3 Catalytic Appel reaction

One year after O'Brien reported the catalytic Wittig reaction, an alternative strategy was introduced by Denton group to circumvent the stoichiometric reduction of the strong P=O double bond, while still achieving phosphine-catalyzed reactivity.[16] This approach was first demonstrated in the catalytic dichlorination of epoxides **35** (Scheme 15).

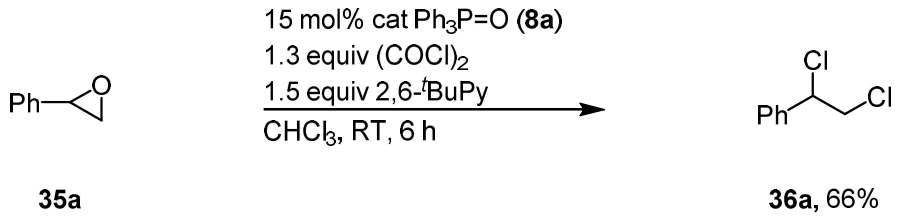

Scheme 15. Catalytic dichlorination of epoxide **35a**.

The mechanism involves a catalytic cycle in which triphenylphosphine oxide (**8a**) is converted *in situ* to a chlorophosphonium salt **37** via reaction with oxalyl chloride, accompanied by the release of CO and CO_2 (Scheme 16). 2,6-di-*tert*-butylpyridine was added, since the generation of HCl under these conditions could potentially lead to side reactions, such as the formation of chlorohydrins. This non-nucleophilic base effectively neutralizes HCl without reacting with oxalyl chloride. The same group applied the principle of P^V/P^V catalysis for the chlorination of primary and secondary alcohols (Scheme 17).[17] This transformation represents the first example of triphenylphosphine oxide (**8a**) catalyzed alcohol chlorination under Appel-type conditions, proceeding via the Appel reaction mechanism. The use of oxalyl chloride can lead to side reactions that compete with the chlorination. The rapid consumption of alcohol substrate **38** (within 10 minutes) results in the formation of chloroglyoxylate and bis-ester byproducts. To address this issue, the authors employed a strategy involving the simultaneous and slow addition of both

oxalyl chloride and alcohol to a solution containing 15 mol% catalyst over a period of 7 h, which afforded yields up to 88%.

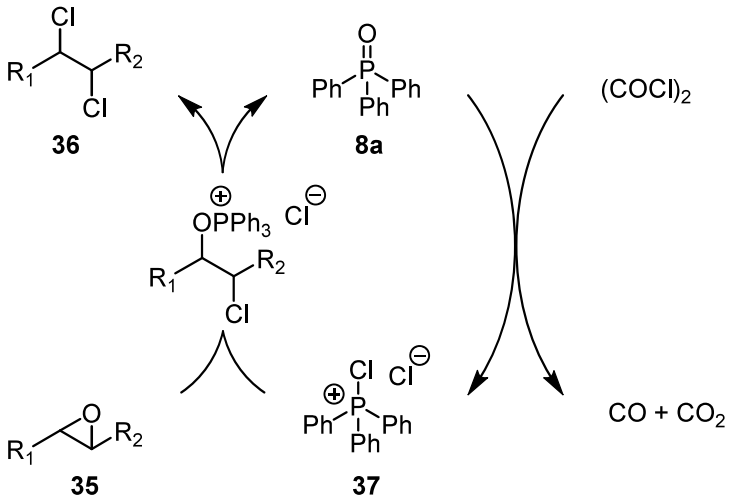

Scheme 16. Proposed mechanism for the dichlorination of epoxides via *in situ* generation of chlorophosphonium salt **37** from triphenylphosphine oxide (**8a**).

The methodology proved effective for a range of acyclic primary and secondary alcohols. In addition to chlorination, successful bromination was also achieved using oxalyl bromide.

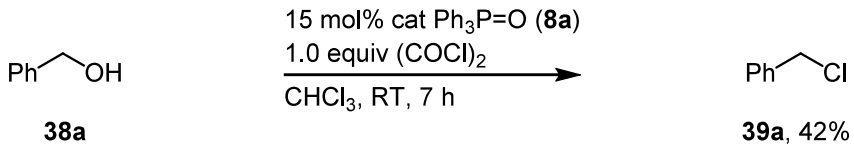

Scheme 17. Phosphine oxide (**8a**) catalyzed chlorination of alcohol **38a**.

Building on the concept of redox catalysis, van Delft and co-workers investigated a redox-catalyzed variant of the catalytic Appel reaction (Scheme 18A) for the synthesis of alkyl bromide **39b**.[15] Given that the reaction aims to convert alcohols **38** into alkyl halides **39**, primarily chlorides and bromides, under mild and non-acidic conditions, careful selection of both the catalyst and the halogenating agent was essential. The five-membered cyclic phosphine oxide catalyst **1a**, which had previously demonstrated excellent performance in the catalytic Wittig reaction, proved unsuitable in this context. As a result, attention shifted to derivatives of dibenzophosphole oxide **1c** as potential catalysts. A separate challenge involved finding a compatible halogenating agent that would not react with the silane reductant. Among several tested, only diethyl bromomalonate (DEBM) functioned

effectively as a brominating agent under the catalytic conditions. The catalytic cycle (Scheme 18B) begins with activation of catalyst **2b** with DEBM, forming bromophosphonium species **40** that reacts with the alcohol **38.** This step generates an oxophosphonium intermediate **41**, which after the nucleophilic attack of the bromide ion leads to the formation of the alkyl bromide **39** and the phosphine oxide **1c**.

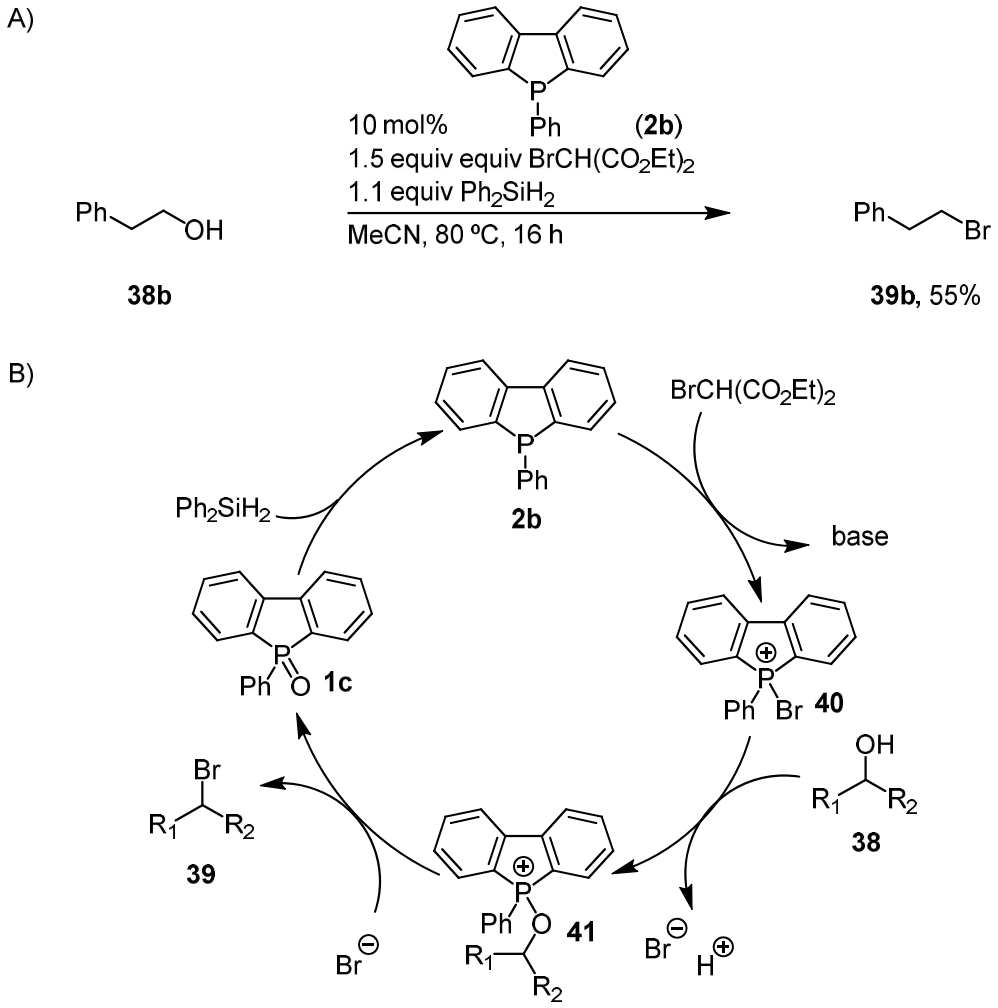

Scheme 18. A) Phosphine catalyzed bromination of alcohol **38b**. B) Proposed mechanism for the bromination of alcohols **38** under Appel reaction-type conditions.

For chlorination, a modified protocol was employed. CCl_4 served as the chlorinating agent, and **2c** was used as the catalyst (Scheme 19). The reaction proceeded with low yield of 40% for **39c.**

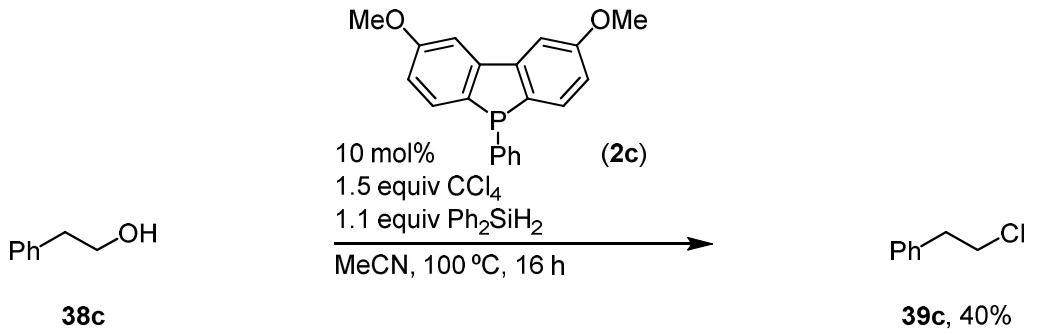

Scheme 19. Chlorination of alcohol **38c** using dibenzophosphole **2c** as a catalyst.

A significantly improved method for the chlorination of alcohols was developed, expanding the substrate scope to secondary and tertiary alcohols, as well as the transformation of epoxides to their corresponding chlorinated derivatives using benzotrichloride as an inexpensive and readily available chlorinating agent.[40] The reaction with trioctylphosphane **13b** as the catalyst and phenylsilane as the terminal reductant proceeds under solvent-free conditions (Scheme 20).

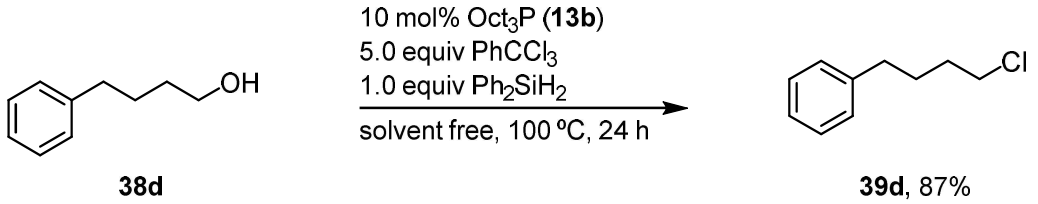

Scheme 20. Chlorination of alcohol **38d** with benzotrichloride via P^{III}/P^{V} redox catalysis.

Alkylphosphanes are generally not utilized in classical Appel reactions as catalysts due to their vigorous reactivity with carbon tetrachloride (CCl_4),[41] however, in this case, the use of trioctylphosphane **13b** proved suitable, since only small amounts are available in the reaction. The proposed mechanism (Scheme 21) involves the chlorophosphonium salt **42** as the activated P-species which undergoes further reaction with an alcohol **38**, yielding an alkoxyphosphonium species **43** along with the formation of dichlorotoluene. The alkoxyphosphonium intermediate **43** undergoes a Michaelis–Arbuzov type rearrangement to release the alkyl chloride **39**. Product **39** may undergo a nucleophilic substitution reaction, resulting in a loss of stereochemical information when chiral alcohols are used as substrates. Another possible pathway is an S_N1 type mechanism, where phosphine oxide **8c** is eliminated to generate a carbocation intermediate **44**, eventually leading to the product ***rac*-39**. The phosphane oxide **8c** is reduced by the organosilane, closing the catalytic cycle.

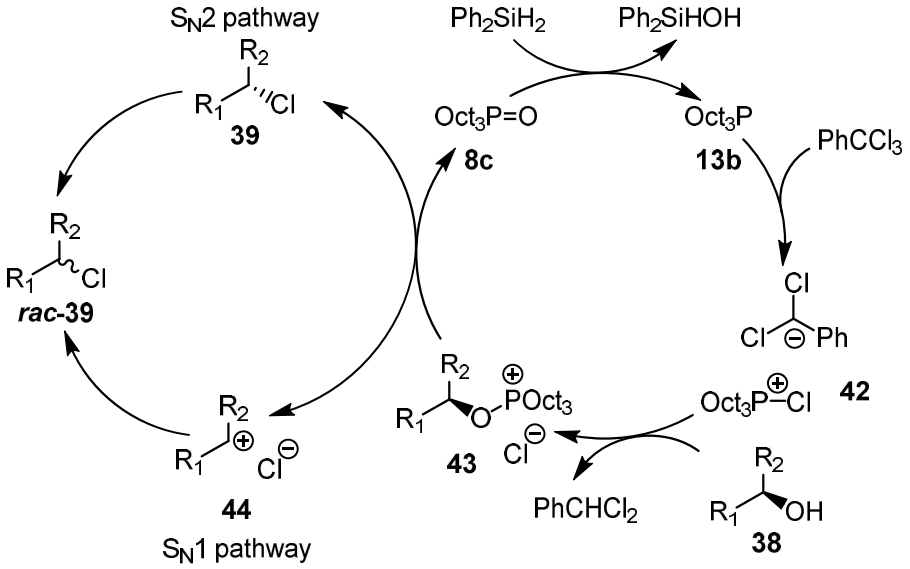

Scheme 21. Proposed mechanism for the chlorination of alcohols **38** via P^{III}/P^{V} redox catalysis.

A similar strategy was used employing the cyclic phosphetane catalyst **19a** (Scheme 22), broadening the substrate scope to secondary and tertiary alcohols which were obtained in good yields with improved stereospecificity.[42] This protocol requires only 1 mol% of catalyst **19a** for the Appel chlorination of both chiral and achiral alcohols. Hexachloroacetone (HCA) was used as a halogen source in substoichiometric quantities (0.7 equivalents), suggesting that two chlorine atoms of HCA participate under the reaction conditions.

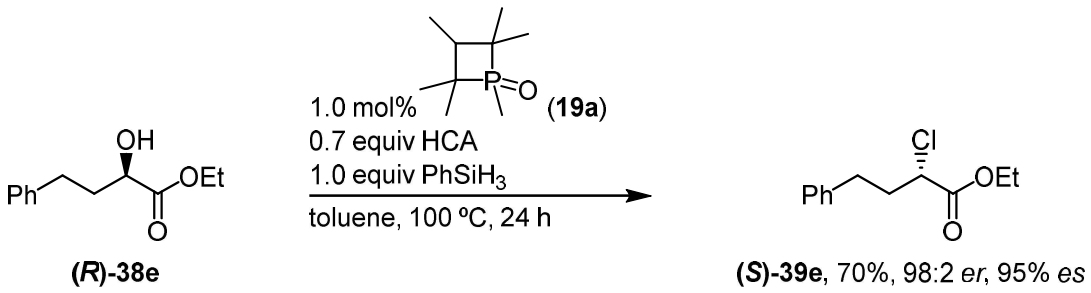

Scheme 22. Chlorination of alcohol **(*R*)-38e** using HCA via P^{III}/P^{V} redox catalysis.

A broad range of alcohol substrates **38** bearing various functional groups, were converted to the corresponding alkyl chlorides **39** with yields up to 97%, and enantiomeric ratios up to 99:1. The methodology was also extended to the chlorination of epoxides **35** (Scheme 23). The epoxide **(*R*)-35b** was converted to the alkyl chloride **(*S*)-36b** with inversion of configuration in 92% yield with 96:4 *er*. This required adjustments to the reaction conditions, including a doubling of the catalyst loading and HCA equivalents.

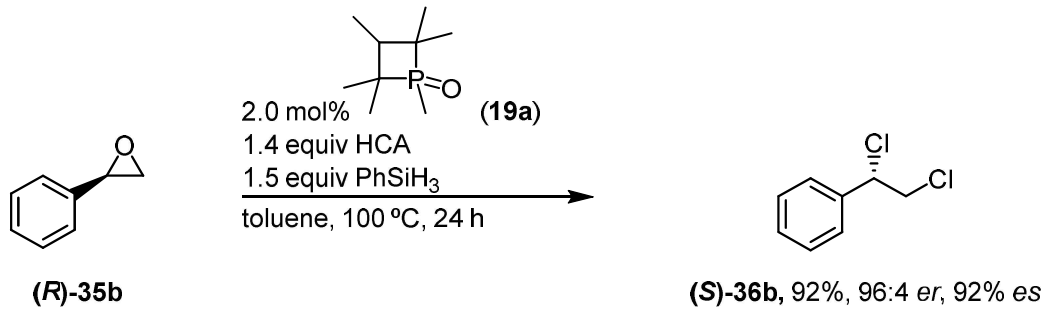

(*R*)-35b **(*S*)-36b,** 92%, 96:4 *er*, 92% *es*

Scheme 23. Chlorination of epoxide **(*R*)-35b** using HCA via P^{III}/P^{V} redox catalysis.

1.5 Amide synthesis and activation via P^{III}/P^{V} redox catalysis

Amides are commonly prepared from carboxylic acids and amines, either via formation of more reactive carboxylic acid anhydrides or acyl chlorides, or by using coupling reagents.[43] In recent years, direct coupling of carboxylic acids with amines under organocatalytic conditions has emerged as a viable alternative, particularly using functionalized arylboronic acids as catalysts.[44] Significant progress has also been made in amide bond formation via phosphorus-based catalysis. A key advancement was reported by Mecinović in 2014,[19] who demonstrated the organocatalytic amidation of unactivated aromatic carboxylic acids with amines. This transformation proceeds in the presence of a catalytic amount of **13c** and a two-fold excess of CCl_4, employing *in situ* reduction using diethoxymethylsilane and bis(4-nitrophenyl)phosphate as an additive, eventually forming **47a** (Scheme 24). The method was compatible with a broad spectrum of unactivated para-substituted benzoic acids, as well as heteroaromatic carboxylic acids such as picolinic and quinaldic acids and aliphatic, aromatic, and heterocyclic amines.

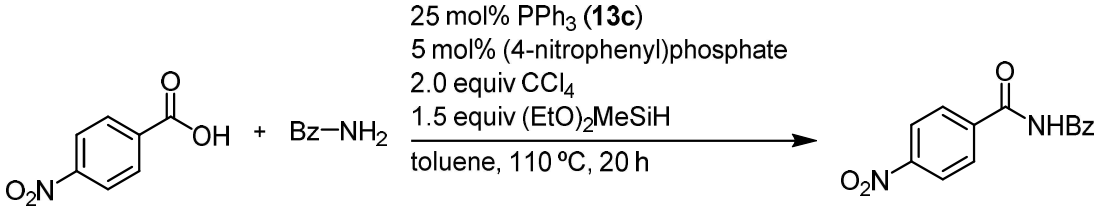

45a **46** **47a,** 64%

Scheme 24. Synthesis of amide **47a** by P^{III}/P^{V} redox catalysis.

In 2022, Arora and co-workers reported an improved organocatalytic method for amide bond formation that eliminates the need for toxic CCl_4, employing instead a dual-component catalytic system (Scheme 25).[45] This strategy utilizes a two-cycle

mechanism involving a phosphine and a selenium redox cycle. In the phosphine cycle, the phosphetane **20a** reacts with a diselenide **48** to form a selenophosphonium salt **49**, which serves as an activating agent for the amino acid **51**. Amino acid **51** is activated forming a selenoester, and regenerating phosphine oxide **19a**. In the selenium cycle, formed selenoester undergoes acyl transfer with amine **52**, yielding the corresponding dipeptide **53** and liberating selenol **50**. The selenol is then oxidized by oxygen from air to regenerate the diselenide **48**, closing the selenium catalytic cycle. The water generated during the oxidation of selenol is effectively scavenged by excess silane, forming silanols or siloxanes as byproducts.

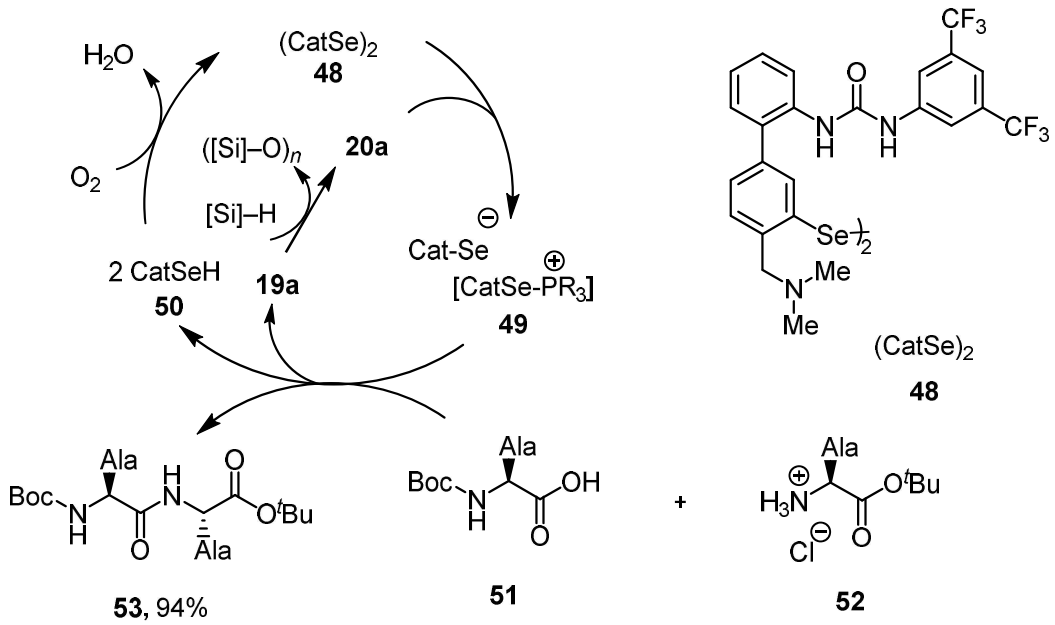

Scheme 25. Dual catalytic cycle for peptide bond formation.

The Radosevich group introduced a method for both amide synthesis and *in situ* amide activation using a P^{III}/P^{V} catalytic system (Scheme 26A).[18] This process for the synthesis of azaheterocycle **55** from carboxylic acid **45b** and amine **54** uses a (diethyl 2-bromo-2-methylmalonate) DEMBM and a terminal hydrosilane reductant to drive sequential C−N and C−C bond formations. The mechanism for amide formation in this system can be compared to the approach of Mecinović in terms of halonium-based catalyst activation. However, in the method of Radosevich, the toxic CCl_4 oxidant is replaced by a milder DEMBM, forming a bromophosphonium ion. This intermediate not only serves as a carboxylic acid activator facilitating the C−N bond formation, but also participates in amide activation during the C−C bond formation phase. Building on this method, the Radosevich group further

demonstrated a three-component condensation reaction involving carboxylic acid **45c**, amine **56**, and pyridine *N*-oxide **57** to synthesize 2-amidopyridine **58** (Scheme 26B).[46] The reaction proceeds via bromophosphonium-mediated activation and condensation with pyridine *N*-oxides. This leads to the formation of a reactive imidoyloxypyridinium intermediate, which undergoes rearrangement to furnish the 2-amidopyridine product.

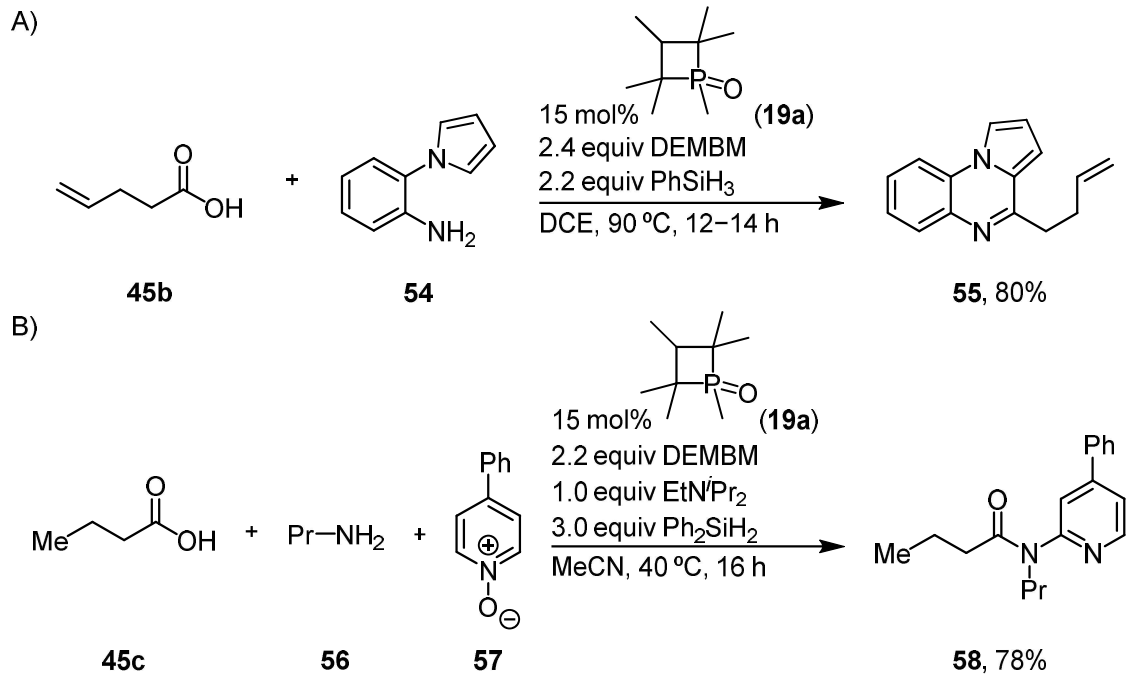

Scheme 26. Synthesis of A) azaheterocycle **55** and B) 2-amidopyridine **58** by P^{III}/P^{V} redox catalysis.

Köring and co-workers reported an alternative method for the amide activation and imidoyl species synthesis (Scheme 27).[47] In this system, 20 mol% of phosphine oxide **8c** is activated to the corresponding P^{V} species by reaction with triphosgene. It then reacts with amide **47b**, and after the nucleophillic attack of the chloride, imidoyl chloride **59b** is formed. Since multiple chlorine atoms from a single triphosgene molecule participate in the activation process, only substoichiometric amounts are required for the reaction.

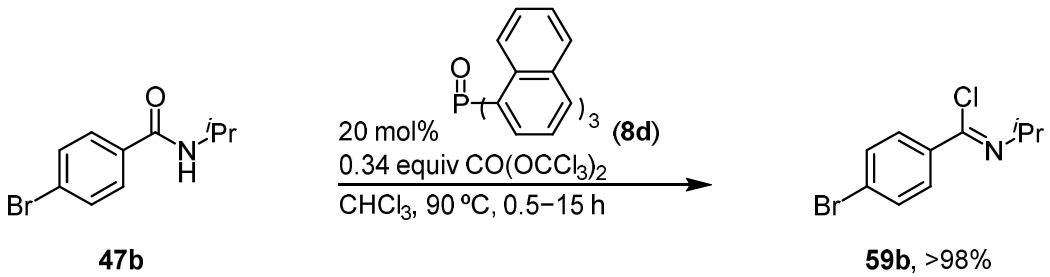

Scheme 27. Synthesis of imidoyl chloride **59b** from amide **47b** using phosphine oxide **8d** and triphosgene.

Xue *et al.* demonstrated a catalytic variant of the Vilsmeier-Haack reaction for the synthesis of indole-3-carboxaldehydes **61** (Scheme 28).[48] In contrast to the traditional Vilsmeier-Haack protocol,[49] which requires stoichiometric and toxic $POCl_3$ or oxalyl chloride[50] for the formylation of electron-rich aromatic systems, this method offers a catalytic alternative that avoids these reagents. The authors achieved catalytic activation of dimethylformamide **47c** and its derivatives, coupling them with indole **60a** and forming indolecarboxaldehydes **61** and ketones under mild conditions.

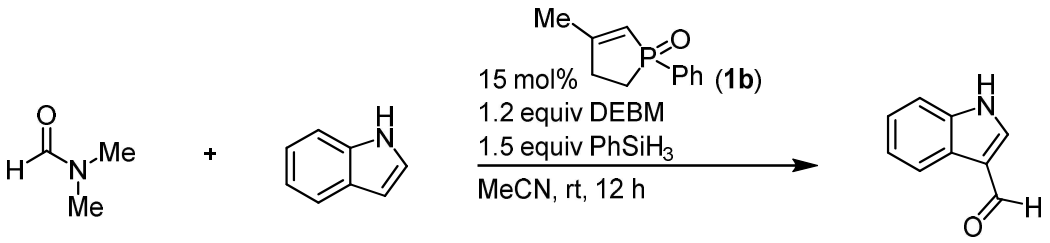

47c **60a** **61**, 95%

Scheme 28. Catalytic Vilsmeyer-Haack reaction for the synthesis of **61**.

1.6 Nitrous oxide decomposition

Nitrous oxide (N_2O) is a potent greenhouse gas and an ozone-depleting substance.[51] Due to its significant environmental impact, recent research has focused on the development of effective methods for its chemical transformation[52,53] or catalytic decomposition.[54] While transition metal systems have been extensively studied for N_2O activation,[55] metal-free approaches have also been explored. For instance, triphenylphosphine (**13c**) can directly reduce N_2O under supercritical conditions (100–140 bar) at 100 °C (Scheme 29).[56]

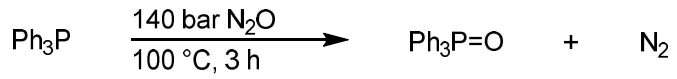

13c **8a**, 94%

Scheme 29. Phosphine-mediated N_2O decomposition.

Additionally, phosphane/borane based frustrated Lewis pairs (FLPs) have been shown to capture and decompose N_2O under milder conditions (Scheme 30).[57] The reaction of an equimolar mixture of **13d** and $B(C_6F_5)_3$ with N_2O results in the precipitation of **62.** Photolysis of **62** or heating it at 135 °C for 44 h resulted in the liberation of N_2 and formation of the Lewis acid-base adduct **63.**

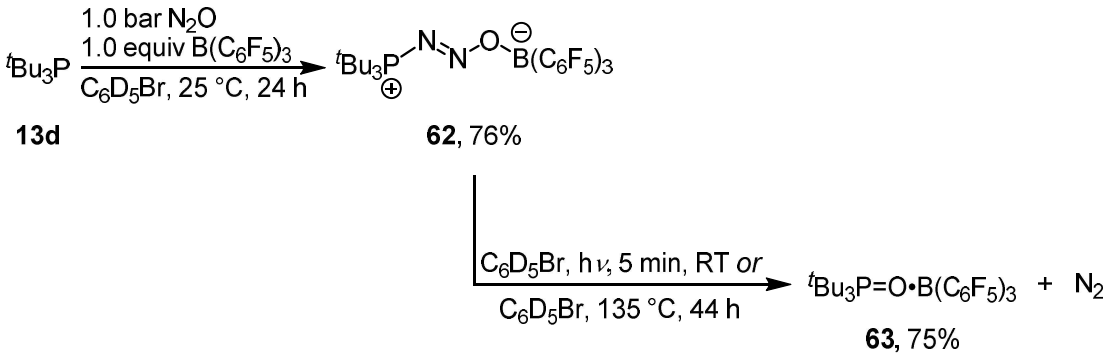

Scheme 30. Decomposition of N_2O by frustrated Lewis pairs.

Despite progress in FLP systems, catalytic turnover has not been achieved, undescoring the necessity for continued investigation in this field.

2. Objective

Phosphorus redox catalysis has emerged in recent years as a versatile strategy for various synthetic transformations. While significant advances have been made, substantial opportunities remain to expand this approach to new reaction types and enhance their synthetic utility. This work aims to explore and expand the scope of P^{III}/P^{V} redox catalysis through several objectives. The first is the development of amidine synthesis based on amide activation via organophosphorus catalysis. Amidines are known to be synthesized via imidoyl halide intermediates from amides, by using toxic, moisture-sensitive dehydrating agents such as PCl_5, $SOCl_2$, and $(COCl)_2$ for the generation of the imidoyl chloride, or by phosphorus mediated approaches generating imidoyl iodide. In the latter approach, phosphine oxide as a byproduct in stoichiometric amount hampers the purification and atom economy. To address this limitation, this work seeks to eliminate the need for toxic and moisture-sensitive reagents as well as to avoid the stoichiometric formation of phosphine oxides. The next objective is to investigate electrophilic aromatic substitution on heterocycles, specifically pyrrole and indole derivatives, using an organocatalytic approach. Building on the amide activation strategy for *in situ* synthesis of imidoyl chlorides, this part of the study aims to investigate the reactivity of pyrrole and indole derivatives toward these intermediates. Another goal of this work is to design a catalytic route to substituted furans. The approach involves the activation of bisacylethenes and acyl acrylates with a phosphorus based catalyst to form a BFW intermediate through Michael addition, followed by an intramolecular Wittig-type cyclization to access furans with underexplored substitution patterns. Finally, the fourth aim is the catalytic reduction of nitrous oxide, a potent greenhouse gas. While phosphine-mediated methods for this transformation have been reported, they require supercritical conditions. The goal of this research is to develop a phosphine-catalyzed approach operating under significantly milder conditions.

3. Results and Discussion

3.1 Synthesis of amidines via P^{III}/P^{V} redox catalyzed in situ formation of imidoyl chloride from amides[58]

Amidines are recognized for their versatility, with broad applications as functional groups in drug design, synthetic intermediates for heterocyclic compounds, and ligands for organometallic complexes.[59] Consequently, the development of efficient and sustainable synthetic methods for amidines remains of significant interest. In this work, amidines are synthesized from amides through P^{III}/P^{V} redox catalysis, employing environmentally benign chlorinating agent to avoid the use of toxic reagents traditionally required in amidine synthesis.

The study commenced with the optimization of the catalytic step for the formation of imidoyl chloride **59d**, from *N*-isopropylbenzamide (**47d**) as a model substrate in BuOAc as solvent, using phosphetane oxide **19a** as catalyst and $PhSiH_3$ as terminal reductant (Table 1). A large focus was put on selecting the most suitable halide source for the formation of imidoyl chloride. Using ethyl 2,2,2-trichloroacetate (ETCA) as a halide source, resulted in 26% yield, while the use of (trichloromethyl)benzene (TCMB) resulted in 68% yield (entries 1 and 2). Imidoyl bromide could also be formed by using DEMBM in 28% yield (entry 3). Notably, when HCA, was used as a chlorinating agent an excellent yield of >99% for the formation of imidoyl chloride **59d** was achieved (entry 4). Lowering the reaction time to 16 h didn't affect the yield (entry 5). Building on the excellent results with HCA, the effects of the solvent were examined, as well as various reaction conditions. Acetonitrile and THF were evaluated as solvents, and gave yields of 63% and 64%, respectively (entry 6 and 7). In addition to BuOAc, the reaction proceeded with the yield of >99% in toluene (entry 8). However, we chose to continue our investigations using BuOAc, as it is a more sustainable alternative to toluene according to the CHEM21 selection guide.[35] Further studies demonstrated that the reaction proceeds efficiently using 1.5 equivalents each of HCA and $PhSiH_3$, with a reduced catalyst loading of 2 mol% (entry 9). The product **59d** was obtained in >99% yield within 1 h under these conditions. To evaluate catalyst performance, alternative candidates were tested under optimized conditions. Phospholene oxide **1b** resulted in a significantly lower yield of 40% (entry 10), while non-cyclic catalysts **8b** and **8a**

gave yields below 20% (entries 11 and 12). Thus the phosphetane catalyst **19a** proved crucial for the effective formation of imidoyl chloride.

Table 1. Optimization of the P^{III}/P^{V} redox catalyzed formation of *N*-isopropylbenzimidoyl chloride (**59d**) from *N*-isopropylbenzamide (**47d**).

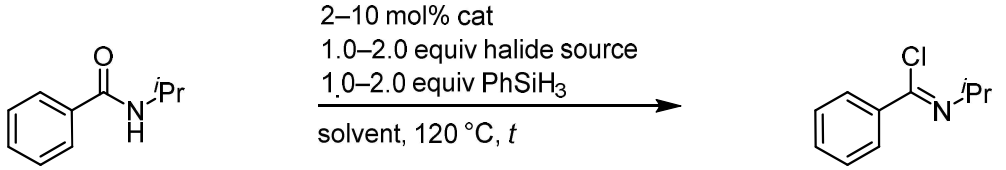

47d **59d**

cat:

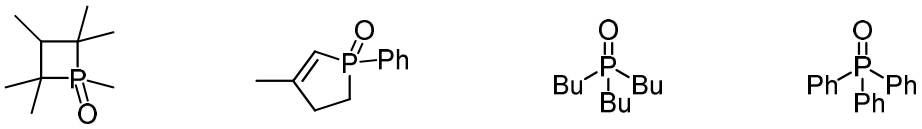

19a **1b** **8b** **8a**

entry	cat (mol%)	halid source (equiv)	silane (equiv)	conditions	yield / %[1]
1	**19a** (10)	ETCA (2.0)	$PhSiH_3$ (2.0)	BuOAc, 24 h	26%
2	**19a** (10)	TCMB (2.0)	$PhSiH_3$ (2.0)	BuOAc, 24 h	68%
3	**19a** (10)	DEMBM (2.0)	$PhSiH_3$ (2.0)	BuOAc, 24 h	28%[2]
4	**19a** (10)	HCA (2.0)	$PhSiH_3$ (2.0)	BuOAc, 24 h	>99%
5	**19a** (10)	HCA (2.0)	$PhSiH_3$ (2.0)	BuOAc, 16 h	>99%
6	**19a** (10)	HCA (2.0)	$PhSiH_3$ (2.0)	MeCN, 16 h	63%
7	**19a** (10)	HCA (2.0)	$PhSiH_3$ (2.0)	THF, 16 h	64%
8	**19a** (10)	HCA (2.0)	$PhSiH_3$ (2.0)	toluene, 16 h	>99%
9	**19a** (2)	HCA (1.5)	$PhSiH_3$ (1.5)	BuOAc, 1 h	99%
10	**1b** (2)	HCA (1.5)	$PhSiH_3$ (1.5)	BuOAc, 1 h	40%
11	**8b** (2)	HCA (1.5)	$PhSiH_3$ (1.5)	BuOAc, 1 h	19%
12	**8a** (2)	HCA (1.5)	$PhSiH_3$ (1.5)	BuOAc, 1 h	10%

Reaction conditions: 1.0 equiv **47d** (0.5 mmol), 2–10 mol% **cat**, 1.0–2.0 equiv halide source, 1.0–2.0 equiv $PhSiH_3$, 1.5 mL BuOAc, 120 °C, 1–24 h. [1]Yields were determined by ^{1}H NMR using mesitylene as the internal standard. [2]*N*-isopropylbenzimidoyl bromide is the product.

Optimization of the second reaction step for the formation of amidine **64a** was carried out by varying the equivalents of nucleophile and the reaction time. Following the *in situ* formation of imidoyl chloride **59d** under optimized conditions,

1.5 and 2.5 equiv of *i*PrNH$_2$ were tested, resulting in conversions of 53% and 71%, respectively, after 4 h (Table 2, entry 1 and 2). Using 3.5 equivalents of ^{i}PrNH$_2$ led to complete conversion and the product **64a** was isolated in an excellent 98% yield (entry 3). Reducing the reaction time to 3 h resulted in decreased conversion and a lower isolated yield of 85% (entry 4).

Table 2. Optimization for the synthesis of amidine **64a** from *in situ* formed **59d**.

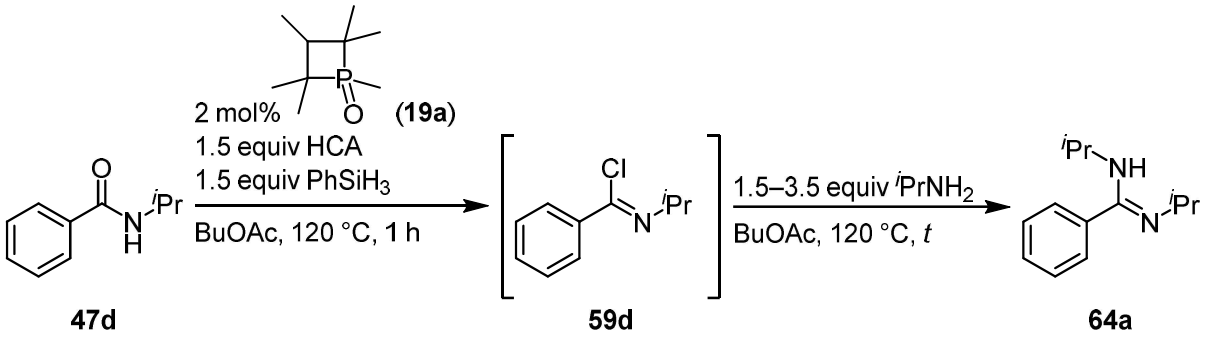

entry	^{i}PrNH$_2$ / equiv	*t* / h	conv. **59d** / %[1]	yield **64a** / %[2]
1	1.5	4	53	n.d.
2	2.5	4	71	n.d.
3	3.5	4	100	98
4	3.5	3	96	85

Reaction conditions: 1.0 equiv **47d** (0.5 mmol), 2 mol% catalyst **19a**, 1.5 equiv HCA, 1.5 equiv PhSiH$_3$, 1.5–3.5 equiv ^{i}PrNH$_2$, 1.5 mL BuOAc, 120 °C. [1]Conversion was determined by GC with mesitylene as internal standard. [2]Isolated yield is given.

The substrate scope was evaluated by converting amides **47** with different amines. In total 20 amidines **64** were synthesized in generally good to excellent yields (Table 3). The reaction with ^{i}PrNH$_2$ and benzylamine as nucleophiles gave the corresponding amidines **64a** and **64b** in 98% yield. Excellent yields were also achieved with aniline derivatives bearing electron-donating or electron-withdrawing groups. The conversion of *p*-ethoxy aniline led to amidine **64c** in 86% yield while the trifluoromethyl derivative **64d** and nitrile-substituted product **64e** were obtained in 98% and 80% yield respectively. When *N*-ethylaniline was used as a nucleophile, 88% yield of amidine **64f** was achieved. The aliphatic secondary amine, diethylamine, gave **64g** in moderate yield of 79%, while the cyclic amines piperidine and morpholine performed slightly better, affording **64h** and **64i** in 88% and 81%

yield, respectively. Further evaluation of the scope was performed by variation of the amide coupling partner. Electron-rich methoxy substituted aryl amide led to **64j** in an excellent yield of 86%, while aryl amide with an electron-acceptor substituent, such as methoxycarbonyl and bromo-substituted derivative produced 64% and 72% of the products **64k** and **64l**, respectively. Thiophene substituted amide gave **64m** in a good yield of 83%. The *N*-substituents of the amide were also varied. The conversion of *N*-cyclohexyl benzamide gave **64n** in 80%, while the *N*-allyl derivative gave **64o** in 74%. Furthermore, piperidin-2-one was also a suitable substrate and the desired amidine **64p** was obtained in moderate yield of 39%.

Table 3. Selected amides **47** converted in one-pot, two-step synthesis to amidines **64** by P^{III}/P^{V} redox catalysis.

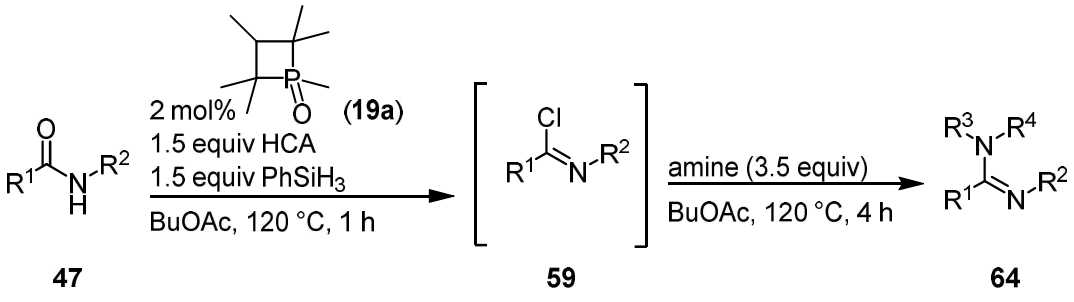

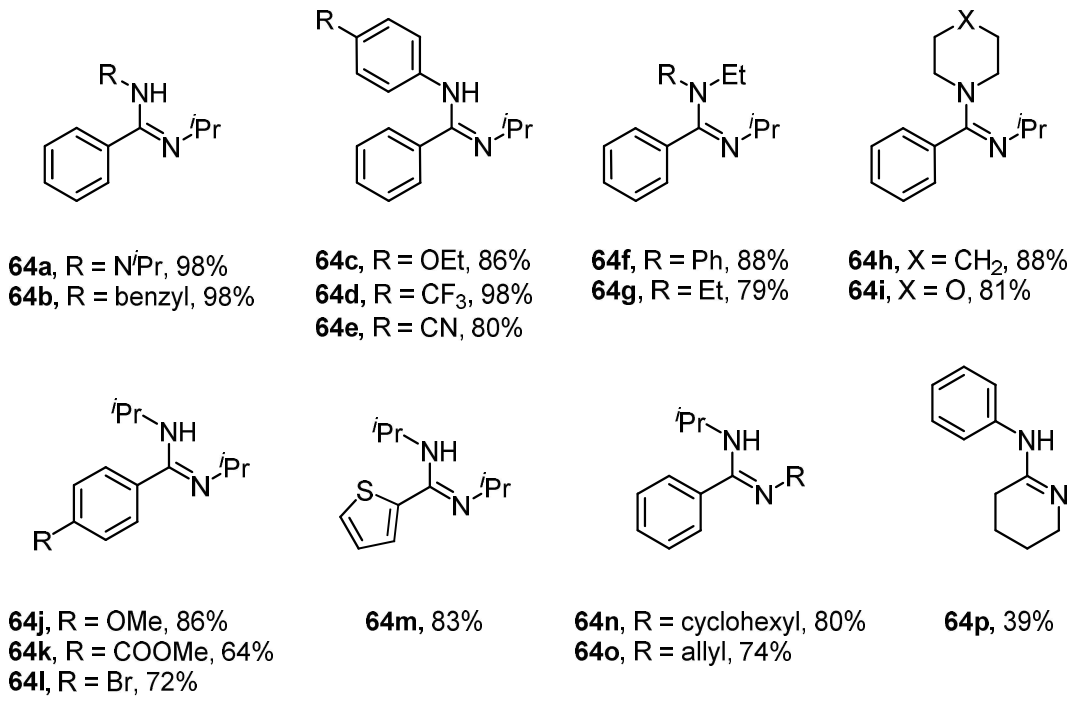

Reaction conditions: Step 1: 1.0 equiv **47** (0.5 mmol), 2 mol% catalyst **19a**, 1.5 equiv HCA, 1.5 equiv $PhSiH_3$, 1.5 mL BuOAc, 120 °C, 1h; Step 2: 3.5 equiv amine, 120 °C, 4 h. Isolated yields are given.

Additionally, Erlotinib (**66**), a tyrosine kinase inhibitor (TKI) used in the treatment of non-small cell lung cancer (NSCLC) and pancreatic cancer[60] was synthesized using one-pot, two-step catalytic protocol (Scheme 31). The synthesis started from commercially available 6,7-bis(2-methoxyethoxy)quinazolin-4(3*H*)-one (**65**), but due to its limited solubility in the standard solvent (BuOAc), the reaction conditions were slightly modified. Erlotinib (**66**) was obtained in a high yield of 81%. This methodology eliminates the requirement for toxic and corrosive oxalyl chloride $(COCl)_2$ in the imidoyl chloride formation step and simplifies the process from a two-step sequence to a more efficient one-pot reaction.

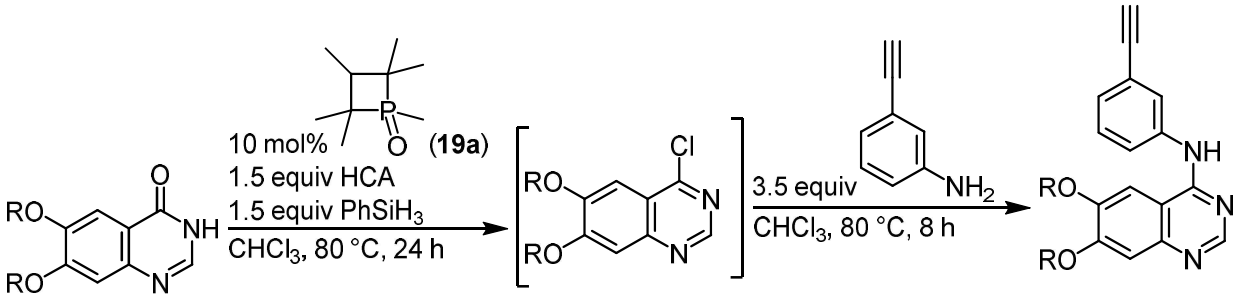

65

66, 81%

R = CH_2CH_2OMe

Scheme **31**. P^{III}/P^{V} redox catalyzed synthesis of Erlotinib **66**.

Mechanistic pathway is proposed based on our previous studies on P^{III}/P^{V} redox catalyzed reactions and control experiments (Scheme 32).[34,36,42] In initial step the phosphine oxide **19a** is reduced by $PhSiH_3$ to phosphine **20a**. When the reduction was performed under the reaction conditions in the absence of HCA, as a control experiment, the phosphine **20a** was formed as a mixture of two diastereoisomers (*dr* 22.3:1) with the chemical shift in the ^{31}P NMR for the major isomer at δ = 28.9 ppm. $^{1}H–^{29}Si$ HMBC NMR experiments indicated the formation of 1,3-diphenyl-disiloxane as one of the major products with a chemical shift δ = - 28.2 ppm which is in accordance with the literature.[61] The siloxane might be formed either by the reaction of the silanol with the silane forming hydrogen or by condensation under liberation of water.[34,36,61] The chlorophosphonium salt **67** is formed by the reaction of **20a** with HCA. In additional control experiments we could show that reaction of **20a** with HCA leads to the formation of **67**, as well as the reaction with **19a** in the presence of HCA and $PhSiH_3$. In both cases a specific signal for **67** was observed in the ^{31}P NMR with a chemical shift of δ = 116.7 ppm for the major isomer. In the

presence of amide **47d** the salt **67** reacts to the proposed oxophosphonium salt intermediate **68** which further converts to imidoyl chloride **59d** under liberation of the catalyst **19a**. The subsequent addition of the amine (^{i}PrNH$_2$) leads to the formation of the desired amidine **64a** as the hydrochloride salt in an addition-elimination sequence.

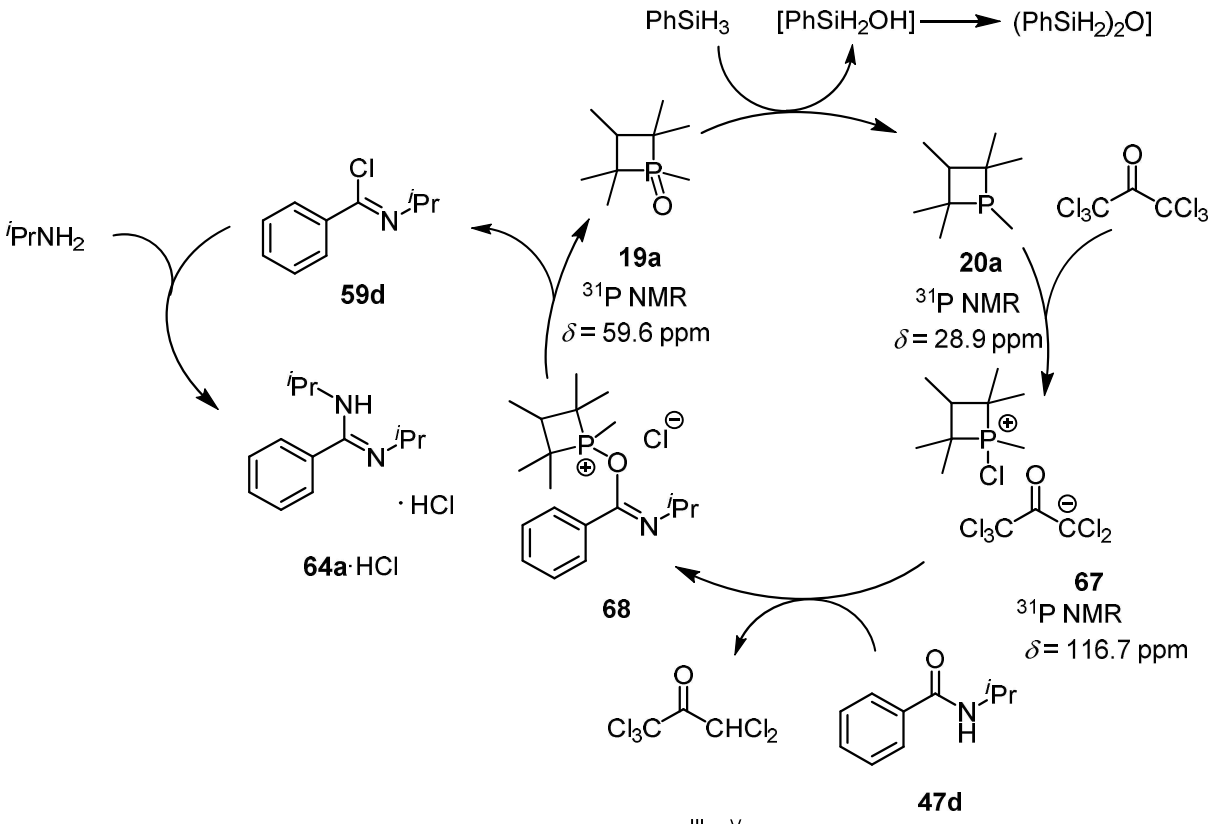

Scheme 32. Proposed mechanistic pathway for the P^{III}/P^{V} catalyzed amidine **64a** formation.

3.2 P^{III}/P^{V}=O redox catalyzed direct amide-to-ketimine transformation via Friedel–Crafts-type C–C bond formation

Friedel–Crafts alkylation and acylation are cornerstone methods in electrophilic aromatic substitution, with over a century of use.[62,63] However, the reliance on strong Lewis acids in this synthetic method and difficulties in achieving selective functionalization limit the applicability.[64] Consequently, there remains a strong demand for alternative methodologies beyond the traditional Friedel–Crafts reactions.[62,65] This project focuses on the functionalization of pyrrole, indole, and their derivatives without the need for strong Lewis acids or metal-catalyst.

Building on the research of activation of amides with phosphine based catalysts described in the previous chapter, this work further explores the use of pyrrole and indole derivatives as nucleophiles, reacting with imidoyl chlorides

generated *in situ*. Based on the optimized first step for the synthesis of imidoyl chlorides, the optimization of the second step was conducted (Table 4). After the *in situ* formation of **59d** under the optimized conditions, the addition of 3.5 and 4.5 equivalents of pyrrole was tested, which resulted in 86% and 81% yield of product **69a**, respectively (entries 1 and 2).

Table 4. Optimization of the reaction conditions for the second step of formation **69a** from *N*-isopropylbenzamide (**47d**).

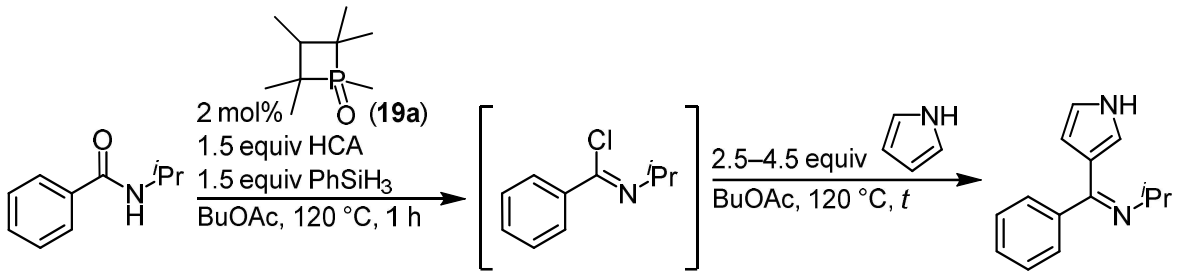

47d **59d** **69a**

entry	pyrrole / equiv	*t* / h	yield / %[1]
1	3.5	4	86
2	4.5	4	81
3	3.5	23	82

Reaction conditions: Step 1: 1.0 equiv **47d** (0.5 mmol), 2 mol% catalyst **19a**, 1.5 equiv HCA, 1.5 equiv $PhSiH_3$, 1.5 mL BuOAc, 120 °C. Step 2: 3.5–4.5 equiv pyrrole, 120 °C, 4–23 h. [1]Yield was determined by ^1H NMR analysis of the crude reaction mixture using mesitylene as the internal standard.

Prolonging the reaction time to 23 h with 3.5 equivalents of pyrrole resulted in 82% yield (entry 3), so the optimized conditions for the second reaction step were set to 4 h and 3.5 equivalents of pyrrole. The substrate scope of the reaction was evaluated (Table 5), commencing with the test of differently substituted pyrroles as nucleophiles in a reaction with imidoyl chlorides **59**. The model substrate **47d** with pyrrole as nucleophile gave the product **69a** in 62% yield. When more electron rich 2-methylpyrrole was used, the product **69b** was formed in a high 77% yield. Pyrrolopyrimidine gave the product **69c** in low 34% yield. Furthermore, indole derivatives were evaluated as nucleophiles. Reaction with indole afforded product **69d** in 70% yield, whereas the more electron-rich 4-methylindole delivered **69e** in an excellent 94% yield. The halo-substituted 5-iodoindole furnished **69f** in a yield of 53%, while conversion of the 5-oxaborolan-substituted indole produced **69g** as a hydrochloride salt in 62% yield.

Table 5. Substrate scope for one-pot two-step reaction of the formation of **69** from amides **47** by P^{III}/P^{V} redox catalysis.

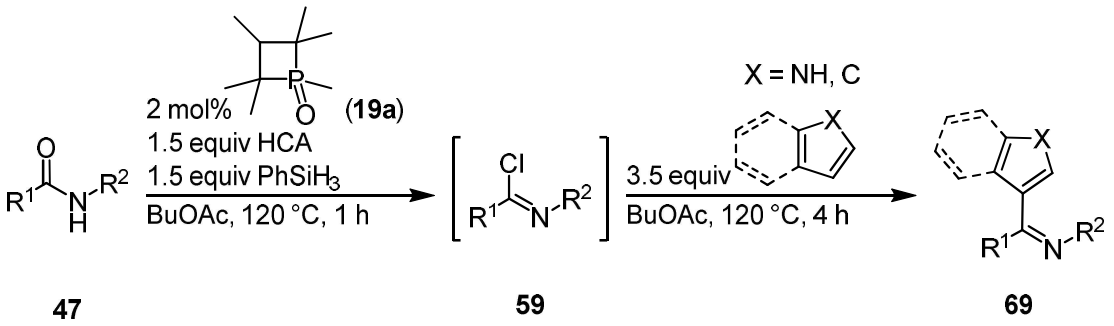

47 **59** **69**

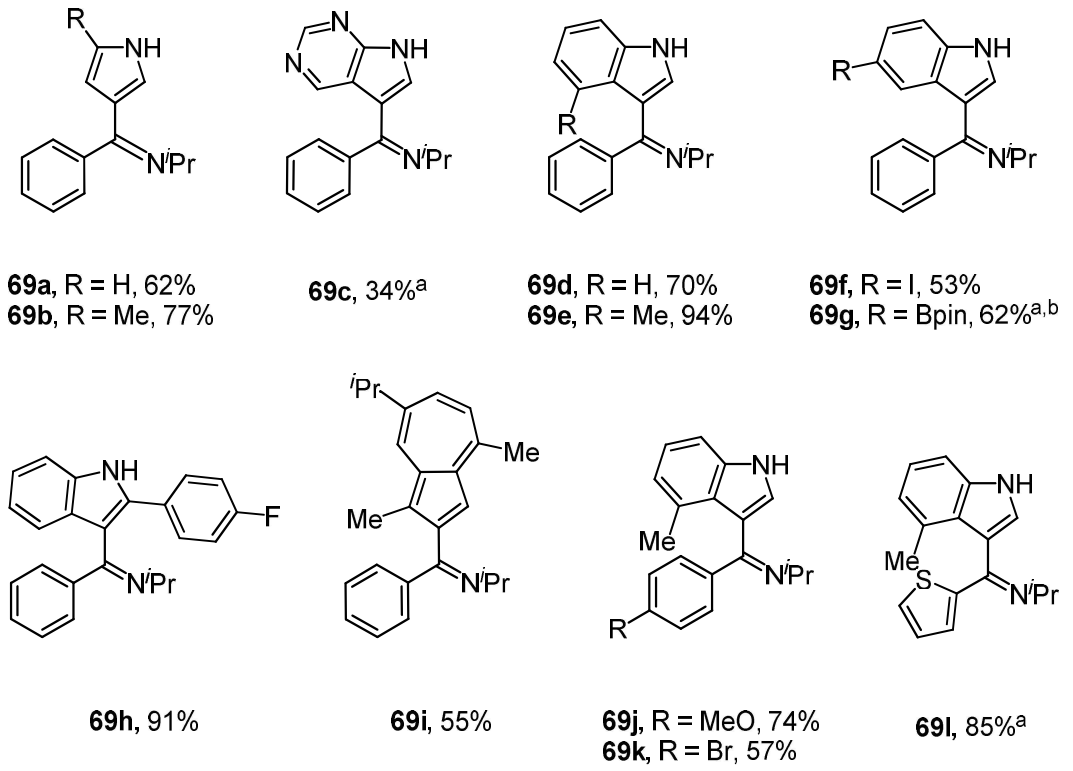

69a, R = H, 62%
69b, R = Me, 77%

69c, 34%[a]

69d, R = H, 70%
69e, R = Me, 94%

69f, R = I, 53%
69g, R = Bpin, 62%[a,b]

69h, 91%

69i, 55%

69j, R = MeO, 74%
69k, R = Br, 57%

69l, 85%[a]

Reaction conditions: Step 1: 1.0 equiv **47** (0.5 mmol), 2 mol% catalyst **19a**, 1.5 equiv HCA, 1.5 equiv $PhSiH_3$, 1.5 mL BuOAc, 120 °C, 1h; Step 2: 3.5 equiv nucleophile, 120 °C, 4 h. Isolated yields are given. [a]Step 2 was prolonged to overnight heating. [b]Product was isolated as a HCl salt.

With 2-*p*-fluorophenyl indole as a nucleophile, product **69h** was formed in 91% yield. In addition, electron-rich azulene derivative was tested, which resulted in a good 55% yield of product **69i.** Additionally, amide coupling partner was varied with 4-methylindole as a nucleophile. Electron-rich methoxy substituted aryl amide led to **69j** in 74% yield, while electron-withdrawing bromo-substituted derivative gave **69k** in 57% yield. Thiophene substituted amide gave the corresponding product **69l** in 85% yield. The mechanism for the imidoyl chloride formation is similar to the mechanism for the synthesis of amidines, reported in the previous chapter (Scheme

32). Following the imidoyl chloride **59d** *in situ* formation, the indole or pyrrole derivatives react with it in an electrophilic aromatic substitution in the subsequent step.

3.3 Synthesis of trisubstituted furans from activated alkenes by P^{III}/P^{V} redox cycling catalysis[66]

Substituted furans are important organic compounds due to their versatile reactivity. They play an important role in producing polymers[67] and they occur as natural products and pharmaceutical agents, even though they are sometimes associated with the formation of toxic metabolites.[68] Furan derivatives used in industrial applications are obtained from biomass sources, but traditional synthetic approaches remain widely used for preparing substituted furans, such as Paal-Knorr reaction for disubstituted furans and Feist-Benary reaction for tetrasubstituted variants.[69] Phosphines can be used for the synthesis of substituted furans under transition metal free conditions. In general, phosphine reacts in a Michael addition with an activated alkene, as shown in one of the previous chapters (Scheme 11), and afterwards, multiple reaction pathways are possible. In this project, the formed enolate reacts with an acyl chloride forming an enol ester, which then reacts in an intramolecular Wittig reaction. In the current literature, the formation of trisubstituted furans from 1,2-diacylethenes or 3-acylacrylates even under stoichiometric conditions has been underexplored with only few published examples.[70]

The investigation of the furan synthesis started with reacting 1,2-dibenzoylethene (**12d**) with benzoyl chloride (**24c**) in THF as solvent, diisopropylethylamine (DIPEA) as base and phenylsilane as the terminal reductant. When different catalysts were tested, phosphetane oxide **19a** afforded the trisubstituted furan **26dc** in a 71% yield (Table 6, entry 1), while less sterically demanding phosphine oxide **19b** afforded **26dc** in 24% (entry 2). Phosphine oxides **1b**, **8c**, and **8b** gave yields <10% (entry 3–5). Lowering the reaction temperature to 40 °C led to a significantly lower yield of 13% (entry 6), whereas at 80 °C **26dc** was obtained in 66% yield (entry 7). Increasing the amount of benzoyl chloride (**24c**) and base to 2.0 and 2.1 equiv respectively, led to the 99% yield (entry 8). The reaction time could be shortened to 4 h (entry 9), but it proved to be viable only for the model substrate **12d**. Test reactions showed the necessity for longer reaction times of 16 h for a broader applicability of the method.

Table 6: Catalyst screening and optimization of the reaction conditions for the formation of triphenylfuran **26dc** from dibenzoylethene **12d**.

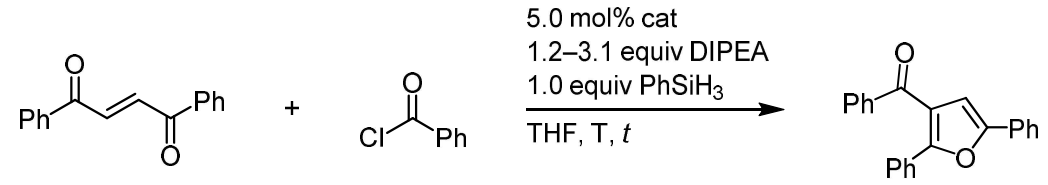

12d **24c** **26dc**

cat:

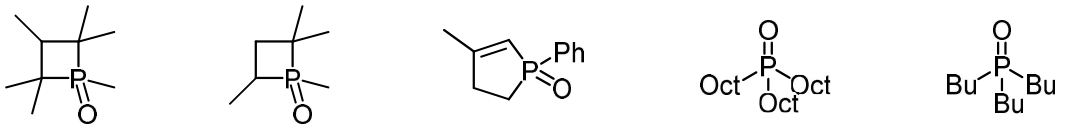

19a **19b** **1b** **8c** **8b**

entry	cat	**24c** / equiv	DIPEA / equiv	*t* / h	T / °C	yield **26dc** / %[1]
1	**19a**	1.1	1.2	16	60	71
2	**19b**	1.1	1.2	16	60	24
3	**1b**	1.1	1.2	16	60	7
4	**8c**	1.1	1.2	16	60	3
5	**8b**	1.1	1.2	16	60	2
6	**19a**	1.1	1.2	16	40	13
7	**19a**	1.1	1.2	16	80	66
8	**19a**	2.0	2.1	16	60	99
9	**19a**	2.0	2.1	4	60	99

Reaction conditions: 1.0 equiv **12d** (0.50 mmol), 1.1–2.0 equiv **24c**, 1.2–2.1 equiv DIPEA, 5.0 mol% catalyst, 1.0 equiv $PhSiH_3$, 1.5 mL solvent. [1]Yield determined by GC-FID with hexadecane as internal standard.

Evaluation of substrate scope was conducted. Model substrate **12d** was converted and corresponding furan **26dc** was isolated in 93% yield after a reaction time of 4 h (Table 7). For the synthesis of other substrates the reaction time was extended to 16 h. Under these conditions, the electron-rich dimethoxy derivative gave the trisubstituted furan **26ec** in a yield of 81%, while the dichloro derivative afforded the furan **26fc** in a moderate yield of 58%. Dithiophene derivative was converted to **26gc** in mediocre 55% yield. When aliphatic, methyl substituted derivative was tested, the product **26hc** was obtained in 40% yield, while phenyl substituted bisacylethene, resulted in a higher product formation **26ic** of 74%. Different acid chlorides **24** were tested in a reaction with dibenzoylethene, and bromo substituted

benzoyl chloride led to the furan **26dd** in a good yield of 89% while the electron-poor methoxycarbonylbenzoyl chloride led to a slightly lower yield of 73% of furan **26de**. Methylbenzoyl chloride led to reduced yield of 28% of furan **26df**. Reaction with cyclopropylcarbonyl chloride led to a surprisingly good yield of 78% of furan **26dg**.

Table 7. Selected examples for the substrate scope of trisubstituted furans **26** from bisacylethenes **12** and acyl chlorides **24**.

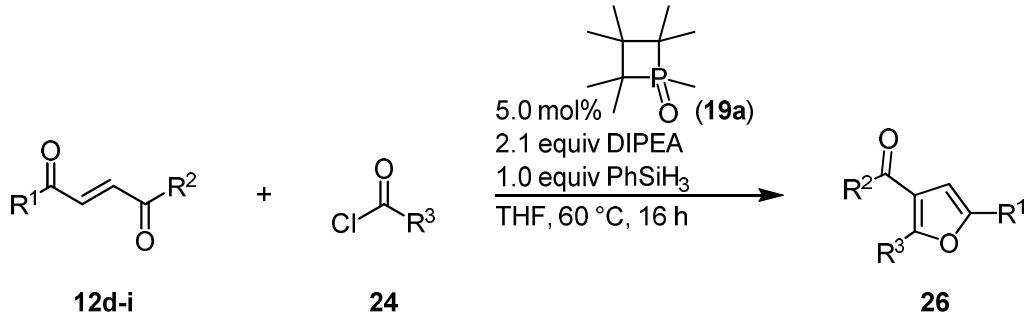

12d-i **24** **26**

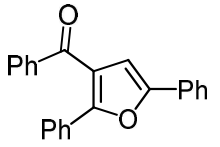

26dc, 93%[a]

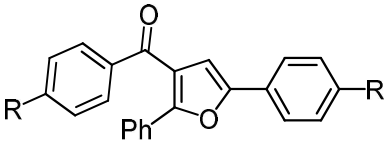

26ec, R = OMe, 81%
26fc, R = Cl, 58%

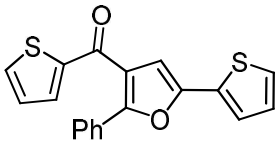

26gc, 55%

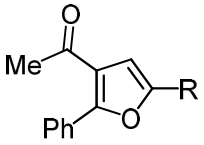

26hc, R = Me, 40%
26ic, R = Ph, 74%

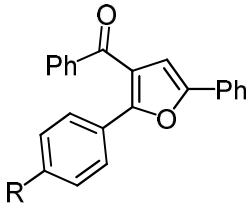

26dd, R = Br, 89%
26de, R = CO_2Me, 73%
26df, R = Me, 28%

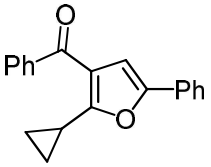

26dg, 78%

Reaction conditions: 1.0 equiv **12d-i** (1.0 mmol), 2.0 equiv **24**, 2.1 equiv DIPEA, 5.0 mol% catalyst **19a**, 1.0 equiv $PhSiH_3$, 3.0 mL THF, 60 °C, 16 h. Isolated yields are given. [a]Reaction time 4 h.

Two mechanistic pathways are possible for this transformation (Scheme 33). After the initial Michael addition, the enolate **21a** reacts with acyl chloride **24c** in a *C*-acylation reaction, followed by nucleophilic attack on the opposing carbonyl group and subsequent deoxygenation in a ring-closure process. Alternatively, *O*-acylation of the enolate could occur, generating enol ester **70**. After deprotonation, **70** would undergo an intramolecular Wittig reaction. The intermediate **71** was synthesized and brought to a reaction in the presence of catalyst **19a** and phenylsilane to check the potential of the ring-closure pathway. The furan was formed so the viability of this

pathway was confirmed. However, when the reaction was conducted in presence of benzoyl chloride (**24c**) and DIPEA, the major product was a tetrasubstituted furan, a product that was previously not observed under these conditions. The ring-closure pathway should theoretically be possible without an added base, but under the optimized conditions of this work, the reaction was not successful without the addition of DIPEA. These results suggest that pathway involving *O*-acylation and an intramolecular Wittig reaction, represents the more plausible mechanistic route.

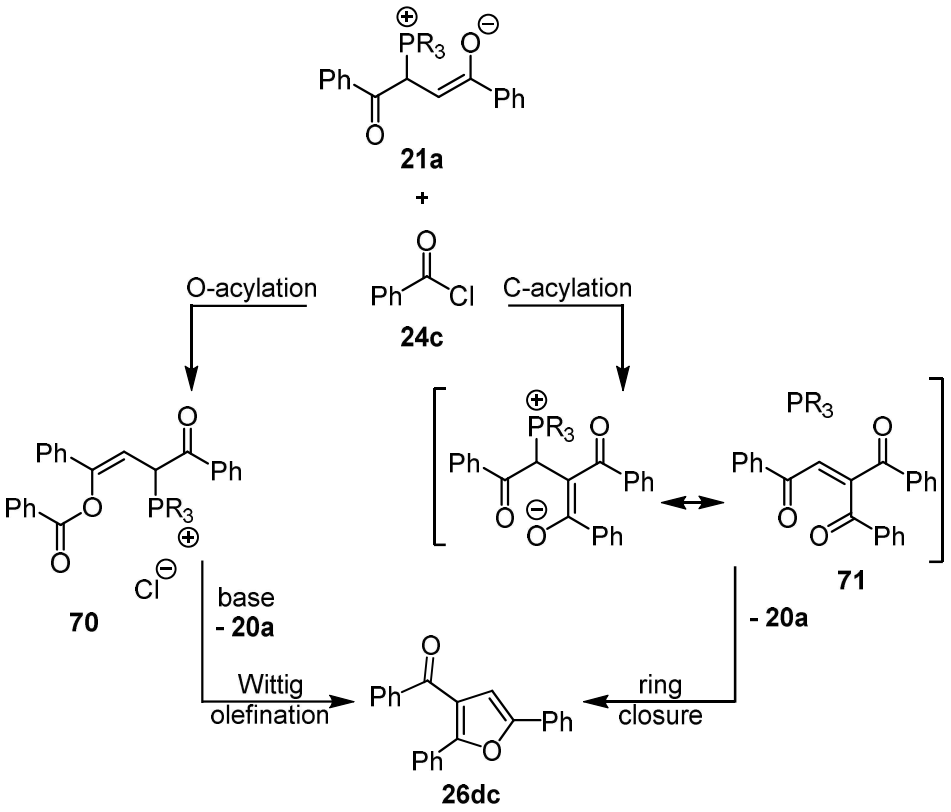

Scheme 33. Possible reaction pathways for the synthesis of trisubstituted furan **26** from diacylethene **12**.

The acrylate **12j** was also tested as substrate under the same reaction conditions (Table 8). When it was converted with benzoylchloride (**24c**), unexpectedly the tetrasubstituted furan **72jc** was formed alongside the the furan **26jc**. The product ratio of the formed furans **26** and **72** was found to be dependent on the phosphine catalyst. Among the tested catalysts, **19a** was the only catalyst leading to an excess formation of the tetrasubstituted furan **72** (entry 1). Less sterically demanding catalyst **19b** produced overall yield of 49% with (entry 2). With the phospholene catalyst **1b** trisubstituted furan **26jc** was preferred, with the 48% yield, and a 6% yield of tetrasubstituted furan **72jc** (entry 3).

Table 8. Catalyst screening and reaction optimization for the formation of trisubstituted furan **26jc** and tetrasubstituted furan **72jc** from acylacrylate **12j**.

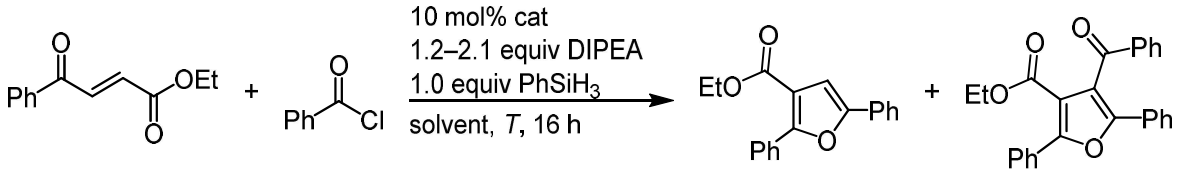

12j **24c** **26jc** **72jc**

cat:

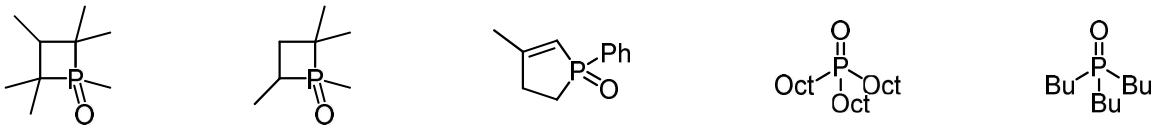

19a **19b** **1b** **8c** **8b**

entry	cat	**24c** / equiv	DIPEA / equiv	solvent	*T* / °C	yield **26jc** / %[a]	yield **72jc** / %[a]	**26ja**:**72jc**
1	**19a**	1.1	1.2	THF	60	11	25	31:69
2	**19b**	1.1	1.2	THF	60	27	22	55:45
3	**1b**	1.1	1.2	THF	60	48	6	89:11
4	**8c**	1.1	1.2	THF	60	2	<2	91:9
5	**8b**	1.1	1.2	THF	60	2	<2	95:5
6	**1b**	1.1	1.2	toluene	100	74	8	90:10
7	**1b**	1.5	1.6	toluene	100	80	10	89:11
8[b]	**1b**	1.5	1.6	toluene	100	82	10	89:11
9	**19a**	5.0	5.0	toluene	60	14	71	16:84

Reaction conditions: 1.0 equiv **12j**, 1.1–5.0 equiv **24c**, 1.2–5.0 equiv DIPEA, 10 mol% **cat**, 1.0 equiv $PhSiH_3$, 1.5 mL solvent, 60–100 °C, 16 h. [a]Yield determined by GC-FID with hexadecane as internal standard, [b]Reaction time: 4 h.

Trisubstituted furan **26jc** was preferred in case with trioctylphosphine oxide (**8c**) and tributylphosphine oxide (**8b**) as catalysts but only led to low yields (entries 4 and 5). When solvent was switched to toluene, and with higher temperature of 100 °C, yield was increased to 82% with the reatio of 90:10 in favour of trisubstituted furan **26jc** (entry 6). Increasing the amount of **24c** and DIPEA to 1.5 and 1.6 equivalents respectively, led to an increased yield 80% of furan **26jc** (entry 7). The reaction time was shortened to 4 h without major changes in yield and selectivity (entry 8). Further optimization was carried out to improve the selective formation of tetrasubstituted furan **72jc**. Under the conditions employing phosphetane catalyst **19a**, an excess of

benzoyl chloride **24c**, and DIPEA at 60 °C, the product was obtained in 71% yield with a ratio of 16:84 in favor of the tetrasubstituted isomer **72jc** (entry 9). Under the conditions optimized for the formation of tetrasubstituted furan, using the phosphetane catalyst **19a**, the **72jc** was isolated in 68% yield, and the trisubstituted furan **26jc** in 13% as the side product (Scheme 34). When *p*-methoxyphenyl substituted alkene **12k** was subjected to a reaction under the same conditions, selectivity problem occurred. Whenever the substituents between the acyl chloride **24** and the acyl acrylates **12k-n** were different, two regioisomers of the tetrasubstituted furan were synthesized. In this case, using acyl acrylate **12k**, tetrasubstituted furans **72kc** in 24% yield, and the **72kc'** in 54% yield were achieved (Scheme 34).

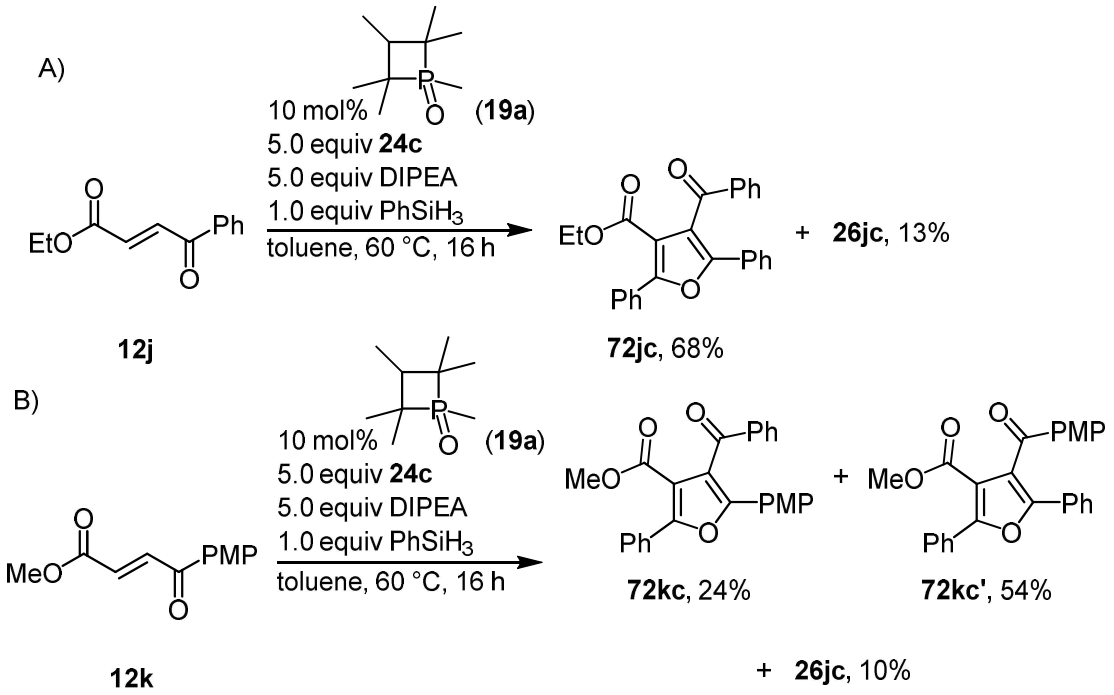

Scheme 34. Selected examples for the synthesis of tetrasubstituted furans **72** from acylacrylates **12**. Reaction conditions: 1.0 equiv **12**, 5.0 equiv **24c**, 5.0 equiv DIPEA, 10 mol% **19a**, 1.0 equiv $PhSiH_3$, 3.0 mL toluene, 60 °C, 16 h; PMP: *p*-methoxyphenyl.

This outcome made this reaction less synthetically valuable. Using the optimized conditions for the synthesis of trisubstituted furans **26** the substrate scope was evaluated (Table 9). The model substrate **12j** was converted with benzoyl chloride **24c** to the diphenylfuran **26jc** in 74% yield. Additionally, the tetrasubstituted furan **72jc** was isolated in a yield of 13%. With *p*-methoxyphenyl substituted alkene **12k**, the furan **26kc** was isolated in 70% yield. The electron-rich methoxy substituted

product **26lc** afforded the yield of 70%, while chloro substituted product **26mc** resulted in a mediocre 59% yield. The heterocyclic, furan derivative **12n** afforded the furanylphenylfuran **26nc** in a 71% yield. Differently substituted benzoyl chlorides were tested in a reaction with ethyl benzoylacrylate. The bromo substituted furan **26jd** was synthesized in a high 70% yield, the methoxycarbonyl derivative **26je** resulted in a lower 59% yield, while the methoxy derivative **26jh** performed with 57% yield. Cyclopropylcarbonyl chloride was also tested with ethyl benzoylacrylate **12j** and yielded the trisubstituted furan **26jg** in 67%.

Table 9. Selected examples for the synthesis of trisubstituted furans from acylacrylates **12j-n** and acyl chlorides **24**.

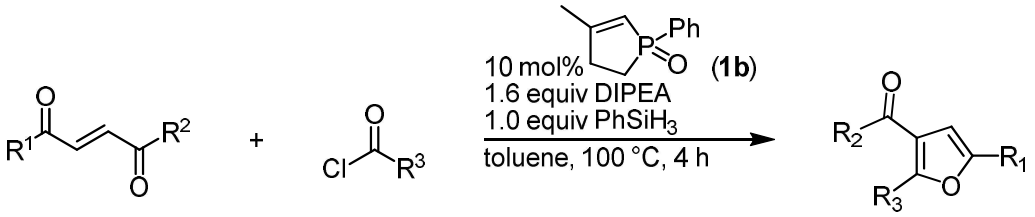

12j-n **24** **26**

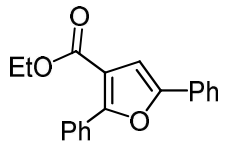

26jc, 74%
+ **72jc**, 13%

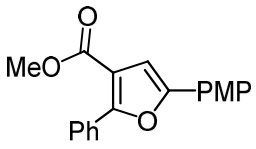

26kc, 70%

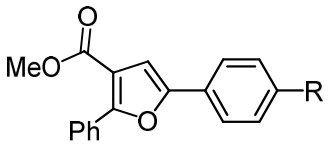

26lc, R = OMe, 70%
26mc, R = Cl, 59%

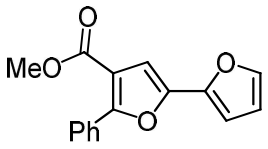

26nc, 71%

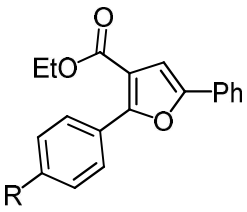

26jd, R = Br, 70%
26je, R = CO_2Me, 59%
26jh, R = OMe, 57%

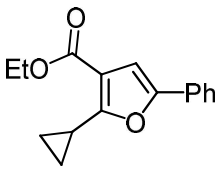

26jg, 67%

Reaction conditions: 1.0 equiv **12j-n** (1.0 mmol), 1.5 equiv **24**, 1.6 equiv DIPEA, 10 mol% **1b**, 1.0 equiv $PhSiH_3$, 3.0 mL toluene, 100 °C, 4 h. Isolated yields are given.

The formation of the tetrasubstituted furans can also be explained by two plausible pathways, both involving *C*-acylation followed by *O*-acylation and an intramolecular Wittig olefination (Scheme 35). Regioisomer formation, observed when the substituents on the acyl acrylate **12** and acyl chloride **24** differ, can only be explained by Michael addition at the *α*-carbon relative to the ester. In this case, Michael addition is followed by *C*-acylation to give the intermediate **73**.

Deprotonation of the acidic proton then enables *O*-acylation at either of two distinct enolate sites. Subsequent deprotonation to generate the ylide, followed by an intramolecular Wittig reaction, affords the two isomeric furans **72kc** and **72kc′**.

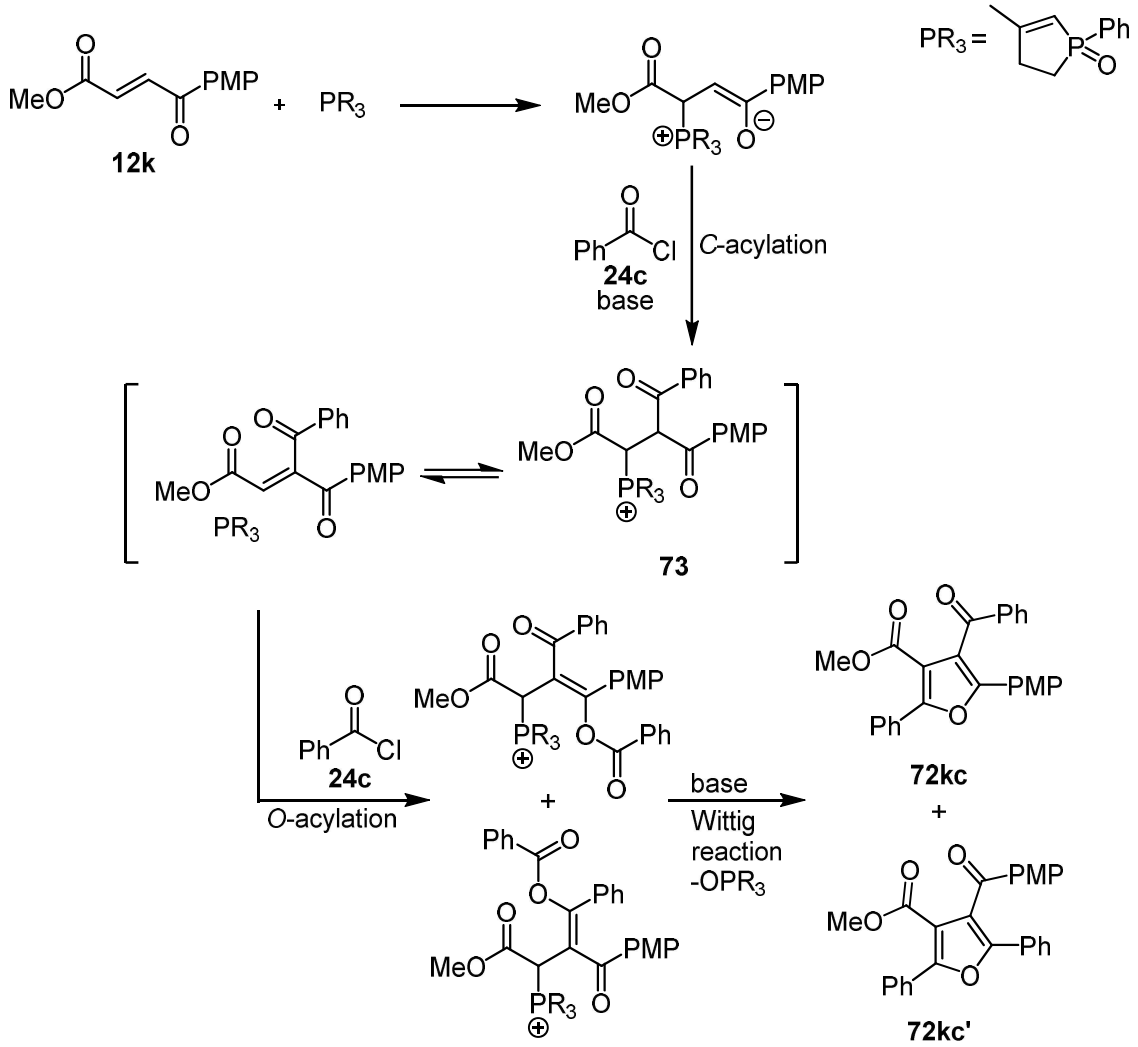

Scheme 35. Possible reaction pathway for the synthesis of tetrasubstituted furans **72kc** and **72kc'** from acylacrylate **12k**.

3.4 Metal-free reduction of nitrous oxide via P^{III}/P^{V} cycling: mechanistic insights and catalytic performance[71]

Nitrous oxide (N_2O) is a potent greenhouse gas that poses environmental challenges, yet it also holds promise in synthetic chemistry as a strong oxidant whose reactions typically yield benign nitrogen gas.[53] Considering the environmental impact of N_2O, efficient strategies for its chemical utilization and catalytic decomposition are urgently needed.[54] This research employes a phosphine-based catalytic system for the reduction of N_2O, circumventing the need

for transition metal catalysts[56] or frustrated Lewis pairs.[57] To investigate the reactivity of phosphetanes toward N_2O, Lewis bases **19** and **20** were reacted with one equivalent of **74** and approximately two equivalents of N_2O at 70 °C (Table 10).

Table 10. Optimization of reaction conditions for the activation of N_2O.

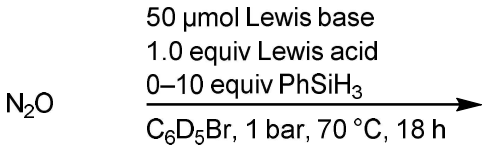

Lewis base: **Lewis acid:**

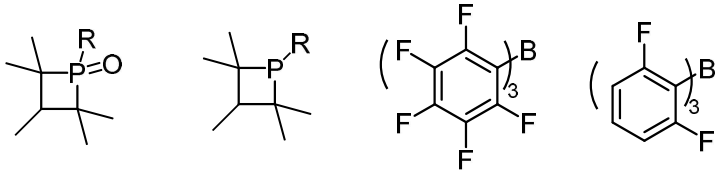

19a, R = Me **20a,** R = Me **74a** **74b**
19c, R = Ph **20b,** R = Ph

entry	Lewis base	Lewis acid	reductant	outcome
1	**20a**	**74a**	-	no reaction
2	**20b**	**74a**	-	no reaction
3	**20a**	**74b**	-	**19a·74b**+N_2
4	**20b**	**74b**	-	**19c·74b**+N_2
5	**19a**	**74b**	$PhSiH_3$	**20a·74b**+N_2
6	**19a**	-	$PhSiH_3$	**20a**+N_2
7	**19c**	-	$PhSiH_3$	**20b**+N_2
8	**20a**	-	-	**19a**+N_2
9	**20b**	-	-	**19c**+N_2
10	-	-	$PhSiH_3$	no reaction

Reaction conditions: 1.0 equiv **Lewis base** (50 µmol), 1.0 equiv **Lewis acid**, 10 equiv $PhSiH_3$, N_2O (1 bar), 0.5 mL C_6D_5Br, 70 °C, 18 h.

When **20a** or **20b** in combination with **74a**, were reacted with N_2O, there was no nitrogen formation (entries 1 and 2). However, when **74a** was replaced with B(2,6-F_2-C_6H_3)$_3$ (**74b**), formation of N_2 was observed in the ^{14}N NMR spectra, along with the formation of the adducts **19a·74b** and **19c·74b** respectively (entries 3 and 4). Since the goal was to explore the catalytic potential of this transformation, 10 equiv of $PhSiH_3$ were added to the reaction mixture of **19a** and **74b**, resulting with formation of nitrogen (entry 5). Subsequently, the reaction of **19a** or **19c** with silane

was examined in the absence of additive **74**, resulting in the formation of N_2, which indicates that phosphetanes alone are capable of catalyzing the reduction of N_2O (entries 6 and 7). The experiments with **20a** or **20b** in the absence of $PhSiH_3$ show the complete conversion to **19a** and **19c**, respectively (entries 8 and 9). Control experiments without the phosphetane resulted in no reaction (entry 10). To demonstrate the catalytic reduction of N_2O, the reaction was monitored using gas chromatography (GC) (Figure 1) and TOF (turnover frequency) and TON (turnover number) were calculated accordingly (Table 11). The results showed that at 70 °C using $PhSiH_3$ as reducing agent, phosphetanes **20a** and **20b** catalyze the reduction of N_2O but with different kinetic profiles, exhibiting turnover frequencies, TOF = 0.4 h^{-1} and 0.1 h^{-1}, respectively (Figure 1, left; Table 11, entries 1 and 2).

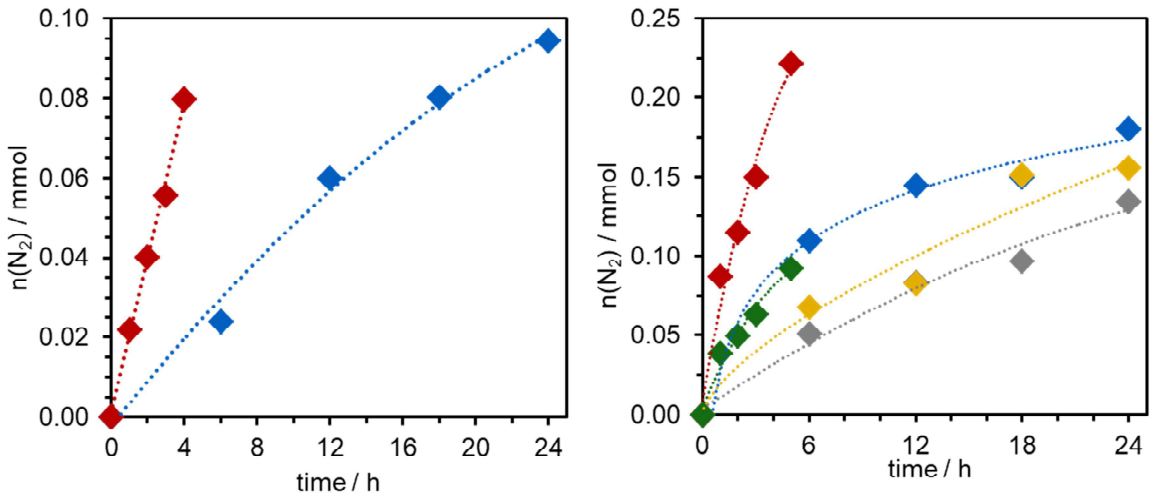

Figure 1. Quantification of N_2 gas evolution vs. time: 0.5 mL C_6H_5Br, 9.5 mL N_2O (0.42 mmol), 0.5 mmol phenyl silane; left: 0.05 mmol **20a** or **20b** at 70 °C and right: 0.025 mmol **20a** or **20b**; or 0.05 mmol **8b**, at 100 °C (◆**20a**, ◆**20b**, ◆ **13c;** ◆**20a**, ◆**20b** with PMHS).

Increasing the reaction temperature to 100 °C significantly enhanced catalytic performance (Figure 1 right; Table 11, entries 3 and 4). The catalyst **13c** was also also tested under these conditions, and although it demonstrated catalytic activity, it had lower efficiency (Figure 1 right, Table 11, entry 5). Additionally, PMHS was tested as an environmentally friendly, low-cost reducing agent. In this case, phosphetanes maintained catalytic activity but with lower efficinecy (Figure 1 right, Table 11, entries 6 and 7). To get the insight into the catalytic mechanism, the reaction orders with respect to the individual reactants were determined. The reduction of the phosphetane oxides **19a** and **19c** by $PhSiH_3$ proceeds with first-order kinetics in both the phosphetane oxide and the silane and requires the

activation energy (E_a) of 10.6±1 kcal·mol^{-1} for **19a** and 10.3±2 kcal·mol^{-1} for **19c**. Similarly, the oxygen transfer from N_2O to the phosphetanes (in the absence of $PhSiH_3$) exhibits a first-order dependence for both **20a** and **20b** with E_a of 11.5±3 kcal·mol^{-1} for **20a** and 18.2±2 kcal·mol^{-1} for **20b**, indicating that this is the rate-determining step.

Table 11. Evaluation of catalysts in the N_2O reduction.

entry	**cat**	reducing agent	T / °C	TON	TOF [h^{-1}]
1	**20a**	$PhSiH_3$	70	1.6[a]	0.4[b]
2	**20b**	$PhSiH_3$	70	0.5[c]	0.1[c]
3	**20a**	$PhSiH_3$	100	8.9[d]	3.3[b]
4	**20b**	$PhSiH_3$	100	4.2[c]	0.7[c]
5	**13c**	$PhSiH_3$	100	0.9[c]	0.1[c]
6	**20a**	PMHS	100	3.5[d]	1.5[b]
7	**20b**	PMHS	100	1.3[c]	0.2[c]

Conditions for entries 1,2,5: 50 µmol **cat**; entries 3,4,6,7: 25 µmol **cat**; both in 0.5 mL C_6H_5Br, 9.5 mL N_2O (0.42 mmol), 0.5 mmol reducing agent; N_2 concentrations were determined by gas chromatography (GC)**;** [a]4h; [b]1h; [c]6h; [d]5h.

The order of the phosphetane catalysts in the full catalytic reaction was determined to be of first-order. Based on these kinetic data, control experiments and earlier reports, a catalytic cycle is proposed. First, the *P*-atom adds to the *N*-terminus of N_2O (Scheme 36), generating the *cis* and *trans*- configured zwitterionic species *cis*-**75** and *trans*-**75** as high energy intermediates. The *cis*-configured diastereomer undergoes intramolecular N_2 extrusion through an intramolecular reaction, resulting in the formation of phosphetane oxide **19a**. The reduction of **19a** by silanes proceeds via the intermediate **76** followed by HO–[Si] elimination. Quantum-chemical calculations at the DLPNO-CCSD(T)/cc-pVTZ//PBEh-3c/def2-mTZVP//openCOSMO-RS level of theory were performed to get mechanistic insight into the reduction of N_2O by the phosphetane. The computational model was performed on simplified 2,2,4,4-tetramethylphosphetane derivatives (**20a′**, Me; **20b′**, Ph), as the methyl substituent in the 3-position is spatially distant from the reactive phosphorus center and unlikely to affect the mechanism. To rationalize the different reactivity of **20a′** and **20b′**, their structural and electronic features were analyzed.

The Me-derivative **20a′** shows a slightly greater pyramidalization than the **20b'**, and a slightly higher partial charge on phosphorous. The reaction of **20a′** with the terminal nitrogen of N_2O is endergonic by 12.5 kcal·mol^{-1} and proceeds via a *cis*-transition state to form *cis*-**75**$_{20a'}$.

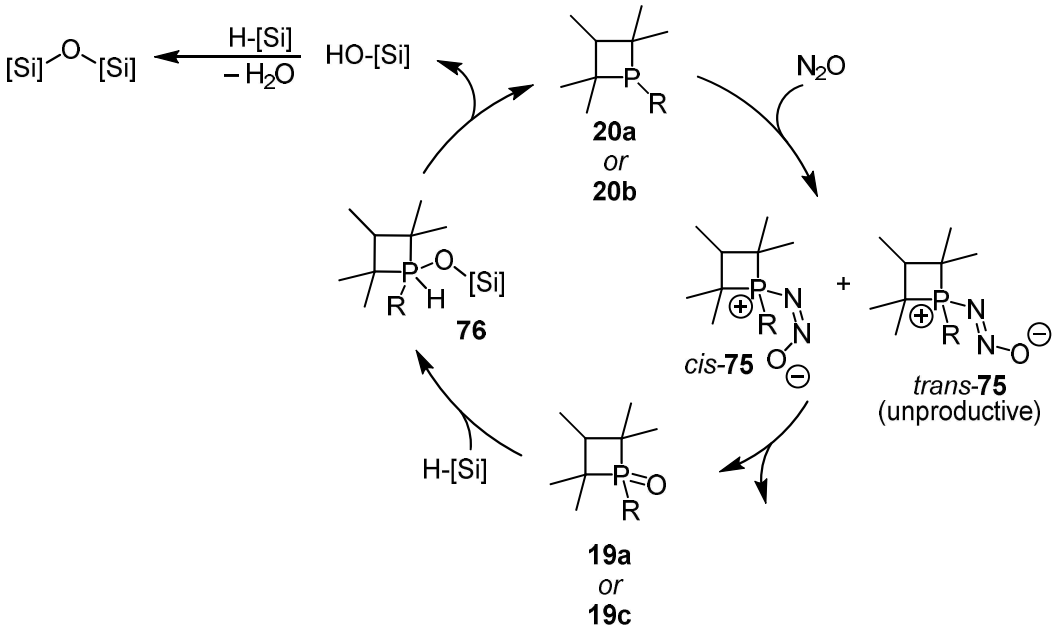

Scheme 36. Proposed catalytic cycle for the phosphetane-catalyzed N_2O reduction.

The *trans*-isomer is by 3.7 kcal·mol^{-1} less stable and forms via a higher barrier of 59.7 kcal·mol^{-1}. The intramolecular *O*-atom transfer to form the corresponding phosphetane oxide is slightly more favorable for **20a′** than for **20b′**. Although the absolute computed barriers are higher than the experimental values by roughly 10–17 kcal·mol^{-1}, the calculated trends are consistent with the experimental kinetics. Oxide transfer is slightly more energy-demanding than the reduction of the oxides **19a′** and **19c′** by silane. Natural population analysis (NPA) calculation of the transition states revealed that formation of the *cis*-**75**$_{20a'}$ is stabilized by donor/acceptor interactions between the phosphorus lone pair and the unoccupied π* and σ* orbitals of N_2O, while such interactions are absent in the in the *trans*-**75**$_{20a'}$, making it less favorable. Local energy decomposition (LED) analysis further showed that, interaction energies between N_2O and the phosphetane are outweighed by the deformation energy required to bend N_2O from linearity. The transition states leading to the *trans*-adducts (*trans*-**75**$_{20a'}$ and *trans*-**75**$_{20b'}$) exhibit higher activation energies due to the higher deformation energy in comparison with the transition states leading to *cis*-**75**$_{20a'}$. The bonding situation in *cis*-**75**$_{20a'}$ and *cis*-

$75_{20b'}$ can be described as zwitterionic, featuring a *cis*-configured azonyl (-N=N-O) group and a weak $LP_{O}{\rightarrow}_{P}$ interaction due to the partial positive polarization of phosphorus. This P–O interactions prime the system for *O*-atom transfer from the N_2O-fragment to the *P*-center.

4. Summary

In this work, new catalytic methods in the field of P^{III}/P^{V} redox catalysis were developed. A phosphine-catalyzed, two-step, one-pot protocol for amidine synthesis from amides was established, involving *in situ* amide activation to form imidoyl chlorides followed by reaction with amines. The method requires low catalyst loading and a mild chlorinating agent, avoiding the harsh, toxic reagents typically used, such as oxalyl chloride $(COCl)_2$. Compared to the phosphine-mediated amidine synthesis, this method offers the advantage of circumventing the stoichiometric generation of phosphine oxide as a byproduct. This transformation was applied to the synthesis of 20 new compounds, including the pharmaceutical tyrosine kinase inhibitor Erlotinib, offering a more efficient alternative to the standard two-step industrial process. The new amide activation strategy also enabled electrophilic aromatic substitution of indole and pyrrole derivatives with the *in situ* generated imidoyl chlorides, providing an organocatalytic alternative to previously metal-catalyzed methods. This underexplored imination of heteroaromatic compounds delivered 20 new compounds in yields up to 94%. Further work explored catalytic furan synthesis via enolate intermediate, usually formed in the base-free Wittig reaction after the Michael addition of the catalyst to the activated olefin. Bisacylethenes and acyl acrylates were reacted with acyl chlorides to access an underrepresented class of substituted furans. Using a phosphetane catalyst, amine base, and phenylsilane as terminal reductant, 12 trisubstituted furans were obtained. Unexpectedly, reactions with acyl acrylates also yielded tetrasubstituted furans, with product ratio dependent on the catalyst. This led to the synthesis of 14 trisubstituted furans using a phospholene catalyst and 6 tetrasubstituted furans using a phosphetane catalyst. In the final project, the first phosphine-catalyzed reduction of nitrous oxide was developed. Although phosphine-mediated and FLP-based systems for N_2O reduction were known, catalytic process had not yet been investigated. Using a phosphetane catalyst with phenylsilane as the terminal reductant, the reaction was performed under mild conditions. Detailed kinetic studies with methyl- and phenyl-substituted phosphetanes, revealed that oxygen transfer to the catalyst is the rate-determining step. The reduction of both phosphetane oxides with phenylsilane and the catalytic deoxygenation step were

first-order in regard to the phospetane. Turnover frequencies (TOF) were quantitatively determined by monitoring nitrogen evolution via gas chromatography.

5. Abbreviations

BFW	base-free Wittig
Bu	butyl
Bz	benzyl
cat	catalyst
cat.	catalytic amount
DIPEA	*N*,*N*-diisopropylethylamine
DEBM	diethyl bromomalonate
DEMBM	diethyl 2-bromo-2-methylmalonate
DMF	dimethylformamide
equiv	equivalents
Et	ethyl
ETCA	ethyl 2,2,2-trichloroacetate
FID	flame ionization detector
FLPs	frustrated Lewis pairs
GC	gas chromatography
HCA	hexachloroacetone
Hex	hexyl
^{i}Pr	*iso*-Propyl
Me	methyl
MeCN	acetonitrile
NMR	nuclear magnetic resonance
NSCLC	non-small cell lung cancer
p	para
Ph	phenyl
PMHS	polymethylhydrosiloxane
PMP	*p*-methoxyphenyl
RT	room temperature
T	temperature
t	time
TOF	turnover frequency
TON	turnover number
TCMB	(trichloromethyl)benzene
THF	tetrahydrofuran
TKI	tyrosine kinaseinhibitor

6. References

[1] M. Mehta, I. La Garcia de Arada, M. Perez, D. Porwal, M. Oestreich, D. W. Stephan, *Organometallics* **2016**, *35*, 1030.

[2] L. Longwitz, T. Werner, *Pure Appl. Chem.* **2019**, *91*, 95.

[3] D. Herault, D. H. Nguyen, D. Nuel, G. Buono, *Chem. Soc. Rev.* **2015**, *44*, 2508.

[4] H. A. van Kalkeren, A. L. Blom, Rutjes, Floris P. J. T., M. A. J. Huijbregts, *Green Chem.* **2013**, *15*, 1255.

[5] P. S.-W. Leung, Y. Teng, P. H. Toy, *Synlett* **2010**, *2010*, 1997.

[6] M. G. Russell, S. Warren, *J. Chem. Soc., Perkin Trans. 1,* **2000**, 505.

[7] D. C. Batesky, M. J. Goldfogel, D. J. Weix, *J. Org. Chem.* **2017**, *82*, 9931.

[8] a) E. A. Broger, US4246204A, **1979**; b) H. Pommer, *Angew. Chem., Int. Ed.* **1977**, *16*, 423; c) D. Hermeling, P. Bassler, P. Hammes, R. H.ugo, P. Lechtken, H. Siegel, *BASF AG, US* **1996**.

[9] a) T. Imamoto, T. Kusumoto, N. Suzuki, K. Sato, *J. Am. Chem. Soc.* **1985**, *107*, 5301; b) T. Imamoto, S. Kikuchi, T. Miura, Y. Wada, *Org. Lett.* **2001**, *3*, 87.

[10] C. A. Busacca, R. Raju, N. Grinberg, N. Haddad, P. James-Jones, H. Lee, J. C. Lorenz, A. Saha, C. H. Senanayake, *J. Org. Chem.* **2008**, *73*, 1524.

[11] T. Coumbe, N. J. Lawrence, F. Muhammad, *Tetrahedron Lett.* **1994**, *35*, 625.

[12] Y. Li, L.-Q. Lu, S. Das, S. Pisiewicz, K. Junge, M. Beller, *J. Am. Chem. Soc.* **2012**, *134*, 18325.

[13] a) D. Moser, K. Jana, C. Sparr, *Angew. Chem., Int. Ed.* **2023**, e202309053; b) T. V. Nykaza, T. S. Harrison, A. Ghosh, R. A. Putnik, A. T. Radosevich, *J. Am. Chem. Soc.* **2017**, *139*, 6839.

[14] a) H. A. van Kalkeren, F. L. van Delft, Rutjes, Floris P. J. T., *Pure Appl. Chem.* **2012**, *85*, 817; b) R. M. Denton, J. An, B. Adeniran, A. J. Blake, W. Lewis, A. M. Poulton, *J. Org. Chem.* **2011**, *76*, 6749.

[15] H. A. van Kalkeren, S. Leenders, C. Rianne, A. Hommersom, F. Rutjes, F. van Delft, *Chem. - Eur. J.* **2011**, *17*, 11290.

[16] R. M. Denton, X. Tang, A. Przeslak, *Org. Lett.* **2010**, *12*, 4678.

[17] R. M. Denton, J. An, B. Adeniran, *Chem. Commun.* **2010**, *46*, 3025.

[18] M. Lecomte, J. M. Lipshultz, S.-H. Kim-Lee, G. Li, A. T. Radosevich, *J. Am. Chem. Soc.* **2019**, *141*, 12507.

[19] D. C. Lenstra, Rutjes, Floris P. J. T., J. Mecinović, *Chem. Commun.* **2014**, *50*, 5763.

[20] G. Wittig, G. Geissler, *Liebigs Ann. Chem.* **1953**, *580*, 44.

[21] a) P. Cao, C.-Y. Li, Y.-B. Kang, Z. Xie, X.-L. Sun, Y. Tang, *J. Org. Chem.* **2007**, *72*, 6628; b) Z.-Z. Huang, Y. Tang, *J. Org. Chem.* **2002**, *67*, 5320; c) Y.-Z. Huang, Y. Liao, *Tetrahedron Lett.* **1990**, *31*, 5897.

[22] A. H. Welch, D. B. Westjohn, D. R. Helsel, R. B. Wanty, *Groundwater* **2000**, *38*, 589.

[23] C. J. O'Brien, J. L. Tellez, Z. S. Nixon, L. J. Kang, A. L. Carter, S. R. Kunkel, K. C. Przeworski, G. A. Chass, *Angew. Chem., Int. Ed.* **2009**, *48*, 6836.

[24] S. Díez-González, S. P. Nolan, *Org. Prep. Proced. Int.* **2007**, *39*, 523.

[25] G. Keglevich, T. Kovács, F. Csatlós, *Heteroat. Chem.* **2015**, *26*, 199.

[26] C. J. O'Brien, Z. S. Nixon, A. J. Holohan, S. R. Kunkel, J. L. Tellez, B. J. Doonan, E. E. Coyle, F. Lavigne, L. J. Kang, K. C. Przeworski, *Chem. - Eur. J.* **2013**, *19*, 15281.

[27] C. J. O'Brien, F. Lavigne, E. E. Coyle, A. J. Holohan, B. J. Doonan, *Chem. - Eur. J.* **2013**, *19*, 5854.

[28] E. E. Coyle, B. J. Doonan, A. J. Holohan, K. A. Walsh, F. Lavigne, E. H. Krenske, C. J. O'Brien, *Angew. Chem., Int. Ed.* **2014**, *53*, 12907.

[29] T. Werner, M. Hoffmann, S. Deshmukh, *Eur. J. Org. Chem.* **2014**, *2014*, 6630.

[30] V. M. Schmiedel, Y. J. Hong, D. Lentz, D. J. Tantillo, M. Christmann, *Angew. Chem., Int. Ed.* **2018**, *57*, 2419.

[31] M.-L. Schirmer, S. Adomeit, T. Werner, *Org. Lett.* **2015**, *17*, 3078.

[32] M.-L. Schirmer, S. Adomeit, A. Spannenberg, T. Werner, *Chem. - Eur. J.* **2016**, *22*, 2458.

[33] A. Grandane, L. Longwitz, C. Roolf, A. Spannenberg, H. Murua Escobar, C. Junghanss, E. Suna, T. Werner, *J. Org. Chem.* **2019**, *84*, 1320.

[34] J. Tönjes, L. Longwitz, T. Werner, *Green Chem.* **2021**, *23*, 4852.

[35] D. Prat, A. Wells, J. Hayler, H. Sneddon, C. R. McElroy, S. Abou-Shehada, P. J. Dunn, *Green Chem.* **2016**, *18*, 288.

[36] L. Longwitz, T. Werner, *Angew. Chem., Int. Ed.* **2020**, *59*, 2760.

[37] C.-J. Lee, T.-H. Chang, J.-K. Yu, G. Madhusudhan Reddy, M.-Y. Hsiao, W. Lin, *Org. Lett.* **2016**, *18*, 3758.

[38] X. Fan, R. Chen, J. Han, Z. He, *Molecules* **2019**, *24*.

[39] Y.-C. Liou, H.-W. Wang, A. Edukondalu, W. Lin, *Org. Lett.* **2021**.

[40] L. Longwitz, S. Jopp, T. Werner, *J. Org. Chem.* **2019**, *84*, 7863.

[41] R. Appel, *Angew. Chem., Int. Ed.* **1975**, *14*, 801.

[42] J. Tönjes, L. Kell, T. Werner, *Org. Lett.* **2023**, *25*, 9114.

[43] a) S.-Y. Han, Y.-A. Kim, *Tetrahedron* **2004**, *60*, 2447; b) E. Valeur, M. Bradley, *Chem. Soc. Rev.* **2009**, *38*, 606.

[44] a) H. Charville, D. Jackson, G. Hodges, A. Whiting, *Chem. Commun.* **2010**, *46*, 1813; b) R. M. Al-Zoubi, O. Marion, D. G. Hall, *Angew. Chem., Int. Ed.* **2008**, *47*, 2876.

[45] Handoko, N. R. Panigrahi, P. S. Arora, *J. Am. Chem. Soc.* **2022**.

[46] J. M. Lipshultz, A. T. Radosevich, *J. Am. Chem. Soc.* **2021**, *143*, 14487.

[47] L. Köring, N. A. Sitte, M. Bursch, S. Grimme, J. Paradies, *Chem. - Eur. J.* **2021**, *27*, 14179.

[48] J. Xue, Y.-S. Zhang, Z. Huan, J.-D. Yang, J.-P. Cheng, *J. Org. Chem.* **2022**, *87*, 15539.

[49] A. Vilsmeier, A. Haack, *Ber. Dtsch. Chem. Ges. A* **1927**, *60*, 119.

[50] M. Gazvoda, M. Kočevar, S. Polanc, *Eur. J. Org. Chem.* **2013**, *2013*, 5381.

[51] A. R. Ravishankara, John S. Daniel, Robert W. Portmann, *Science* **2009**, *326*, 123.

[52] a) K. Severin, *Trends Chem.* **2023**, *5*, 574; b) I. R. Landman, F. Fadaei-Tirani, K. Severin, *Chem. Commun.* **2021**, *57*, 11537.

[53] K. Severin, *Chem. Soc. Rev.* **2015**, *44*, 6375.

[54] Z. Zhuang, B. Guan, J. Chen, C. Zheng, J. Zhou, T. Su, Y. Chen, C. Zhu, X. Hu, S. Zhao et al., *Chem. Eng. J.* **2024**, *486*, 150374.

[55] a) P. Molinillo, B. Lacroix, F. Vattier, N. Rendón, A. Suárez, P. Lara, *Chem. Commun.* **2022**, *58*, 7176; b) R. Deeba, S. Chardon-Noblat, C. Costentin, *ACS Catal.* **2023**, *13*, 8262.

[56] S. Poh, R. Hernandez, M. Inagaki, P. G. Jessop, *Org. Lett.* **1999**, *1*, 583.

[57] E. Otten, R. C. Neu, D. W. Stephan, *J. Am. Chem. Soc.* **2009**, *131*, 9918.

[58] V. Medvarić, J. Paradies, T. Werner, *Adv. Synth. Catal.* **2025**, *367*, e70059.

[59] a) F. T. Edelmann, *Chem. Soc. Rev.* **2012**, *41*, 7657; b) A. A. Aly, S. Bräse, M. A.-M. Gomaa, *Arkivoc* **2019**, *2018*, 85; c) S. Liu, Y. Tang, S. Chen, X. Li, H. Liu, *Angew. Chem., Int. Ed.* **2024**, *63*, e202407952.

[60] Y.-T. Wang, P.-C. Yang, J.-Y. Zhang, J.-F. Sun, *Molecules* **2024**, *29*, 1448.

[61] C. Laye, J. Lusseau, F. Robert, Y. Landais, *Adv. Synth. Catal.* **2021**, *363*, 3035.

[62] V. Dočekal, Y. Niderer, A. Kurčina, I. Císařová, J. Veselý, *Org. Lett.* **2024**, *26*, 6993.

[63] L. Jiao, E. Herdtweck, T. Bach, *J. Am. Chem. Soc.* **2012**, *134*, 14563.

[64] a) H. Kong, K. Li, J. Zhang, H. Yan, L. Jing, Y. Liu, C. Song, P. Zhou, B. Wang, *Adv. Synth. Catal.* **2024**, e202401128; b) M. Bandini, A. Eichholzer, *Angew. Chem., Int. Ed.* **2009**, *48*, 9608.

[65] a) J. A. Leitch, C. L. McMullin, M. F. Mahon, Y. Bhonoah, C. G. Frost, *ACS Catal.* **2017**, *7*, 2616; b) A. Taheri, B. Lai, C. Cheng, Y. Gu, *Green Chem.* **2015**, *17*, 812; c) J. Märsch, S. Reiter, T. Rittner, R. E. Rodriguez-Lugo, M. Whitfield, D. J. Scott, R. J. Kutta, P. Nuernberger, R. de Vivie-Riedle, R. Wolf, *Angew. Chem., Int. Ed.* **2024**, *63*, e202405780; d) T.-Y. Wang, X.-X. Chen, D.-X. Zhu, L. W. Chung, M.-H. Xu, *Angew. Chem., Int. Ed.* **2022**, *61*, e202207008.

[66] J. Tönjes, V. Medvarić, T. Werner, *J. Org. Chem.* **2024**, *89*, 10729.

[67] C. Post, D. Maniar, V. S. D. Voet, R. Folkersma, K. Loos, *ACS Omega* **2023**, *8*, 8991.

[68] M. D. Delost, D. T. Smith, B. J. Anderson, J. T. Njardarson, *J. Med. Chem.* **2018**, *61*, 10996.

[69] K. I. Galkin, V. P. Ananikov, *ChemSusChem* **2019**, *12*, 2976.

[70] a) K.-W. Chen, S. Syu, Y.-J. Jang, W. Lin, *Org. Biomol. Chem.* **2011**, *9*, 2098; b) Y. Wang, Y.-C. Luo, X.-Q. Hu, P.-F. Xu, *Org. Lett.* **2011**, *13*, 5346.

[71] R. Zhou, V. Medvarić, T. Werner, J. Paradies, *J. Am. Chem. Soc.* **2025**, *147*, 37879.

7. Appendix

7.1 Synthesis of amidines via P^{III}/P^{V} redox catalyzed in situ formation of imidoyl chloride from amides

V. Medvarić, J. Paradies, T. Werner, *Adv. Synth. Catal.* **2025**, *367*, e70059.
DOI: 10.1002/adsc.70059

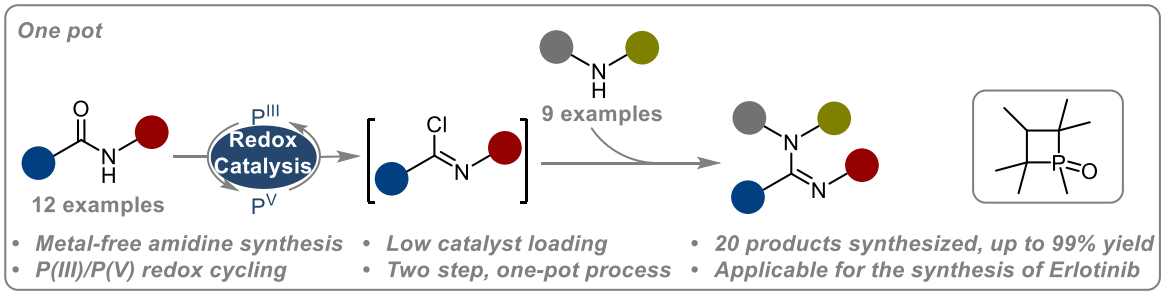

Abstract:

Amidines are a ubiquitous class of bioactive compounds found in a wide variety of natural products; thus, efficient strategies for their preparation are in great demand. Herein we report a novel protocol for the synthesis of amidines based on P^{III}/P^{V} redox catalysis. This two-step, one-pot approach involves the activation of amides via P^{III}/P^{V} catalyzed *in situ* formation of imidoyl chloride intermediates which are directly converted with amines to the corresponding amidines. Instead of traditionally used toxic and corrosive chloride sources, hexachloroacetone was successfully employed as a halide source. The reaction proceeds with low catalyst loading (2 mol%) in BuOAc as the solvent. Under the optimized conditions 20 amidines were prepared in yields up to 99%. A feasible mechanism is proposed based on experimental results. The synthetic potential of this method was evaluated in the preparation of the tyrosine kinase inhibitor (TKI) Erlotinib.

RESEARCH ARTICLE doi.org/10.1002/adsc.70059 ADVANCED SYNTHESIS & CATALYSIS

Synthesis of Amidines Via P(III)/P(V)=O Redox Catalyzed In Situ Formation of Imidoyl Chlorides From Amides

Viktorija Medvarić,[a,b] Jan Paradies,[a] and Thomas Werner[a,b,*]

[a] Department of Chemistry and Center for Sustainable Systems Design (CSSD), Paderborn University, Warburger Str. 100 D-33098 Paderborn, Germany
E-mail: th.werner@uni-paderborn.de
[b] Leibniz Institute for Catalysis at the University of Rostock (LIKAT Rostock), Albert Einstein Str. 29a, D-18059 Rostock, Germany

Manuscript received: April 7, 2025; Revised manuscript received: July 14, 2025;
Version of record online: August 28, 2025

Supporting information for this article is available on the WWW under https://doi.org/10.1002/adsc.70059

Abstract: Amidines are a ubiquitous class of bioactive compounds found in a wide variety of natural products; thus, efficient strategies for their preparation are in great demand. Herein, a novel protocol is reported for the synthesis of amidines based on P^{III}/P^{V}=O redox catalysis. This two-step, one-pot approach involves the activation of amides via P^{III}/P^{V}=O catalyzed in situ formation of imidoyl chloride intermediates which are directly converted upon reaction with amines into the corresponding amidines. Instead of traditionally used toxic and corrosive chloride sources, hexachloroacetone (HCA) is successfully employed as a halide source. The reaction proceeds with low catalyst loading (2 mol%) in BuOAc as the solvent. Under the optimized conditions, 20 amidines are prepared in yields up to 99%. A feasible mechanism is proposed based on experimental results. The synthetic potential of this method is evaluated in the preparation of the tyrosine kinase inhibitor (TKI) Erlotinib.

Keywords: amide activation, amidines, C–N, catalysis, organocatalysis, P^{III}/P^{v}=O, redox cycling

1. Introduction

Amidines are a well-established class of organic compounds and are valued by chemists for their unique chemical and physical properties.[1] Amidines often show high basicity, e.g. 1,8-diazabicyclo[5.4.0] undec-7-ene (DBU) and are frequently employed as a non-nucleophilic bases and organocatalysts in synthetic chemistry.[2] They have also been utilized as ligands in organometallic complexes[3] and as starting material for the synthesis of heterocycles.[4,5] The amidine moiety is recognized as surrogate for peptide bonds[6,7] and has been identified in natural products such as polycyclic alkaloids[8] and polysaccharides.[9,10] This substructure can also be found in various agrochemicals[11] and drug candidates[12] such as Viagra, Abacavir, Clozapine, and Erlotinib (**Scheme 1**).

Several synthetic strategies for the construction of amidine structures are known.[1,4,13] Recent examples include [Ag],[14] [Cu],[15] [Pd],[16] as well as metal-free multicomponent reactions[17] for the synthesis of *N*-Acyl and *N*-tosyl amidines, respectively. Among various precursors amides are especially useful starting materials for the synthesis of amidines due to their readily availability and ease of preparation. The synthesis of *N,N′*-disubstituted or *N,N,N′*-trisubstituted amidines from amides proceeds via an activated secondary amide intermediates and subsequent conversion with an amine (**Scheme 2**A).[7,18] In this approach commonly imidoyl chlorides are used. Their synthesis from amides usually requires toxic and moisture-sensitive dehydrating agents such as PCl_5,[19] $SOCl_2$,[20] and $(COCl)_2$.[21]

In 2017, Phakhodee reported a Ph_3P/I_2mediated process for the one-pot synthesis of amidines from amides

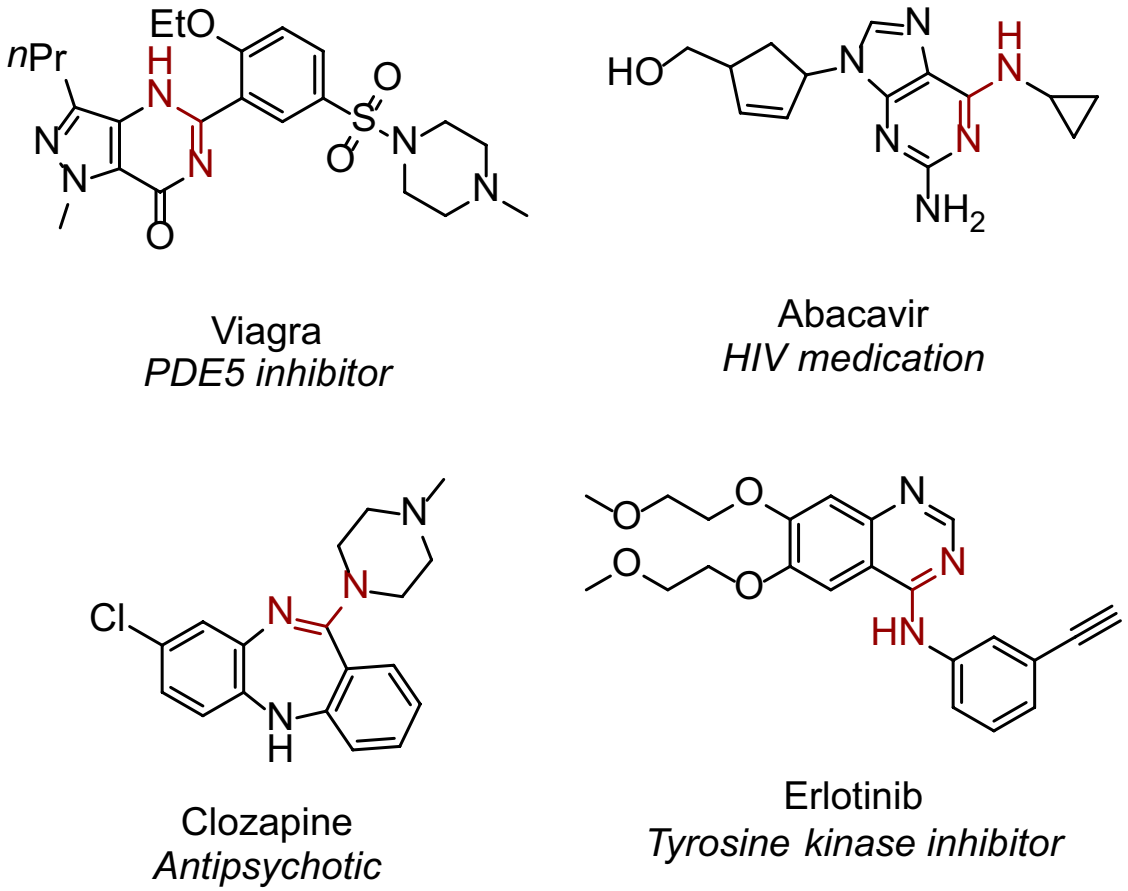

Scheme 1. Pharmaceutical drugs containing amidine moiety.

via the respective imidoyl iodide (Scheme 2B).[22] However this methodology requires the use of stoichiometric quantities of the phosphine, culminating in the stoichiometric generation of phosphine oxide, which hampers the purification process and leads to enlarged waste streams. To the best of our knowledge, there are only two documented methods to catalytically activate amides using phosphorus-based catalysts. In 2021, Paradies and coworkers reported the formation of imidoyl chlorides by a redox-neutral phosphine oxide catalyzed reaction using triphosgene as chloride source.[23] Xue et al. developed a catalytic Vilsmeier-Haack reaction which is based on P^{III}/P^{V}=O redox-catalysis.[24] In this process amides are activated using 4-methyl-1-phenyl-2,3-dihydrophosphole 1-oxide as catalyst and dimethylbromomalonate as bromine ion source. Within the past 10 years a growing number of organopnictogen redox catalytic methods have emerged especially in terms of P^{III}/P^{V}=O redox catalysis.[25] Due to our interest in this field[26–29] and based on our experience in P^{III}/P^{V}=O halogenation reactions,[29,30] we aimed to develop a catalytic one-pot synthesis of *N,N,N′*-trisubstituted amidines from amides (Scheme 2C). Our approach sought to avoid the critical dehydrating agents mentioned above.

2. Results and Discussion

Our study began by optimizing the catalytic reaction step, forming imidoyl chloride **3a**, from *N*-isopropylbenzamide (**1a**) as a model substrate in BuOAc as solvent, using phosphetane oxide **2a** as catalyst and $PhSiH_3$ as terminal reductant (**Table 1**). The initial focus was selecting the most suitable halide source for the formation of imidoyl chloride **3a**. The formation of imidoyl chloride **3a** with ethyl 2,2,2-trichloroacetate (ETCA) resulted in 26% yield, while the use of (trichloromethyl)benzene (TCMB) resulted in 68% yield (Table 1, entry 1 and 2). Notably, in the presence of hexachloroacetone (HCA), a chlorinating agent previously employed by our group as effective reagent for catalytic Appel reactions,[29,30] an excellent yield of >99% for the formation of imidoyl chloride was achieved (entry 3). The formation of imidoyl bromide was also feasible. The use of diethyl 2-bromo-2-methylmalonate (DEMBM) gave the corresponding imidoyl bromide in 28% yield (entry 4). Based on the excellent result achieved with HCA, we evaluated the impact of the solvent and other reaction parameters.[31] Besides BuOAc, toluene proved to be a suitable solvent, yielding the desired product in >99% yield.[31] We focused on performing our further investigations in

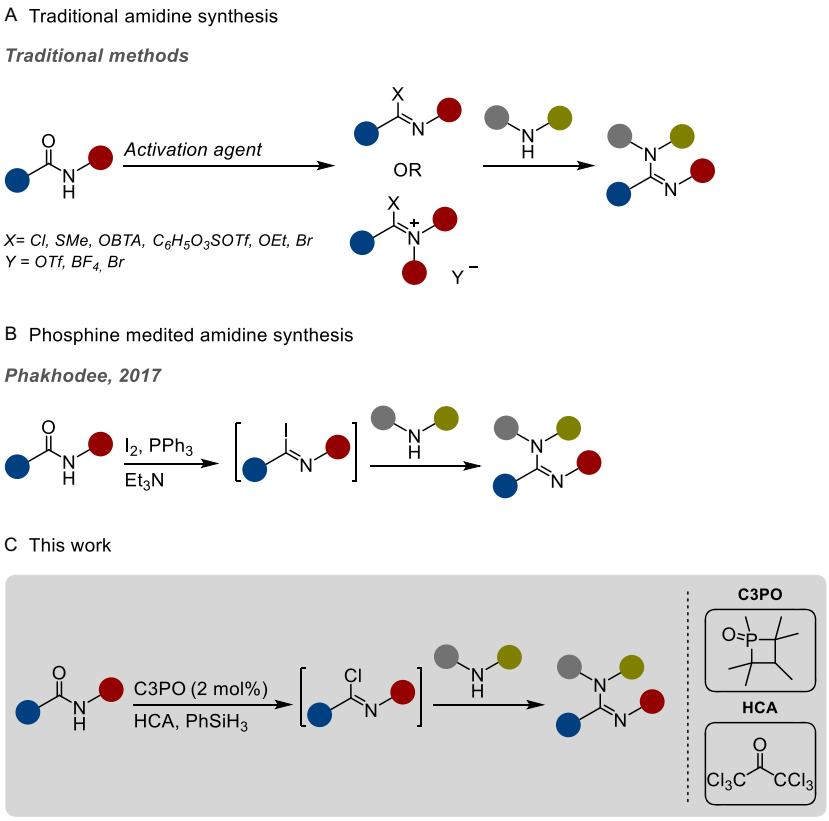

Scheme 2. Synthetic approaches to amidines. A) Traditional amidine synthesis. B) Phosphine medited amidine synthesis. C) This work.

BuOAc since it is more sustainable alternative in comparison to toluene according to the CHEM21 selection guide.[32] Further studies revealed that the reaction can be efficiently performed utilizing 1.5 equivalents of HCA and 1.5 equivalents of the terminal reductant at lower catalyst loading of 2 mol% (entry 5). Under these conditions the desired product **3a** was obtained in >99% yield after 1 h. The four-membered phosphetane catalyst **2a** appears crucial for the efficient formation of imidoyl chloride. Under the optimized conditions other potential catalysts were tested. However, the use of phospholene oxide **2b** as catalyst resulted in a significantly lower yield of 40% (entry 6), while noncyclic catalysts previously used in catalytic P^{III}/P^{V}=O Wittig[33] and Appel[30] reactions, gave even lower yields, <20% (entries 7 and 8). When equimolar amounts of HCA and $PhSiH_3$ were used, **3a** was obtained in 82% (entry 9). At lower reaction temperature of 100 °C the yield decreased to 69% (entry 10).

Subsequently, the second reaction step was optimized by varying the equivalents of added nucleophile and reaction time. After the in situ formation of **3a** under the optimized conditions, 1.5 and 2.5 equivalents of *i*$PrNH_2$ were tested, leading to conversions of 53% and 71%, respectively (**Table 2**, entry 1 and 2) after conducting the reaction for 4 h. Using 3.5 equivalents of *i*$PrNH_2$ resulted in 100% conversion, thus we isolated the product **4a** in an excellent 98% yield (entry 3). Reducing the reaction time of the second step resulted in a lower conversion and 85% of isolated yield (entry 4). Therefore, the optimized conditions for the second reaction step were set to a reaction time of 4 h.

Having established the optimal conditions, we set out to explore the substrate scope of the reaction (**Figure 1**). We started our evaluation by treating **1a** with different amines. The reaction with *i*$PrNH_2$ and benzylamine as nucleophiles gave the corresponding amidines **4a** and **4b** in 98% yield, respectively. Excellent yields were also achieved with aniline derivatives bearing electron-donating or electron-withdrawing groups. The conversion of *p*-ethoxy aniline led to amidine **4c** in 86% yield while the trifluoromethyl derivative **4d** and nitrile-substituted product **4e** were obtained in 98% and 80% yield, respectively. When *N*-ethylaniline was used as a nucleophile, 88% yield of amidine **4f** was achieved. The aliphatic secondary amine, diethylamine, gave **4g** in good yield of 79%, while the cyclic amines piperidine and morpholine performed slightly better, affording **4h** and **4i** in 88% and 81% yield, respectively. When ammonia was employed as a nucleophile the desired product **4j** was not obtained. Further evaluation of the scope was performed by variation of the amide coupling partner. Electron-rich methoxy substituted aryl amide **1k** led

Table 1. Optimization of the P^{III}/P^{V}=O redox catalyzed formation of *N*-isopropylbenzimidoyl chloride (**3a**) from *N*-isopropylbenzamide (**1a**).

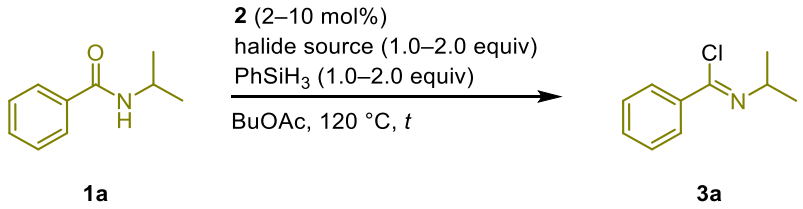

Catalysts:

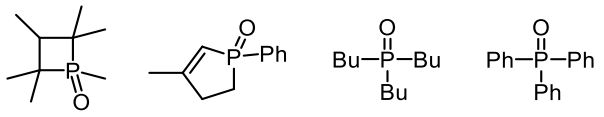

2a **2b** **2c** **2d**

Halide source:

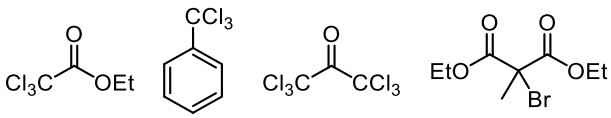

ETCA **TCMB** **HCA** **DEMBM**

Entry	2 [mol%]	Halide source [equiv]	Silane [equiv]	*t* [h]	Yield [%][a]
1	**2a** (10)	ETCA (2.0)	$PhSiH_3$ (2.0)	24	26
2	**2a** (10)	TCMB (2.0)	$PhSiH_3$ (2.0)	24	68
3	**2a** (10)	HCA (2.0)	$PhSiH_3$ (2.0)	24	>99
4	**2a** (10)	DEMBM (2.0)	$PhSiH_3$ (2.0)	24	28[b]
5	**2a** (2)	HCA (1.5)	$PhSiH_3$ (1.5)	1 h	>99
6	**2b** (2)	HCA (1.5)	$PhSiH_3$ (1.5)	1 h	40
7	**2c** (2)	HCA (1.5)	$PhSiH_3$ (1.5)	1 h	19
8	**2d** (2)	HCA (1.5)	$PhSiH_3$ (1.5)	1 h	10
9	**2a** (2)	HCA (1.0)	$PhSiH_3$ (1.0)	1 h	82
10[c]	**2a** (2)	HCA (1.5)	$PhSiH_3$ (1.5)	1 h	69

Reaction conditions: 1.0 equiv **1a** (0.5 mmol), 2–10 mol% catalyst **2**, 1.0–2.0 equiv halide source, 1.0–2.0 equiv $PhSiH_3$, 1.5 mL BuOAc, 120 °C, 1–24 h;
[a] Yields were determined by ^{1}H NMR using mesitylene as an internal standard;
[b] *N*-isopropylbenzimidoyl bromide is the product;
[c] 100 °C.

Table 2. Optimization for the synthesis of amidine **4a** from in situ formed **3a**.

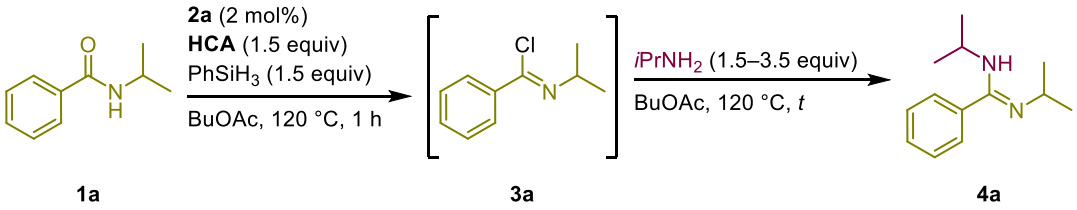

Entry	*i*PrNH$_2$ [equiv]	*t* [h]	Conv. 1a [%][a]	Yield 4a [%][b]
1	1.5	4	53	n.d.
2	2.5	4	71	n.d.
3	3.5	4	100	98
4	3.5	3	96	85

Reaction conditions: 1.0 equiv **1a** (0.5 mmol), 2 mol% catalyst **2a**, 1.5 equiv HCA, 1.5 equiv $PhSiH_3$, 1.5–3.5 equiv *i*PrNH$_2$, 1.5 mL BuOAc, 120 °C;
[a] Conversion was determined by GC with mesitylene as internal standard;[31]
[b] Isolated yield is given.

to **4k** in a good yield of 86%, while aryl amide with an electron-acceptor substituent, such as methoxycarbonyl **1l** and bromo-substituted derivative **1m** produced 64% and 73% of the products **4l** and **4m**, respectively. As shown by Kalz et al.,[34] there are different possible isomeric forms of *N*,*N*′-disubstituted amidines which can

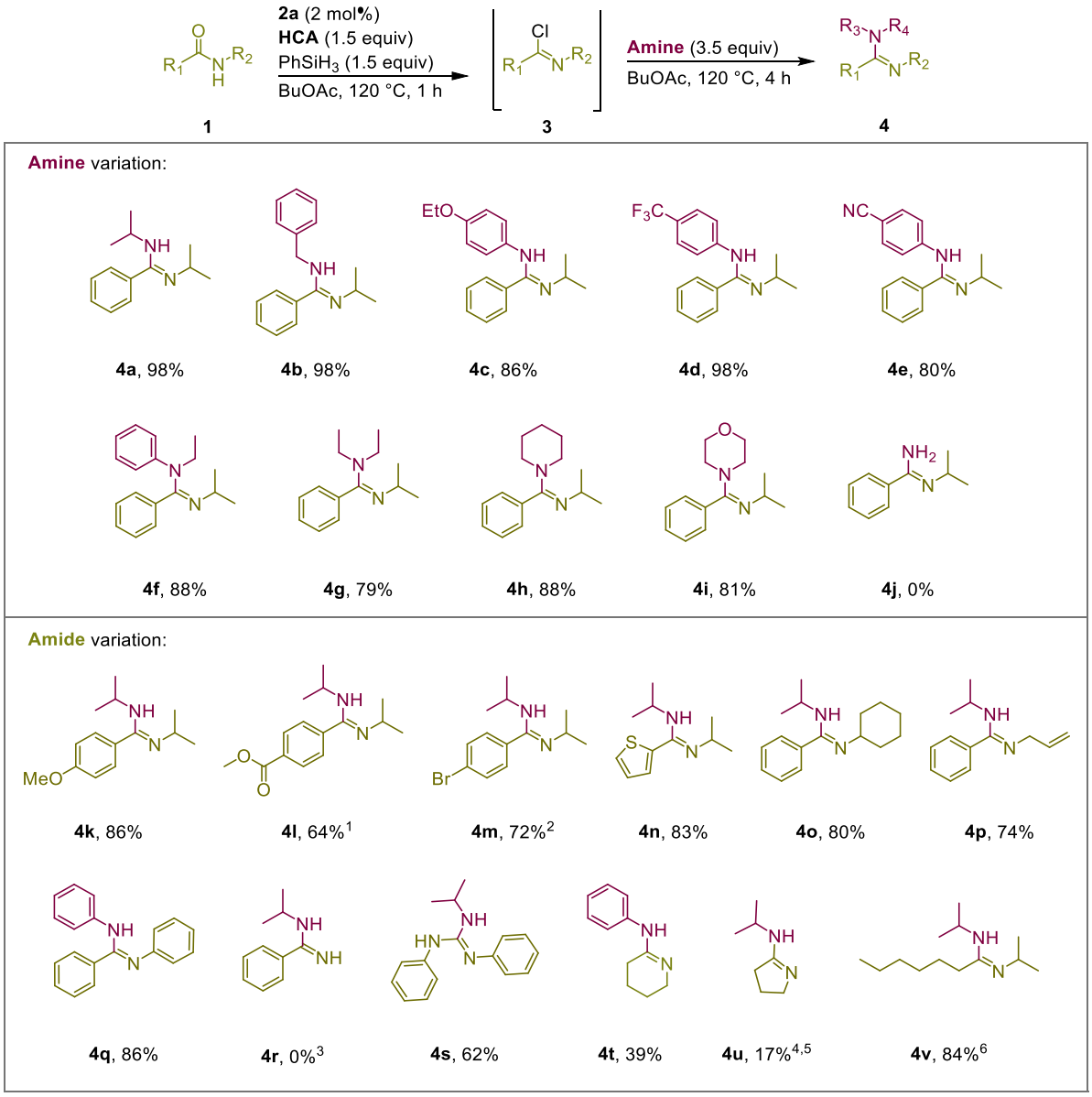

Figure 1. Substrate scope for one-pot two-step synthesis of amidines **4** from amides **1** by P^{III}/P^{V}=O redox catalysis. Reaction conditions: Step 1: 1.0 equiv **1** (0.5 mmol), 2 mol% catalyst **2a**, 1.5 equiv HCA, 1.5 equiv $PhSiH_3$, 1.5 mL BuOAc, 120 °C, 1 h; Step 2: 3.5 equiv amine, 120 °C, 4 h. Isolated yields are given. Mixture of two isomers [1]1:0.24 and [2]1:0.25. [3]Product is reduced to nitrile. [4]1 mmol scale. [5]Yield was determined by ^{1}H NMR analysis of the crude reaction mixture using triethylamine as internal standard. [6]Mesitylene was used as internal standard.

result from C=N isomerization, C–N rotation or tautomerism. In our hands, products **4l** and **4m** were obtained as a mixture of two isomers in a ratio of 1:0.24 and 1:0.25, respectively. Thiophene substituted amide **1n** gave **4n** in a good yield of 83%. The *N*-substituents of the amide were also varied. The conversion of *N*-cyclohexyl benzamide **1o** gave **4o** in 80%, *N*-allyl derivative **1p** gave **4p** in 74%, and *N*-phenyl benzamide (**1q**) led to **4q** in 86% yield. Under the reaction conditions the conversion of **1r** did not lead to the desired product **4r**. Instead, the benzonitrile was observed due to the evolution of hydrogen under catalytic conditions.[35] In addition, diphenylurea (**1s**) was tested as a substrate under the standard reaction conditions, and **4s** was obtained in 62% yield. Furthermore, piperidin-2-one (**1t**) and pyrrolidine-2-one (**1u**) were also suitable substrates even though the desired amidines **4t** and **4u** were obtained in moderate yields of 39% and 17%, respectively. Also, the aliphatic amide **1v**, was successfully converted to the desired amidine **4v** in 84% yield.

The amidine substructure is present in various biologically active compounds, including Erlotinib (**5b**), a TKI

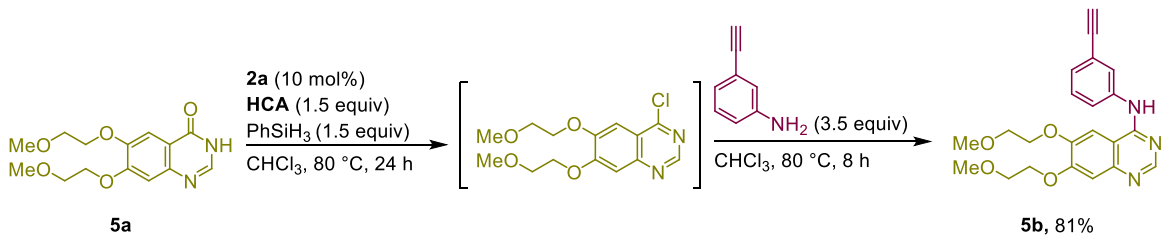

Scheme 3. P^{III}/P^{V}=O redox catalyzed synthesis of Erlotinib (**5b**) from **5a**.

used in the treatment of non-small cell lung cancer and pancreatic cancer.[36] To highlight the synthetic utility of our protocol, we synthesized Erlotinib (**5b**) starting from commercially available 6,7-bis(2-methoxyethoxy) quinazolin-4(3H)-one (**5a**) (**Scheme 3**). Due to the limited solubility of quinazolinone **5a** in the standard solvent (BuOAc), the reaction conditions were slightly modified. Under these adjusted conditions, **5a** was successfully converted using our one-pot, two-step catalytic protocol. Notably, the target compound, Erlotinib (**5b**), was obtained in a high yield of 81%. This methodology eliminates the requirement for toxic and corrosive oxalyl chloride $(COCl)_2$ in the imidoyl chloride formation step and simplifies the process from a two-step sequence to a more efficient one-pot reaction.

Based on our previous studies on P^{III}/P^{V}=O redox catalyzed reactions and control experiments,[27–31,37] we propose the following pathway leading to the formation of amidine **4** from amides **1** and amines (**Scheme 4**). The initial step is the reduction of phosphine oxide **2a** by $PhSiH_3$ to phosphine **6**. As a control experiment, the reduction was performed under the reaction conditions in the absence of HCA. This reaction leads directly to the phosphine **6,** as a mixture of two diastereoisomers (*dr* 22.3:1) with the chemical shift in the ^{31}P NMR for the major isomer at $\delta = 28.9$ ppm. The proposed silanol was not observed. However, ^{1}H—^{29}Si HMBC NMR experiments indicated the formation of 1,3-diphenyldisiloxane as one of the major products with a chemical shift of $\delta = -28.2$ ppm, which is in accordance with the literature.[38] The siloxane might be formed either by the reaction of the silanol with the silane forming hydrogen or by condensation under liberation of water.[27,28,38] The subsequent reaction of **6** with HCA leads to the chlorophosphonium salt **7**. In additional control experiments we could show that starting from **6,** the reaction with HCA leads to the formation of **7**. Moreover, **7** was obtained from **2a** in the presence of HCA and $PhSiH_3$ as a reducing agent. In both cases a specific signal for **7** was observed in the ^{31}P NMR with a chemical shift of $\delta = 116.7$ ppm for the major isomer. In the presence of amide **1a,** the salt **7** reacts to the proposed oxyphosphonium salt intermediate **8,** which further converts to imidoyl chloride **3a** under liberation of the catalyst **2a**. As indicated above, **3a** was observed in >99% yield under the optimized conditions (Table 1, entry 5). The subsequent addition of the amine (iPrNH$_2$) leads to the formation of the desired amidine **4a** in ≥98% yield

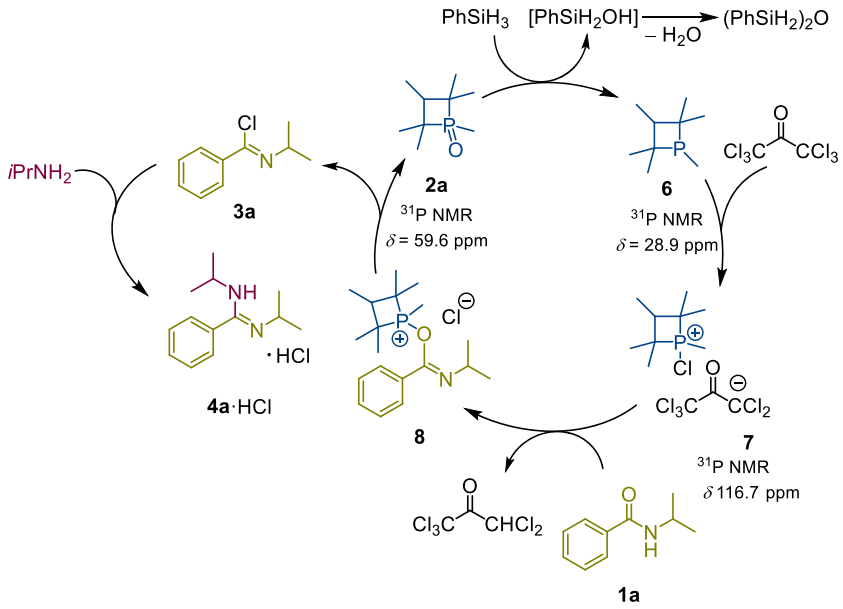

Scheme 4. Proposed mechanistic pathway for the P^{III}/P^{V}=O catalyzed amidine formation.

as the hydrochloride salt in an addition–elimination sequence (Table 2, entry 3).

3. Conclusion

A one-pot protocol for the synthesis of amidines from amides via the construction of C─N bonds using P^{III}/P^{V}═O redox catalysis was developed. Hexachloroacetone is used as a mild chlorinating agent for the in situ formation of imidoyl chlorides. The reaction is performed in BuOAc which is considered a green solvent. Under the optimized conditions 20 amidines from a wide range of amides and amines were prepared in yields up to 99%. The potential of the developed protocol was shown in the synthesis of the potent TKI Erlotinib. Additionally, this method demonstrates potential applicability in the synthesis of guanidines and the derivatization of heterocyclic compounds. Based on previous work and control experiments a feasible mechanism was proposed. Our laboratory is currently investigating the utilization of alternative nucleophiles in place of amines.

4. Experimental Section

Catalyst **2a** was synthesized according to the previously reported literature.[31] Catalysts **2a**, **2c,** and **2d** are commercially available from the following providers: *TCI Chemicals*, *BLD Pharm*, *abcr*, *Merck*. Catalyst **2b** is commercially available from *TCI Chemicals* and *BLD Pharm*.

General Procedure: An oven-dried Schlenk flask equipped with a stir bar was charged with an amide **1** (1.00 equiv) and the catalyst 1,2,2,3,4,4-hexamethylphosphetane 1-oxide (**2a**, 2.00 mol%). The flask was evacuated and flashed with argon three times. BuOAc (0.33 M) and subsequently $PhSiH_3$ (1.50 equiv) and 1,1,1,3,3,3-hexachloropropan-2-one (1.50 equiv) were added. The reaction mixture was heated under argon to 120 °C in an oil bath. After 1 h, amine (3.50 equiv) was added dropwise via syringe if it was liquid. If the amine was a solid, it was transferred into a Schlenk tube, cycled onto a Schlenk line, and dissolved in the lowest possible amount of BuOAc (0.5–1.5 mL), added via syringe to the reaction mixture dropwise, and the heating was continued for 4 h. The reaction was then cooled to room temperature. 3.0 mL of 2 M NaOH and 2.0 mL of Et_2O were added and the reaction mixture was stirred overnight. The reaction mixture was then transferred to a separatory funnel. The organic phase was separated, and the aqueous phase was extracted two times with Et_2O. The combined organic layers were dried over Na_2SO_4. All volatiles were removed, and the crude product was purified by column chromatography.

Acknowledgements

J.P. acknowledges the German Science Foundation (DFG) for financial support (PA1562/18–1).

Open Access funding enabled and organized by Projekt DEAL.

Conflict of Interest

The authors declare no conflict of interest.

Author Contributions

Viktorija Medvarić, ***Jan Paradies***, *and* ***Thomas Werner*** *planned the experiments and the project.* ***Viktorija Medvarić*** *conducted experimental work.* ***Viktorija Medvarić***, ***Jan Paradies***, *and* ***Thomas Werner*** *wrote the manuscript.*

References

[1] R. L. Shriner, F. W. Neumann, *Chem. Rev.* **1944**, *3*, 351.
[2] a) A. C. Savoca, S. Urgaonkar, in *Diazabicyclo[5.4.0]undec-7-ene-Diazabicyclo[5.4.0]undec-7-ene, 1st ed., e-EROS Encycl. Reagents Org. Synth*., John Wiley & Sons, **2006**, pp. 1–8, ISBN: 9780470842898. b) B. Nand, G. Khanna, A. Chaudhary, A. Lumb, J. M. Khurana, *Curr. Org. Chem.* **2015**, *19*, 790.
[3] a) F. T. Edelmann, *Chem. Soc. Rev.* **2012**, *41*, 7657. b) A. Hill, M. Fink, *Advances in Organometallic Chemistry*, 1st ed., Academic Press **2013**, p. 55, ISBN: 9780124078413. c) S.-F. Yuan, Y. Yan, G. A. Solan, Y. Ma, W.-H. Sun, *Coord. Chem. Rev.* **2020**, *411*, 213254.
[4] A. A. Aly, S. Bräse, M. A.-M. Gomaa, *Arkivoc* **2019**, *2018*, 85.
[5] a) W. Guo, M. Zhao, W. Tan, L. Zheng, K. Tao, X. Fan, *Org. Chem. Front.* **2019**, *6*, 2120. b) Y. Zuo, P. Zuo, M. Liu, X. Wang, J. Du, X. Li, P. Zhang, Z. Xu, *Org. Biomol. Chem.* **2024**, *22*, 5014.
[6] S. Kumari, A. V. Carmona, A. K. Tiwari, P. C. Trippier, *J. Med. Chem.* **2020**, *63*, 12290.
[7] E. A. O'Brien, K. K. Sharma, J. Byerly-Duke, L. A. Camacho, B. VanVeller, *J. Am. Chem. Soc.* **2022**, *144*, 22397.
[8] a) S. C. Joergen, C. Christophersen, *J. Am. Chem. Soc.* **1979**, *101*, 4012. b) S. M. Verbitski, C. L. Mayne, R. A. Davis, G. P. Concepcion, C. M. Ireland, *J. Org. Chem.* **2002**, *67*, 7124. c) P. N. Solís, A. G. Ravelo, J. A. Palenzuela, M. R. Gupta, A. González, J. D. Phillipson, *Phytochemistry* **1997**, *44*, 963.
[9] A. Maciejewska, J. Lukasiewicz, T. Niedziela, Z. Szewczuk, C. Lugowski, *Carbohydr. Res.* **2009**, *344*, 894.
[10] S. N. Senchenkova, A. S. Shashkov, Y. A. Knirel, C. Esteve, E. Alcaide, S. Merino, J. M. Tomás, *Carbohydr. Res.* **2009**, *344*, 1009.
[11] M. N. C. Soeiro, K. Werbovetz, D. W. Boykin, W. D. Wilson, M. Z. Wang, A. Hemphill, *Parasitology* **2013**, *140*, 929.
[12] a) S. Liu, Y. Tang, S. Chen, X. Li, H. Liu, *Angew. Chem., Int. Ed. Engl.* **2024**, *63*, e202407952. b) D. Y. Travin, M. Metelev, M. Serebryakova, E. S. Komarova, I. A. Osterman, D. Ghilarov, K. Severinov, *J. Am. Chem. Soc.* **2018**, *140*, 5625. c) M.-J. Wang, Y.-Q. Liu, L.-C. Chang, et al, *J. Med. Chem.* **2014**, *57*, 6008.

d) D. K. Lang, R. Kaur, R. Arora, B. Saini, S. Arora, *Anti-Cancer Agents Med. Chem.* **2020**, *20*, 2150.
[13] a) G. V. Boyd, *Amidines and Imidates*, 1st ed., John Wiley & Sons **1991**, p. 339, ISBN: 9780470772478. b) Z. W. in, *Comprehensive Organic Name Reactions and Reagents*, John Wiley & Sons **2010**, pp. 2237–2240. c) L. M. Fleury, E. E. Wilson, M. Vogt, T. J. Fan, A. G. Oliver, B. L. Ashfeld, *Angew. Chem., Int. Ed., Engl.* **2013**, 52–11589. d) A. Rouzi, R. Hudabaierdi, A. Wusiman, *Tetrahedron* **2018**, *74*, 2475. e) Y. Zheng, J. Mao, J. Chen, G. Rong, D. Liu, H. Yan, Y. Chi, X. Xu, *RSC Adv.* **2015**, *5*, 50113.
[14] B. Liu, Y. Ning, M. Virelli, G. Zanoni, E. A. Anderson, X. Bi, *J. Am. Chem. Soc.* **2019**, *141*, 1593.
[15] K. M. van Vliet, L. H. Polak, M. A. Siegler, J. I. van der Vlugt, C. F. Guerra, B. de Bruin, *J. Am. Chem. Soc.* **2019**, *141*, 15240.
[16] W. Chang, Z. Lei, Y. Yang, S. Dai, J. Feng, J. Yang, Z. Zhang, *Org. Lett.* **2023**, *25*, 1392.
[17] Z. Alassad, A. AboRaed, M. S. Mizrachi, M. H. Pérez-Temprano, A. Milo, *J. Am. Chem. Soc.* **2022**, *144*, 20672.
[18] a) Z.-K. Wan, S. Wacharasindhu, E. Binnun, T. Mansour, *Org. Lett.* **2006**, *8*, 2425. b) K.-J. Xiao, A.-E. Wang, P.-Q. Huang, *Angew. Chem., Int. Ed. Engl.* **2012**, *51*, 8314. c) A. B. Charette, M. Grenon, *Tetrahedron Lett.* **2000**, *41*, 1677. d) A. R. Katritzky, C. Cai, S. K. Singh, *J. Org. Chem.* **2006**, *71*, 3375. e) B. A. Phillips, G. Fodor, J. Gal, F. Letourneau, J. J. Ryan, *Tetrahedron* **1973**, *29*, 3309.
[19] a) N. Ramu, T. M. Krishna, R. Kapavarapu, S. Narsimha, *RSC Adv.* **2024**, *14*, 8921. b) S. Grintsevich, A. Sapegin, E. Reutskaya, S. Peintner, M. Erdélyi, M. Krasavin, *Eur. J. Org. Chem.* **2020**, *2020*, 5664. c) M. Hong, X. Tang, L. Falivene, L. Caporaso, L. Cavallo, E. Y.-X. Chen, *J. Am. Chem. Soc.* **2016**, *138*, 2021. d) I. Semenyuta, O. Golovchenko, O. Bahrieieva, R. Vydzhak, V. Zhirnov, V. Brovarets, *ChemMedChem* **2024**, *19*, e202400205.
[20] a) M. A. Epishina, A. S. Kulikov, N. V. Ignat'ev, M. Schulte, N. N. Makhova, *Mendeleev Commun.* **2015**, *25*, 126. b) Z. Liu, L. Zhou, W. H. Liu, *Chem. Eur. J.* **2023**, *29*, e202301729. c) K. P. Kawahara, W. Matsuoka, H. Ito, K. Itami, *Angew. Chem., Int. Ed. Engl.* **2020**, *59*, 6383.
[21] a) P. J. Manley, M. T. Bilodeau, *Org. Lett.* **2002**, *4*, 3127. b) J.-P. Lin, F.-H. Zhang, Y.-Q. Long, *Org. Lett.* **2014**, *16*, 2822. c) M. Gazvoda, M. Kočevar, S. Polanc, *Eur. J. Org. Chem.* **2013**, *2013*, 5381. d) W. S. Ham, H. Choi, J. Zhang, D. Kim, S. Chang, *J. Am. Chem. Soc.* **2022**, *144*, 2885. e) L.-H. Li, X.-T. Gu, M. Shi, Y. Wei, *Chem. Sci.* **2022**, *13*, 12851.
[22] a) W. Phakhodee, S. Wangngae, N. Wiriya, M. Pattarawarapan, *Tetrahedron Lett.* **2016**, *57*, 5351. b) W. Phakhodee, S. Wangngae, M. Pattarawarapan, *J. Org. Chem.* **2017**, *82*, 8058.
[23] L. Köring, N. A. Sitte, M. Bursch, S. Grimme, J. Paradies, *Chem. Eur. J.* **2021**, *27*, 14179.
[24] J. Xue, Y.-S. Zhang, Z. Huan, J.-D. Yang, J.-P. Cheng, *J. Org. Chem.* **2022**, *87*, 15539.
[25] a) J. M. Lipshultz, G. Li, A. T. Radosevich, *J. Am. Chem. Soc.* **2021**, *143*, 1699. b) Z. Lao, P. H. Toy, *Beilstein J. Org. Chem.* **2016**, *12*, 2577. c) M. Pei, A. Tian, Q. Yang, N. Huang, L. Wang, D. Li, *Green Synth. Catal.* **2023**, *4*, 135. d) L. Longwitz, T. Werner, *Pure Appl. Chem.* **2019**, *91*, 95.
[26] a) L. Longwitz, A. Spannenberg, T. Werner, *ACS Catal.* **2019**, *9*, 9237. b) J. Tönjes, V. Medvarić, T. Werner, *J. Org. Chem.* **2024**, *89*, 10729.
[27] L. Longwitz, T. Werner, *Angew. Chem., Int. Ed. Engl.* **2020**, *59*, 2760.
[28] J. Tönjes, L. Longwitz, T. Werner, *Green Chem.* **2021**, *23*, 4852.
[29] J. Tönjes, L. Kell, T. Werner, *Org. Lett.* **2023**, *25*, 9114.
[30] L. Longwitz, S. Jopp, T. Werner, *J. Org. Chem.* **2019**, *84*, 7863.
[31] See supporting information.
[32] D. Prat, A. Wells, J. Hayler, H. Sneddon, C. R. McElroy, S. Abou-Shehada, P. J. Dunn, *Green Chem.* **2016**, *18*, 288.
[33] a) M.-L. Schirmer, S. Adomeit, T. Werner, *Org. Lett.* **2015**, *17*, 3078. b) T. Werner, M. Hoffmann, S. Deshmukh, *Eur. J. Org. Chem.* **2014**, *2014*, 6873. c) M. Hoffmann, S. Deshmukh, T. Werner, *Eur. J. Org. Chem.* **2015**, *2015*, 4532.
[34] K. F. Kalz, A. Hausmann, S. Dechert, S. Meyer, M. John, F. Meyer, *Chemistry* **2016**, *22*, 18190.
[35] S. Zhou, K. Junge, D. Addis, S. Das, M. Beller, *Org. Lett.* **2009**, *11*, 2461.
[36] Y.-T. Wang, P.-C. Yang, J.-Y. Zhang, J.-F. Sun, *Molecules* **2024**, *29*, 1448.
[37] R. Appel, *Angew. Chem., Int. Ed.* **1975**, *14*, 801.
[38] C. Laye, J. Lusseau, F. Robert, Y. Landais, *Adv. Synth. Catal.* **2021**, *363*, 3035.

7.2 P^{III}/P^{V}=O redox catalyzed direct amide-to-ketimine transformation via Friedel–Crafts-type C–C bond formation

V. Medvarić, N. Mergard, T. Werner, *submitted manuscript*.

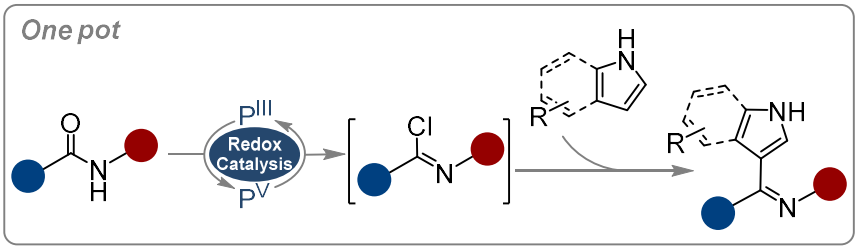

Abstract:

A direct and efficient transformation of common secondary amides into aromatic ketimines via C–C bond formation is reported. The process relies on in situ activation of secondary amides through P^{III}/P^{V}=O redox catalysis to generate reactive imidoyl chloride intermediates. Utilizing hexachloroacetone as a chlorinating agent and only 2 mol% of the phosphorus catalyst, subsequent addition of indole and pyrrole derivatives affords selective C3-functionalization products. This one-pot, two-step protocol provides access to a broad range of C3-ketimines from diverse secondary amides and heteroarenes, delivering up to 94% yield across 20 newly synthesized compounds. The transformation represents a formal Friedel–Crafts-type reaction employing secondary amides as electrophilic partners, expanding the synthetic utility of P^{III}/P^{V}=O redox catalysis and amide activation in heteroarene functionalization.

P^{III}/P^{V}=O redox catalyzed direct amide-to-ketimine transformation via Friedel–Crafts-type C–C bond formation

Viktorija Medvarić [a], Niklas Mergard[a], Thomas Werner*[a,b]

[a] V. Medvarić, N. Mergard, Prof. T. Werner
Department of Chemistry and Center for Sustainable Systems Design (CSSD)
Paderborn University
Warburger Str. 100, D-33098 Paderborn, Germany
E-mail: vmedvaric@mail.uni-paderborn.de, niklas.mergard@uni-paderborn.de, th.werner@uni-paderborn.de

[b] Prof. T. Werner
Leibniz Institute for Catalysis at the University of Rostock (LIKAT Rostock)
Albert Einstein Str. 29a, D-18059 Rostock, Germany

Supporting information for this article is given via a link at the end of the document.

Abstract: A direct and efficient transformation of common secondary amides into aromatic ketimines via C–C bond formation is reported. The process relies on in situ activation of secondary amides through P^{III}/P^{V}=O redox catalysis to generate reactive imidoyl chloride intermediates. Utilizing hexachloroacetone as a chlorinating agent and only 2 mol% of the phosphorus catalyst, subsequent addition of indole and pyrrole derivatives affords selective C3-functionalization products. This one-pot, two-step protocol provides access to a broad range of C3-ketimines from diverse secondary amides and heteroarenes, delivering up to 94% yield across 20 newly synthesized compounds. The transformation represents a formal Friedel–Crafts-type reaction employing secondary amides as electrophilic partners, expanding the synthetic utility of P^{III}/P^{V}=O redox catalysis and amide activation in heteroarene functionalization.

Introduction

Pyrrole and indole are fundamental heterocyclic building blocks found in a vast array of natural products and pharmaceuticals, with significant biological activity.[1–11] Significant efforts have been devoted to the development of efficient synthetic protocols for the preparation and direct functionalization of these compounds.[12] Among other electrophilic aromatic substitution reactions, Friedel–Crafts acylation is one of the most widely used techniques.[13,14] Despite its historical importance, traditional Friedel–Crafts reaction is hindered by several limitations, such as the need for strong Lewis acid catalysts and challenges associated with selective functionalization.[12,15] Although extensive efforts have been made, a strong demand for methodologies beyond Friedel–Crafts acylation as well as the use of readily available and bench stable starting materials still remains.[13,16–21] With regard to the latter, the use of readily available secondary amides is of particular interest. Based on previous work on the activation of amides with triflic anhydride (Tf_2O),[22–25] Huang and coworkers reported the Tf_2O-mediated coupling of arenes with secondary amides (Figure 1A).[26] Notably, depending on the work-up, aromatic ketimines or ketones were accessible. The direct synthesis of ketimines is of particular interest since imines are valuable synthetic intermediates typically formed through the dehydration condensation of corresponding carbonyl compounds and amines.[27,28] While aldimines can often be synthesized under simple reflux conditions without the need for additives, the preparation of ketimines from less reactive substrates generally requires the use of acid catalysts.[29–31] Examples on the direct synthesis of ketimines from pyrrols and indols which are not based on condensation are rare. Tobisu reported Lewis acid promoted insertion of isocyanides into aromatic C−H bonds leading to aromatic imines (Figure 1B).[32] In this process stochiometric amounts of $AlCl_3$ are required. Following this, Giles et al. described the synthesis of imine functionalized indoles.[33] The imine moiety was generated with *N*-alkylnitrilium tetrafluoroborate to afford iminium salts which was subsequently converted to the imine under basic conditions.

P^{III}/P^{V} redox catalysis has emerged as a powerful tool for the activation of various substrates in organic synthesis.[34,35] In regard to amide activation and electrophilic aromatic substation Xue developed P^{III}/P^{V} redox catalyzed method for acylation of indole (Figure 1C).[36] This method facilitates the *in situ* generation of the Vilsmeier–Haack intermediate, which subsequently undergoes reaction with indole to yield the acylated product. Activation of various substrates through P^{III}/P^{V} redox catalysis has emerged as a prominent area of research. Our

group demonstrated the activation of alcohols via the phosphorus redox catalysis, enabling their transformation into alkyl chlorides.[37,38] Mecinović used the P^{III}/P^{V} redox catalysis for the activation of carboxylic acids and their subsequent coupling with amines to form amides.[39] This approach was later refined by Radosevich, further expanding the scope and utility of P^{III}/P^{V} catalyzed transformations.[40,41] In contrast, the activation of amides via phosphine catalysis remains relatively underexplored, representing a critical gap that forms the focus of our current research.[36,40,41] Recently, we reported the activation of amides for the synthesis of amidines via P^{III}/P^{V} redox catalysis.[42] Based on this work, we envisioned that the direct synthesis of ketimine functionalized, valuable building blocks from indols and pyrrols should be feasible. Herein we report the selective C-3 functionalization of indoles and pyrroles via P^{III}/P^{V}=O redox catalysis utilizing readily available amides as substrates (Figure 1D).

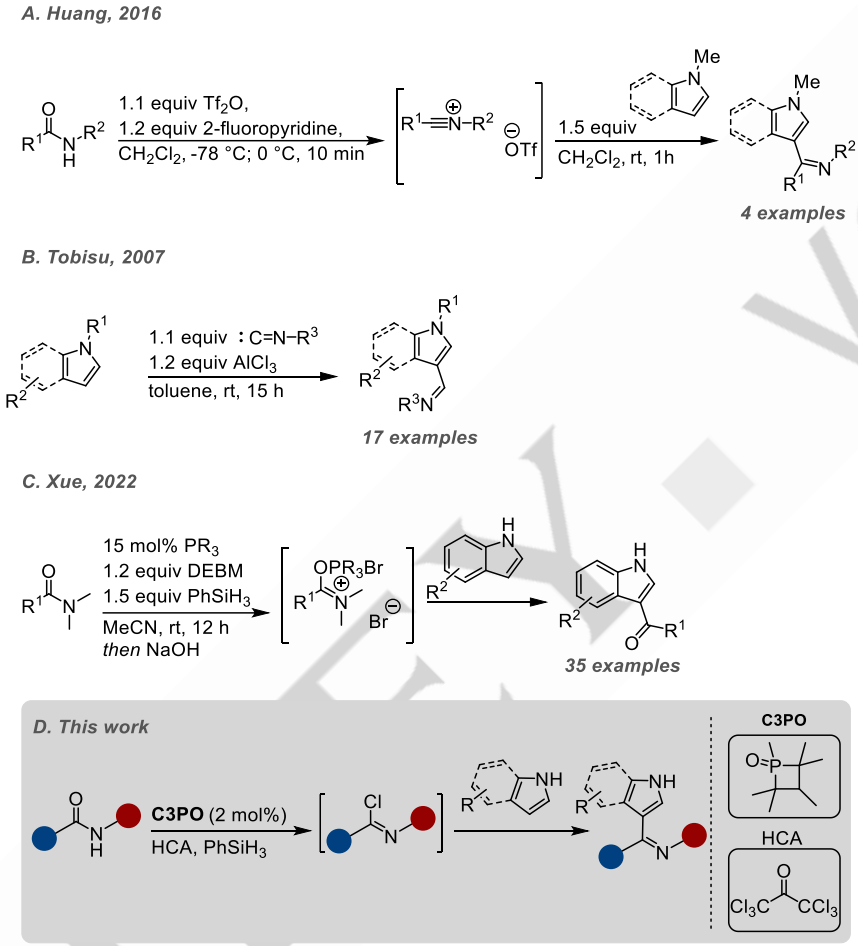

Figure 1. Examples for the functionalization of pyrrole and indole derivatives.

Results and Discussion

The first step of this one-pot synthesis is the *in situ* formation of imidoyl chlorides from amides via P^{III}/P^{V} redox catalysis.[42] For the in situ reduction of phosphine oxide, $PhSiH_3$ proved to be the most effective reagent. The optimized conditions for the first step comprised 1.5 equivalents hexachloroacetone (HCA) and $PhSiH_3$, 2 mol% catalyst **C3PO** and BuOAc as green solvent.[42] Under these conditions the imidoyl chloride intermediate **2a** is obtained in >99% yield after 1 h. Initially, we optimized the reaction conditions for the electrophilic substitution of pyrrol (**3a**) with isopropylbenzamide (**1a**) by varying the amount of **3a** and the reaction time (Table 1). After the *in situ* formation of **2a**, 2.5 equivalents of **3a** were added. After 4 h at 120 °C **4aa** was obtained in 70% yield (Table 1, entry 1). When 3.5 equivalents were used, **4aa** was formed in 86% yield (Table 1, entry 2). A further increase in the amount of **3a** to 4.5 equivalents resulted in a slight decrease of the yield and **4aa** was obtained in 81% (Table 1, entry 3). Conducting the reaction with 3.5 equivalents of **3a** for 1 h gave also a lower yield of 64% (Table 1, entry 4). Prolonging the reaction time to 23 h led to 82% yield (Table 1, entry 5). Lower reaction temperature of 100 °C was also tested, giving **4aa** in 53% yield (Table 1, entry 6).

Table 1. Optimization of reaction conditions for the second step for the synthesis of **4aa** from *N*-isopropylbenzamide (**1a**) and pyrrole (**3a**).

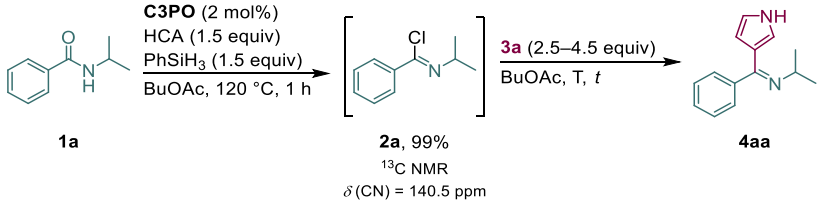

entry	3a / equiv	*t* / h	T / °C	yield / %[1]
1	2.5	4	120	70
2	3.5	4	120	86
3	4.5	4	120	81
4	3.5	1	120	64
5	3.5	23	120	82
6	3.5	4	100	53

Reaction conditions: Step 1: 1.0 equiv **1a** (0.5 mmol), 2 mol% catalyst **C3PO**, 1.5 equiv HCA, 1.5 equiv $PhSiH_3$, 1.5 mL BuOAc, 120 °C. Step 2: 2.5–4.5 equiv pyrrole **3a**, 100–120 °C, 1–23 h. [1]Yield was determined by ^1H NMR analysis of the reaction mixture after extraction using mesitylene as an internal standard.

With optimal conditions in hand, we explored the substrate scope of the reaction (Table 2), commencing with testing differently substituted pyrroles **3a-f** as nucleophiles in a reaction with **1a**. Using pyrrole **3a** as a nucleophile, we were able to isolate the product **4aa** in 62% yield, while more electron rich 2-methylpyrrole (**3b**) gave the product **4ab** in high 77% yield. More reactive 2,4-dimethylpyrrole (**3c**) resulted in high 82% yield of the product **4ac**. The conversion of *N*-methylfuran pyrrole derivative **3d** gave **4ad** as a mixture of *E*/*Z* isomers (1:1.7) in a total yield of 72%. The reaction with pyrrolopyridine **3e** gave amidine **4ae** in 55% yield. It is not unusual to form amidines under these conditions, as reported before.[42] Notably, pyrrolopyrimidine **3f** derivative resulted in product **4af** in 34% yield. When indazole **3g** was used as a nucleophile, 36% of the product **4ag** was obtained. We turned our attention to the functionalization of indole derivatives as nucleophiles. Using indole **3h** as the nucleophile resulted in the formation of **4ah** in 70% yield as a mixture of *E*/*Z* isomers (3.5:1), while more electron rich 4-methyl indole **3i** gave the corresponding **4ai** in excellent 94%. Iodo-indole derivative **3j** gave 53% yield of the product **4aj** in 5.7:1 *E*/*Z* ratio, while 6-trifluoro indole **3k** resulted with the product **4ak** in 61% yield. The conversion of 5-oxaborolan substituted indole **3l** led to 62% yield of **4al** as a hydrochloride salt, while the 2-*p*-fluorophenyl derivative **3m** gave the product **4am** in 91%. In addition, we tested the electron-rich azulene derivative **3n**, which to our surprise resulted in a good 55% yield of product **4an**.

Table 2. Substrate scope for the variation of nucleophiles **3a-3n** in the one-pot two-step reaction for the formation of **4aa-4an** from amide **1a** by P^{III}/P^{V}=O redox catalysis.

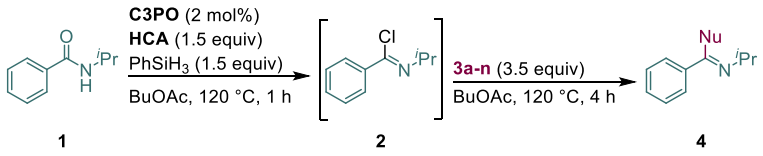

Variation of nucleophile

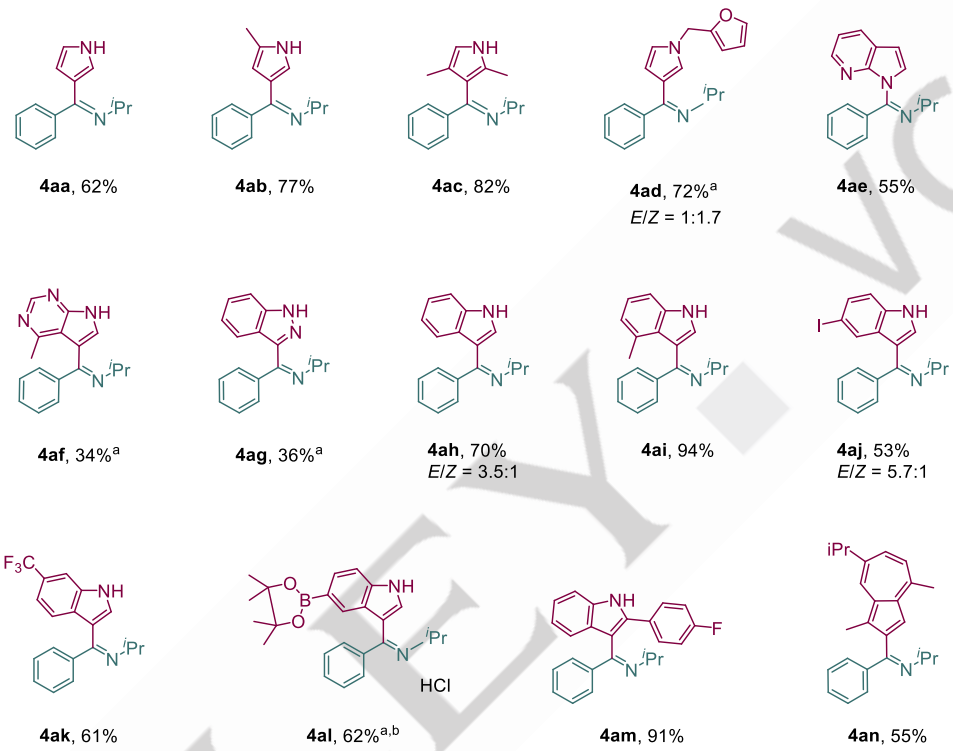

4aa, 62%

4ab, 77%

4ac, 82%

4ad, 72%[a]
E/*Z* = 1:1.7

4ae, 55%

4af, 34%[a]

4ag, 36%[a]

4ah, 70%
E/*Z* = 3.5:1

4ai, 94%

4aj, 53%
E/*Z* = 5.7:1

4ak, 61%

4al, 62%[a,b]

4am, 91%

4an, 55%

Reaction conditions: Step 1: 1.0 equiv **1a** (0.5 mmol), 2mol% catalyst **C3PO**, 1.5 equiv HCA, 1.5 equiv $PhSiH_3$, 1.5 mL BuOAc, 120 °C, 1h; Step 2: 3.5 equiv nucleophile, 120 °C, 4 h. Isolated yields are given. [a]Step 2 was prolonged to overnight heating. [b]Product was isolated as a HCl salt.

Aditionally, further evaluation of the substrate scope was performed by variation of the amide coupling partner **1b-1i** with **3i** as the nucleophile (Table 3). Electron-rich methoxy substituted aryl amide **1b** led to **4bi** in 74% yield. Bromo-substituted derivative **1c** gave **4ci** in 57% yield. Benzyl substituted amide **1d** was converted to the product **4di** in 55% yield, while the thiophene substituted amide **1e** gave the corresponding product **4ei** in 85% yield. Aliphatic heptanamide **1f** led to 55% yield of the product **4fi**. The *N*-substituents of the amide were also varied, and *N*-phenylheptanamide (**1g**) led to **4gi** in 22% yield, while aromatic *N*-phenylbenzamide (**1h**) afforded the product **4hi** in 61% yield. Furthermore, we tested lactam **1i** as a substrate. Unfortunately the formation of the desired product **4ii** was not observed.

Table 3. Substrate scope for the variation of amide **1** in a one-pot two-step reaction for the formation of **4** by P^{III}/P^{V}=O redox catalysis.

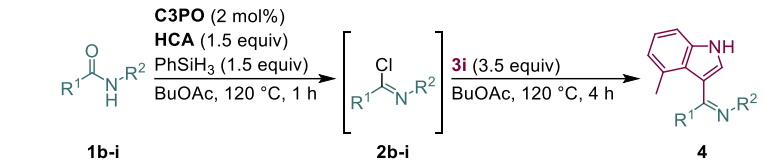

Variation of amide

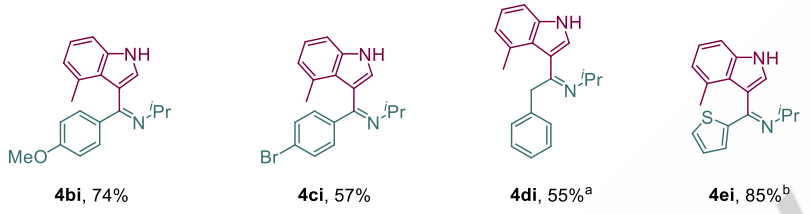

4bi, 74% **4ci**, 57% **4di**, 55%[a] **4ei**, 85%[b]

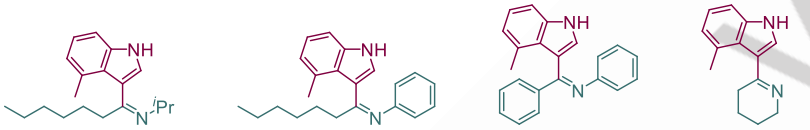

4fi, 55%[a] **4gi**, 22%[a] **4hi**, 61% **4ii**, 0%

Reaction conditions: Step 1: 1.0 equiv **1** (0.5 mmol), 2 mol% catalyst **C3PO**, 1.5 equiv HCA, 1.5 equiv $PhSiH_3$, 1.5 mL BuOAc, 120 °C, 1h; Step 2: 3.5 equiv nucleophile, 120 °C, 4 h. Isolated yields are given. [a]Yields were determined by ^{1}H NMR using mesitylene as an internal standard. [b]Step 2 was prolonged to overnight heating.

Based on our previous studies on P^{III}/P^{V}=O redox catalyzed reactions we propose the mechanism shown in Figure 4.[37,38,42] Initially, the phosphine oxide **C3PO** is reduced by $PhSiH_3$ to **C3P**, accompanied with the formation of 1,3-diphenyl-disiloxane. Phosphine **C3P** further reacts with hexachloroacetone to form a chlorophosphonium salt **5**. In the presence of amide **1a** the salt **5** reacts to the proposed oxophosphonium salt intermediate **6** which further converts to imidoyl chloride **2a** under liberation of the catalyst **C3PO** completing the catalytic cycle. The subsequent addition of **3a** leads to the formation of the desired product **4aa**.

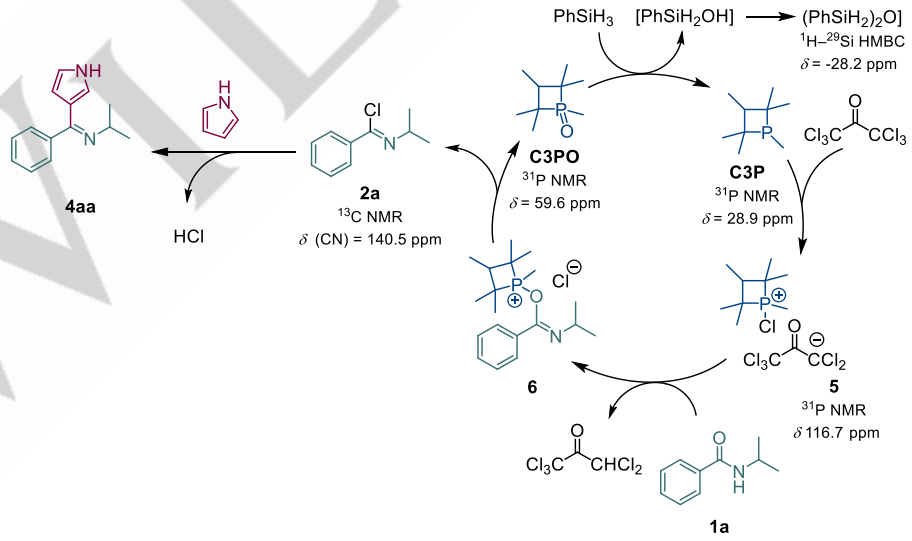

Figure 4. Proposed mechanistic pathway for the electrophilic aromatic substitution via P^{III}/P^{V}=O catalyzed *in situ* imidoyl chloride formation.

Conclusion

In conclusion, a concise and efficient two-step, one-pot protocol has been developed for the electrophilic aromatic substitution of indoles, pyrroles, and their derivatives using secondary amides as electrophilic partners. The reaction proceeds via in situ formation of imidoyl chlorides through P^{III}/P^{V} redox catalysis, with hexachloroacetone serving as a mild and effective chlorinating agent. This strategy enables direct C–C bond formation under mild conditions, affording aromatic ketimines as valuable synthetic intermediates. Systematic evaluation of substrate scope demonstrated the broad applicability of the method: 13 nucleophiles (pyrroles and indoles) and 7 electrophiles (amides) were successfully coupled to furnish 20 novel ketimine products in yields of up to 94%. The proposed reaction mechanism, consistent with established amide activation pathways, provides further insight into P^{III}/P^{V}-catalyzed transformations. Overall, this work expands the synthetic utility of secondary amides as electrophiles in Friedel–Crafts-type reactions and highlights the versatility of phosphorus redox catalysis in C–C bond formation.

Keywords: organocatalysis • phosphorus redox catalysis • C–C bond formation • amide activation • functionalization

References

[1] S.-F. Duan, L. Song, H.-Y. Guo, H. Deng, X. Huang, Q.-K. Shen, Z.-S. Quan, X.-M. Yin, "Research status of indole-modified natural products", *RSC Med. Chem.* **2023**, 14, 2535.
[2] C. Zheng, S.-L. You, "Catalytic asymmetric dearomatization (CADA) reaction-enabled total synthesis of indole-based natural products", *Nat. Prod. Rep.* **2019**, 36, 1589.
[3] N. K. Kaushik, N. Kaushik, P. Attri, N. Kumar, C. H. Kim, A. K. Verma, E. H. Choi, "Biomedical importance of indoles", *Molecules* **2013**, 18, 6620.
[4] S. M. Umer, M. Solangi, K. M. Khan, R. S. Z. Saleem, "Indole-Containing Natural Products 2019-2022: Isolations, Reappraisals, Syntheses, and Biological Activities", *Molecules* **2022**, 27, 7586.
[5] E. Vitaku, D. T. Smith, J. T. Njardarson, "Analysis of the structural diversity, substitution patterns, and frequency of nitrogen heterocycles among U.S. FDA approved pharmaceuticals", *J. Med. Chem.* **2014**, 57, 10257.
[6] B. H. Ganesh, A. G. Raj, B. Aruchamy, P. Nanjan, C. Drago, P. Ramani, "Pyrrole: A Decisive Scaffold for the Development of Therapeutic Agents and Structure-Activity Relationship", *ChemMedChem* **2024**, 19, e202300447.
[7] L. Long, H. Zhang, Z. Zhou, L. Duan, D. Fan, R. Wang, S. Xu, D. Qiao, W. Zhu, "Pyrrole-containing hybrids as potential anticancer agents: An insight into current developments and structure-activity relationships", *Eur. J. Med. Chem.* **2024**, 273, 116470.
[8] B. S. Manya, M. R. P. Kumar, K. Rajagopal, M. A. Hassan, S. O. Rab, M. A. Alshehri, T. B. Emran, "Insights into the Biological Activities and Substituent Effects of Pyrrole Derivatives: The Chemistry-Biology Connection", *Chem. Biodiversity* **2024**, 21, e202400534.
[9] T. V. Sravanthi, S. L. Manju, "Indoles - A promising scaffold for drug development", *Eur. J. Pharm. Sci.* **2016**, 91, 1.
[10] A. Kumari, R. K. Singh, "Medicinal chemistry of indole derivatives: Current to future therapeutic prospectives", *Bioorg. Chem.* **2019**, 89, 103021.
[11] W. Yan, S. S. Zhao, Y. H. Ye, Y. Y. Zhang, Y. Zhang, J. Y. Xu, S. M. Yin, R. X. Tan, "Generation of Indoles with Agrochemical Significance through Biotransformation by Chaetomium globosum", *J. Nat. Prod.* **2019**, 82, 2132.
[12] M. Bandini, A. Eichholzer, "Catalytic functionalization of indoles in a new dimension", *Angew. Chem., Int. Ed.* **2009**, 48, 9608.
[13] V. Dočekal, Y. Niderer, A. Kurčina, I. Císařová, J. Veselý, "Regio- and Enantioselective N-Heterocyclic Carbene-Catalyzed Annulation of Aminoindoles Initiated by Friedel-Crafts Alkylation", *Org. Lett.* **2024**, 26, 6993.
[14] L. Jiao, E. Herdtweck, T. Bach, "Pd(II)-catalyzed regioselective 2-alkylation of indoles via a norbornene-mediated C-H activation: mechanism and applications", *J. Am. Chem. Soc.* **2012**, 134, 14563.
[15] H. Kong, K. Li, J. Zhang, H. Yan, L. Jing, Y. Liu, C. Song, P. Zhou, B. Wang, "Trifluoroacetic Acid Promotes Umpolung of 2-Methylindole to Achieve C(sp3)−H Activation", *Adv. Synth. Catal.* **2024**, e202401128.

[16] J. A. Leitch, C. L. McMullin, M. F. Mahon, Y. Bhonoah, C. G. Frost, "Remote C6-Selective Ruthenium-Catalyzed C–H Alkylation of Indole Derivatives via σ-Activation", *ACS Catal.* **2017**, 7, 2616.
[17] J. Kim, S. H. Hong, "Dual Activation of Nucleophiles and Electrophiles by N-Heterocyclic Carbene Organocatalysis: Chemoselective N-Imination of Indoles with Isocyanides", *Org. Lett.* **2017**, 19, 3259.
[18] J. Märsch, S. Reiter, T. Rittner, R. E. Rodriguez-Lugo, M. Whitfield, D. J. Scott, R. J. Kutta, P. Nuernberger, R. de Vivie-Riedle, R. Wolf, "Cobalt-Mediated Photochemical C-H Arylation of Pyrroles", *Angew. Chem., Int. Ed.* **2024**, 63, e202405780.
[19] J.-C. Wu, R.-J. Song, Z.-Q. Wang, X.-C. Huang, Y.-X. Xie, J.-H. Li, "Copper-catalyzed C-H oxidation/cross-coupling of α-amino carbonyl compounds", *Angew. Chem., Int. Ed.* **2012**, 51, 3453.
[20] A. Taheri, B. Lai, C. Cheng, Y. Gu, "Brønsted acid ionic liquid-catalyzed reductive Friedel–Crafts alkylation of indoles and cyclic ketones without using an external reductant", *Green Chem.* **2015**, 17, 812.
[21] T.-Y. Wang, X.-X. Chen, D.-X. Zhu, L. W. Chung, M.-H. Xu, "Rhodium(I) Carbene-Promoted Enantioselective C-H Functionalization of Simple Unprotected Indoles, Pyrroles and Heteroanalogues: New Mechanistic Insights", *Angew. Chem., Int. Ed.* **2022**, 61, e202207008.
[22] S. Régnier, W. S. Bechara, A. B. Charette, "Synthesis of 3-Aminoimidazo1,2-apyridines from α-Aminopyridinyl Amides", *J. Org. Chem.* **2016**, 81, 10348.
[23] K. L. White, M. Mewald, M. Movassaghi, "Direct Observation of Intermediates Involved in the Interruption of the Bischler-Napieralski Reaction", *J. Org. Chem.* **2015**, 80, 7403.
[24] W. S. Bechara, G. Pelletier, A. B. Charette, "Chemoselective synthesis of ketones and ketimines by addition of organometallic reagents to secondary amides", *Nat. Chem.* **2012**, 4, 228.
[25] A. Romanens, G. Bélanger, "Preparation of conformationally restricted β(2,2)- and β(2,2,3)-amino esters and derivatives containing an all-carbon quaternary center", *Org. Lett.* **2015**, 17, 322.
[26] P.-Q. Huang, Y.-H. Huang, K.-J. Xiao, "Metal-Free Intermolecular Coupling of Arenes with Secondary Amides: Chemoselective Synthesis of Aromatic Ketimines and Ketones, and N-Deacylation of Secondary Amides", *J. Org. Chem.* **2016**, 81, 9020.
[27] R. W. Layer, "The Chemistry of Imines.", *Chem. Rev.* **1963**, 63, 489.
[28] R. D. Patil, S. Adimurthy, "Catalytic Methods for Imine Synthesis", *Asian J. Org. Chem.* **2013**, 2, 726.
[29] Y. Liu, Q. Yang, D. Hao, W. Zhang, "Facile Synthesis of Triarylmethanimine Promoted by a Lewis Acid - Base Pair: Theoretical and Experimental Studies", *Aust. J. Chem.* **2012**, 65, 1390.
[30] M. Higuchi, A. Kimoto, S. Shiki, K. Yamamoto, "Selective synthesis of novel cyclic phenylazomethine trimers", *J. Org. Chem.* **2000**, 65, 5680.
[31] T. Yasukawa, H. Nakajima, R. Masuda, Y. Yamashita, S. Kobayashi, "Effect of Activation Methods of Molecular Sieves on Ketimine Synthesis", *J. Org. Chem.* **2022**, 87, 13750.
[32] M. Tobisu, S. Yamaguchi, N. Chatani, "Lewis acid-promoted imine synthesis by the insertion of isocyanides into C-H bonds of electron-rich aromatic compounds", *Org. Lett.* **2007**, 9, 3351.
[33] R. G. Giles, H. Heaney, M. J. Plater, "Reactions of nitrilium salts with indole and pyrrole and their derivatives in the synthesis of imines, ketones and secondary amines", *Tetrahedron* **2015**, 71, 7367.
[34] J. M. Lipshultz, G. Li, A. T. Radosevich, "Main Group Redox Catalysis of Organopnictogens: Vertical Periodic Trends and Emerging Opportunities in Group 15", *J. Am. Chem. Soc.* **2021**, 143, 1699.
[35] L. Longwitz, T. Werner, "Recent advances in catalytic Wittig-type reactions based on P(III)/P(V) redox cycling", *Pure Appl. Chem.* **2019**, 91, 95.
[36] J. Xue, Y.-S. Zhang, Z. Huan, J.-D. Yang, J.-P. Cheng, "Catalytic Vilsmeier-Haack Reactions for C1-Deuterated Formylation of Indoles", *J. Org. Chem.* **2022**, 87, 15539.
[37] L. Longwitz, S. Jopp, T. Werner, "Organocatalytic Chlorination of Alcohols by P(III)/P(V) Redox Cycling", *J. Org. Chem.* **2019**, 84, 7863.
[38] J. Tönjes, L. Kell, T. Werner, "Organocatalytic Stereospecific Appel Reaction", *Org. Lett.* **2023**, 25, 9114.
[39] D. C. Lenstra, Rutjes, Floris P. J. T., J. Mecinović, "Triphenylphosphine-catalysed amide bond formation between carboxylic acids and amines", *Chem. Commun.* **2014**, 50, 5763.

[40] M. Lecomte, J. M. Lipshultz, S.-H. Kim-Lee, G. Li, A. T. Radosevich, "Driving Recursive Dehydration by PIII/PV Catalysis: Annulation of Amines and Carboxylic Acids by Sequential C–N and C–C Bond Formation", *J. Am. Chem. Soc.* **2019**, 141, 12507.
[41] J. M. Lipshultz, A. T. Radosevich, "Uniting Amide Synthesis and Activation by PIII/PV–Catalyzed Serial Condensation: Three-Component Assembly of 2-Amidopyridines", *J. Am. Chem. Soc.* **2021**, 143, 14487.
[42] V. Medvarić, J. Paradies, T. Werner, "Synthesis of Amidines Via P(III)/P(V)=O Redox Catalyzed In Situ Formation of Imidoyl Chlorides From Amides", *Adv. Synth. Catal.* **2025**, 367, e70059.

7.3 Synthesis of trisubstituted furans from activated alkenes by P^{III}/P^{V} redox cycling catalysis

J. Tönjes, V. Medvarić, T. Werner, *J. Org. Chem.* **2024**, *89*, 15, 10729.

DOI: 10.1021/acs.joc.4c00985

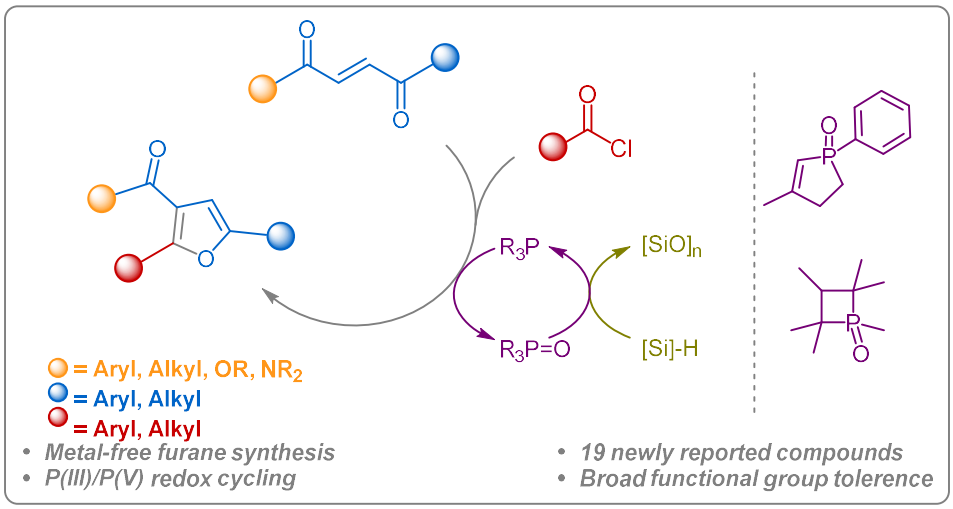

Abstract:

The organocatalytic formation of an underrepresented family of tri- and tetrasubstituted furans from activated alkenes and acyl chlorides is reported. In a reaction sequence based on P^{III}/P^{V} redox cycling catalysis, the cyclic phosphine catalysts react with bisacylethenes or acylacrylates in a Michael addition, followed by an acylation and either an intramolecular Wittig reaction or a ring closure reaction, liberating the furans. The formed phosphine oxides are reduced in situ by phenylsilane as terminal reductant. In a first step, 12 diacylethenes were converted to the respective trisubstituted furans. The reaction of acylacrylates showed a surprising, catalyst dependent alternate reaction forming tetrasubstituted furans. Two additional methods were developed, giving 14 trisubstituted furans using a phospholene catalyst and an additional 6 tetrasubstituted furans using a phosphetane catalyst. This encompassed 19 newly described compounds.

JOC The Journal of Organic Chemistry

pubs.acs.org/joc Article

Synthesis of Trisubstituted Furans from Activated Alkenes by P(III)/P(V) Redox Cycling Catalysis

Jan Tönjes, Viktorija Medvarić, and Thomas Werner*

Cite This: J. Org. Chem. 2024, 89, 10729−10735 Read Online

ACCESS | Metrics & More | Article Recommendations | Supporting Information

ABSTRACT: The organocatalytic formation of an underrepresented family of trisubstituted and tetrasubstituted furans from activated alkenes and acyl chlorides is reported. In a reaction sequence based on P(III)/P(V) redox cycling catalysis, the cyclic phosphine catalysts react with diacylethenes or acyl acrylates in Michael addition, followed by acylation and either an intramolecular Wittig reaction or a ring closure reaction, liberating the furans. The formed phosphine oxides are reduced in situ by phenylsilane as a terminal reductant. In the first step, 12 diacylethenes were converted to the respective trisubstituted furans. The reaction of acyl acrylates showed a surprising, catalyst-dependent alternate reaction forming tetrasubstituted furans. Two additional methods were developed, giving 14 trisubstituted furans using a phospholene catalyst and an additional 6 tetrasubstituted furans using a phosphetane catalyst. This encompassed 19 newly described compounds.

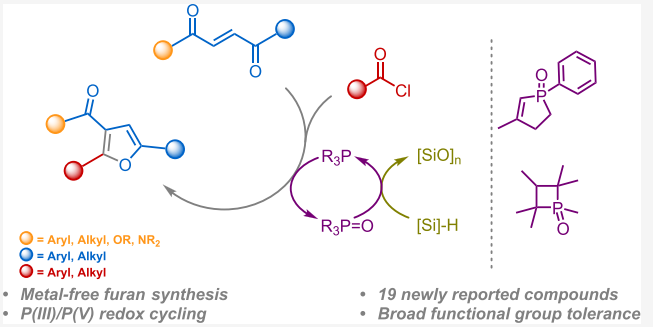

INTRODUCTION

Substituted furans are a valuable synthetic target, not only due to their wide occurrence in natural products and active compounds, including approved pharmaceuticals, despite their propensity to lead to toxic metabolites.[1,2] They can also serve as an interesting synthon for the synthesis of natural or complex products due to their versatile reactivity.[3,4] This can be exemplified by their ability to react in Diels−Alder type cycloadditions by the formation of synthetically useful products with different oxidants or exchange of oxygen with different heteroatoms.[5−7]

While furan derivatives for technical applications are mostly derived from biomass, classical reactions for the formation of substituted furans include the Paal−Knorr synthesis for disubstituted products or the Feist−Benary synthesis for tetrasubstituted furans.[8−10] Following this, a multitude of methods have been developed to form furans with diverse substitution patterns and to employ various starting materials.[11−16] A large number of methods employ transition metal catalysts, especially on the basis of silver and gold using alkynes or ketenes as substrates, although catalysts on the basis of palladium, copper, and others have also been reported.

Phosphines can be used for the synthesis of substituted furans under transition metal-free conditions. Some substrates can be activated by catalytic amounts of phosphine, forming substituted furans by rearrangement.[17] In a more general method, the phosphine can react in Michael addition with an activated alkene, which, in turn, can be acylated with acid anhydrides or acid chlorides. Deprotonation of this intermediate leads to the formation of a substituted furan via an intramolecular Wittig reaction.[18−21] Here, stoichiometric amounts of phosphine have to be employed to form phosphine oxide as a byproduct, which can lead to separation problems and an enlarged waste stream.

First steps to alleviate this general issue were done by O'Brien et al. in 2009 with the development of P(III)/P(V) redox cycling catalysis.[22] In this reaction principle, the phosphine oxide formed in a reaction of this type is reduced in situ using silanes as terminal reductants. Thus, catalytic amounts of phosphines are sufficient, reducing the phosphine oxide waste stream, simplifying the purification of the products and making the use of specialized phosphines more economically viable. This methodology was adapted for different reactions, including reductive C−N coupling reactions, Morita−Baylis−Hilman/Wittig cascade, Vilsmeier−Haack reaction, Staudinger/Aza-Wittig reaction, base-free Wittig reaction, and the reduction of activated alkenes.[23−28] P(III)/P(V) redox cycling catalysis has also been employed for the formation of substituted furans. Lin and co-workers reworked their method for the synthesis of tetrasubstituted furans from trisubstituted activated alkenes using stoichiometric amounts of tributylphosphine toward the use of

Received: April 23, 2024
Revised: June 21, 2024
Accepted: July 8, 2024
Published: July 15, 2024

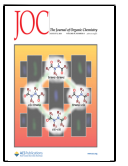

catalytic amounts of a phospholane catalyst with silyl chlorides as promoters and phenylsilane as a terminal reductant (Scheme 1a).[21,29] He and co-workers updated their synthesis of

Scheme 1. Different Approaches toward Substituted Furans by P(III)/P(V) Redox Cycling Catalysis

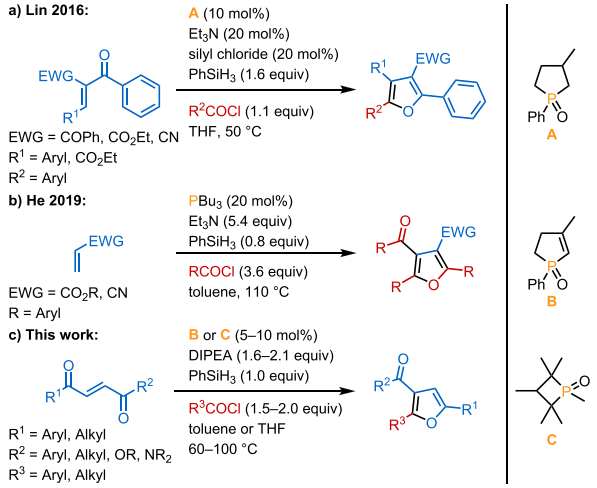

tetrasubstituted furans starting from acrylates toward the use of catalytic amounts of tributylphosphine at elevated temperatures with the same terminal reductant (Scheme 1b).[20,30] Recently, Lin and co-workers also revised their method toward the synthesis of furo[2,3-*f*]dibenzotropones.[31]

In the field of activated alkenes, neither the use of 1,2-diacylethenes nor 3-acyl acrylates has been explored for the metal-free, catalytic synthesis of substituted furans, and only few examples can be found in the literature under stoichiometric conditions.[32] Thus, our aim was to explore these activated alkenes in a Michael-addition/acylation/Wittig sequence under phosphine redox cycling catalysis and develop methods for the synthesis of new products in the valuable field of substituted furans (Scheme 1c).

RESULTS AND DISCUSSION

We started our investigation with the reaction of 1,2-dibenzoylethene (**1a**) with benzoyl chloride (**2a**) in THF as the solvent, diisopropylethylamine (DIPEA) as the base, and phenylsilane as the terminal reductant. In the first step, the reactivity of various phosphine catalysts was evaluated. The use of hexamethylphosphetane oxide **3a** afforded the desired trisubstituted furan **4a** in a satisfactory yield of 71% (Table 1, entry 1). This highly active catalyst was used in various transformations in recent years.[28,33−35] In the presence of the more sterically demanding phosphine oxide **3b**, no product formation was observed (entry 2). Surprisingly, the less sterically demanding tetramethylphospetane oxide **3c**, which was recently introduced by the group of Radosevich, gave the product **4a** in only 24% yield (entry 3).[23,36] Several other phosphine oxides **3d**−**3g** were employed as catalysts. However, **4a** was obtained in low yields <10% in all cases (entries 4−7). This is especially unexpected for phospholene **3d**, which is widely used in P(III)/P(V) redox cycling catalysis.

The exchange of THF with cyclopentyl methyl ether (CPME), butyl acetate, or MeTHF gave all similar but lower yields of furan **4a** between 43 and 55%, while the use of toluene and MeCN led to significantly lower yields of 34% and

Table 1. Catalyst Screening and Optimization of the Reaction Conditions for the Formation of Triphenylfuran 4a from Dibenzoylethene 1a[b]

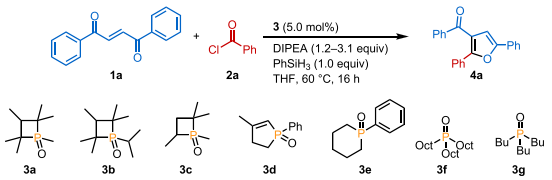

entry	3	2a/equiv	DIPEA/equiv	modification	4a yield[a]/%
1	**3a**	1.1	1.2		71
2	**3b**	1.1	1.2		0
3	**3c**	1.1	1.2		24
4	**3d**	1.1	1.2		7
5	**3e**	1.1	1.2		3
6	**3f**	1.1	1.2		3
7	**3g**	1.1	1.2		2
8	**3a**	1.1	1.2	40 °C	13
9	**3a**	1.1	1.2	80 °C	66
10	**3a**	1.5	1.6		87
11	**3a**	2.0	2.1		99
12	**3a**	2.0	2.1	4 h	99
13	**3a**	2.0	2.1	2 h	82

[a]Yield determined by GC-FID with hexadecane as the internal standard. [b]Reaction conditions: 1.0 equiv of **1a** (0.50 mmol), 1.1−2.0 equiv of BzCl (**2a**, 0.55−1.0 mmol), 1.2−2.1 equiv of DIPEA (0.60−1.05 mmol), 5.0 mol % catalyst **3** (25 μmol), 1.0 equiv of $PhSiH_3$ (0.50 mmol), 1.5 mL of solvent, 60 °C, 16 h.

2%, respectively.[37] Different amine bases, sodium carbonate and butylene oxide, as a capped base were also tested.[37] Butylene oxide proved to be an alternative to DIPEA, affording the furan **4a** in a yield of 69%, whereas the other tested bases only gave **4a** in yields <10%. A reduction in the reaction temperature to 40 °C led to a significantly lower yield of 13% (entry 8), whereas at 80 °C, **4a** was obtained in 66% yield (entry 9). An increase in the amounts of base and benzoyl chloride (**2a**) led to improved yields. In the presence of 1.5 equiv of **2a**, the desired product was obtained in 87% yield, while 99% yield was achieved when 2.0 equiv of **2a** was used (entries 10 and 11). Notably, the reaction time could be shortened to 4 h without a reduction in the amount of product **4a**, while even 2 h led to a good yield of 82% (entries 12 and 13). In the absence of phenylsilane or catalyst **3a**, no product was formed, while in the absence of DIPEA, traces of furan **4a** were obtained.[37]

When the optimized conditions were employed, dibenzoylethene **1a** yielded the product **4a** in an isolated yield of 93% after a reaction time of 4 h. However, test reactions for other substrates led to unsatisfactory yields (Figure 1). For the further evaluation of the substrate scope, the reaction time was extended to 16 h. Under these conditions, the electron-rich dimethoxyderivative **1b** was converted to the trisubstituted furan **4b** in a yield of 81%, while the dichlorocompound **1c** afforded the respective furan **4c** in a moderate yield of 58%. Both the more challenging dithiophene compound **1d** and more sterically hindered dinaphthyl compound **1e** gave comparable yields of 50 and 54% of the respective furans **4d** and **4e**, respectively. The hexenedione **1f** could be converted to the methylsubstituted furan **4f** in a yield of 40%, whereas the phenylpentenedione **1g** afforded 3-acetyl-2,5-diphenylfuran (**4g**) in a yield of 74%. Only less than 7% of the isomer was

https://doi.org/10.1021/acs.joc.4c00985
J. Org. Chem. 2024, 89, 10729−10735

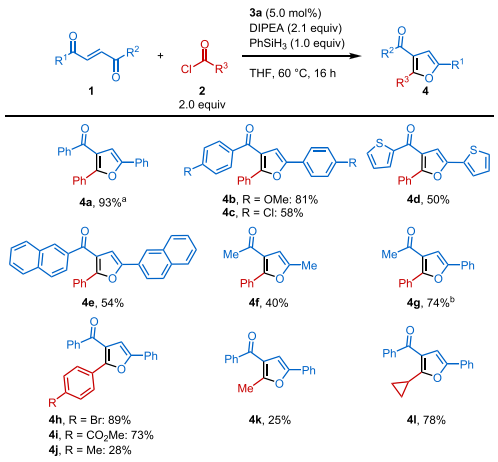

Figure 1. Substrate scope for the conversion of diacylalkenes **1**. Reaction conditions: 1.0 equiv of **1** (1.0 mmol), 2.0 equiv of **2** (2.0 mmol), 2.1 equiv of DIPEA (2.1 mmol), 5.0 mol % catalyst **3a** (50 μmol), 1.0 equiv of $PhSiH_3$ (1.0 mmol), 3.0 mL of solvent, 60 °C, 16 h. [a]Reaction time, 4 h. [b]<7% of isomeric 3-benzoyl-5-methyl-2-phenylfuran was formed. Isolated yields are given.

formed. With less distinctly different acyl groups, a less favorable isomeric mixture is to be expected. By exchanging the acid chloride for derivative **2b**, the bromophenyl substituted furan **4h** was isolated in a good yield of 89%. The electron-poor methoxycarbonylbenzoyl chloride (**2c**) led to a slightly lower yield of 73% of furan **4i**, whereas the more electron-rich methylbenzoyl chloride **2d** led to a reduced yield of 28% of furan **4j**. Similarly, the reaction of model compound **1a** with acetyl chloride (**2e**) led to the expected trisubstituted furan **4k** in a yield of 25%, whereas a surprisingly good yield of 78% of furan **4l** was obtained in the reaction of cyclopropylcarbonyl chloride **2f**.

Based on the work of He and co-workers, two reaction pathways are plausible for the reaction of diketone **1** with acyl chloride **2** using the phosphetane catalyst **3a** and phenylsilane as the terminal reductant.[30] In the first reaction pathway, after Michael addition of reduced phosphine **5** to activated alkene **1**, formed enolate **I-1** reacts with acyl chloride under *C*-acylation and subsequent deprotonation to form enolate **I-2** (Figure 2, reaction pathway **I**). A nucleophilic attack of the enolate leads to a ring closure reaction, and the subsequent deoxygenation results in the formation of trisubstituted furan **4** and phosphine oxide **3**, which can be reduced by the terminal reductant. In the second reaction pathway, the formed enolate **II-1** reacts under *O*-acylation to form the enolester **II-2** (Figure 2, reaction pathway **II**). Deprotonation of the phosphonium salt forms an ylide, which reacts in an intramolecular Wittig reaction, forming the trisubstituted furan **4** and the phosphine oxide **3**.

The triketone **6** was synthesized and converted to the trisubstituted furan **4a** using phosphetane catalyst **3a** and phenylsilane under 60 °C in THF, demonstrating the general viability of the ring closure reaction. Upon the addition of benzoyl chloride (**2a**) and DIPEA to the reaction mixture, only a little trisubstituted furan **4a** was formed, while the tetrasubstituted furan **7** was isolated as the main product in a yield of 64%. The formation of this product was not previously observed in the reaction of diketone **1** with acyl chloride **2**. Additionally, without an added base, only traces of trisubstituted furan **4a** were formed in the reaction of diketone

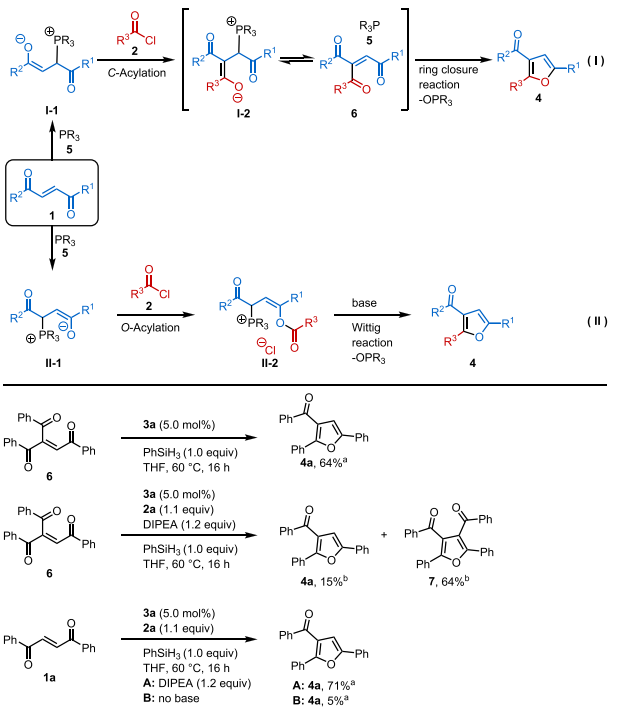

Figure 2. Plausible reaction pathways and test reactions for the synthesis of trisubstituted furan **4** from diacylethene **1**. The reduction of phosphine oxide **3** using phenylsilane as the terminal reductant was omitted from the scheme. [a]Yield determined by GC-FID with hexadecane as an internal standard. [b]Isolated yields are given.

1a with acyl chloride **2a**, while an insoluble salt was formed. Thus, reaction path **II**, which includes the intramolecular Wittig reaction, depicts a more plausible reaction mechanism.

Furthermore, the reaction of ethyl benzoyl acrylate (**8a**) with benzoyl chloride **2a** using phosphetane catalyst **3a** was conducted (Table 2). Surprisingly, in addition to the expected trisubstituted furan **9a**, also the tetrasubstituted furan **10a** was formed. The ratio of the formed furans **9a** and **10a** was found to be dependent on phosphine catalyst **3** used. The hexamethylphosphetane **3a** was the only catalyst tested, which led to an excess in the formation of the tetrasubstituted furan **10a** (entry 1). The isopropyl-substituted furan **3b** achieved only a low yield, while the less sterically demanding tetramethylphosphetane **3c** led to a good overall yield of 49% but with a nearly equal product distribution (entries 2 and 3). The formation of trisubstituted furan **9a** was clearly favored when using the phospholene catalyst **3d** with a 48% yield of trisubstituted furan **9a** and a 6% yield of tetrasubstituted furan **10a** (entry 4). While also clearly preferring the formation of trisubstituted furan **9a**, the phosphinane catalyst **3e**, as well as trioctylphosphine oxide (**3f**) and tributylphosphine oxide (**3g**), only led to yields in the single digit range (entry 5−7). The trialkyl catalysts **3f** and **3g** were also brought to reaction at higher temperatures, but only slight improvements in yield were observed, while the product ratio remained similar.[37] Higher reaction temperatures were shown to be advantageous for the formation of trisubstituted furan **9a**. Thus, an increased temperature of 100 °C in CPME and toluene improved the yields to 69% and 74%, respectively (entries 8 and 9). Even higher temperatures of 120 and 140 °C yielded nearly identical results.[37]

Increasing the amounts of benzoyl chloride (**2a**) and DIPEA to 1.5 and 1.6 equiv led to an increased yield of furan **9a**

https://doi.org/10.1021/acs.joc.4c00985
J. Org. Chem. 2024, 89, 10729−10735

Table 2. Catalyst Screening and Reaction Optimization for the Formation of Trisubstituted Furan 9a and Tetrasubstituted Furan 10a from Acylacrylate 5a[d]

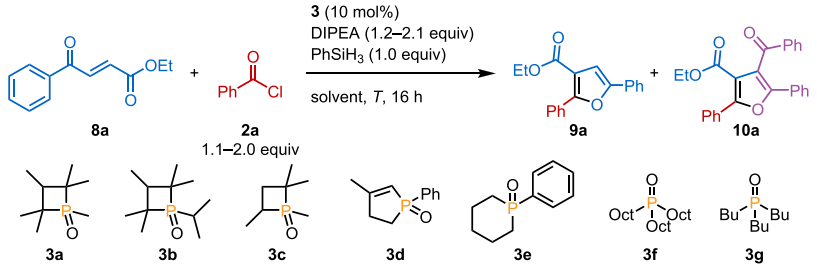

entry	3	2a/equiv	DIPEA/equiv	solvent	T/°C	9a yield[a]/%	10a yield[a]/%	9a:10a
1	**3a**	1.1	1.2	THF	60	11	25	31:69
2	**3b**	1.1	1.2	THF	60	5	3	68:33
3	**3c**	1.1	1.2	THF	60	27	22	55:45
4	**3d**	1.1	1.2	THF	60	48	6	89:11
5	**3e**	1.1	1.2	THF	60	4	<2	98:3
6	**3f**	1.1	1.2	THF	60	2	<2	91:9
7	**3g**	1.1	1.2	THF	60	2	<2	95:5
8	**3d**	1.1	1.2	CPME	100	69	6	92:8
9	**3d**	1.1	1.2	toluene	100	74	8	90:10
10	**3d**	1.5	1.6	toluene	100	80	10	89:11
11	**3d**	2.0	2.1	toluene	100	81	12	87:13
12[b]	**3d**	1.5	1.6	toluene	100	82	10	89:11
13[c]	**3d**	1.5	1.6	toluene	100	67	9	88:12
14	**3a**	5.0	5.0	toluene	60	14	71	16:84

[a]Yield determined by GC-FID with hexadecane as the internal standard. [b]Reaction time: 4 h. [c]Reaction time: 2 h. [d]Reaction conditions: 1.0 equiv of **8a** (0.50 mmol), 1.1−5.0 equiv of BzCl (**2a**, 0.55−2.5 mmol), 1.2−5.0 equiv of DIPEA (0.60−2.5 mmol), 10 mol % catalyst **3** (50 μmol), 1.0 equiv of $PhSiH_3$ (0.50 mmol), 1.5 mL of solvent, 60−100 °C, 2−16 h.

(80%), while a further increased loading to 2.0 and 2.1 equiv only resulted in an increased formation of side product **10a** (entries 10 and 11). The reaction time could be shortened to 4 h without large changes in yield and selectivity, while shorter reaction times led to reduced yields (entries 12 and 13). Test reactions without a catalyst or phenylsilane did not lead to product formation, while in the absence of a base, still 53% of the trisubstituted furan **9a** was formed.[37] The tetrasubstituted furan **10a** was best formed utilizing phosphetane catalyst **3a**, an excess of benzoyl chloride **2a**, and DIPEA at a reaction temperature of 60 °C (entry 14). Under these conditions, tetrasubstituted furan **10a** was formed in a yield of 71%.

Under these reaction conditions, the model substrate was converted to diphenylfuran **9a** in an isolated yield of 74% (Figure 3). Additionally, tetrasubstituted furan **10a** was isolated in a yield of 13%. The electron-rich methoxy derivative **8b** led to the formation of the trisubstituted furan **9b** in a yield of 70%. Attempts to isolate the tetrasubstituted side product revealed a property of the reaction that was concealed during the optimization due to the choice of reactants. If R^1 and R^3 are distinct, two isomers of tetrasubstituted furan **10** are formed in a substrate-specific ratio, which happens due to the formation of a symmetric diacyl-intermediate (see discussion of the mechanism). The more sterically hindered 1-naphthyl derivative **8c** led to furan **9c** in a good yield of 78%. Similarly, the furan derivative **8d** gave the furanylphenylfuran **9d** in a good yield of 71%, while chloro derivative **8e** and piperonyl derivative **8f** formed their respective trisubstituted furans **9e** and **9f** in slightly lower yields of 59% and 57%, respectively. Also, the conversion of ethyl oxopentenoate **8g** was possible, resulting in the respective methyl-substituted furan **9g** in a yield of 60%.

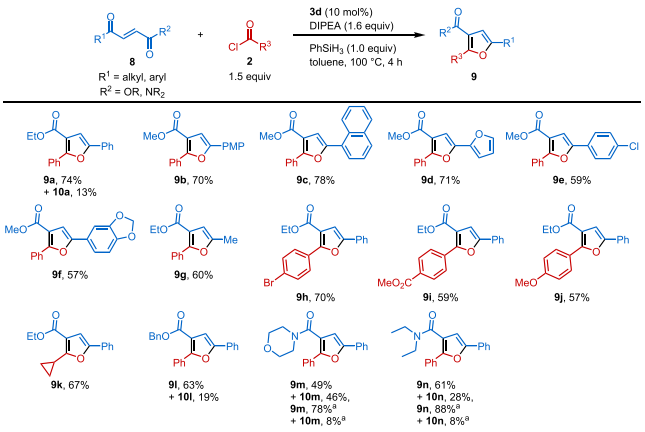

Figure 3. Substrate scope for the conversion of acyl acrylates **8**. Reaction conditions: 1.0 equiv of **8** (1.0 mmol), 1.5 equiv of **2** (1.5 mmol), 1.6 equiv of DIPEA (1.6 mmol), 10 mol % catalyst **3d** (0.10 mmol), 1.0 equiv of $PhSiH_3$ (1.0 mmol), 3.0 mL of toluene, 100 °C, 4 h. Isolated yields are given. PMP: *p*-methoxyphenyl.[a]Reaction conditions: 1.0 equiv of **8** (1.0 mmol), 5.0 equiv of **2** (5.0 mmol), 5.0 equiv of DIPEA (5.0 mmol), 10 mol % catalyst **3a** (0.10 mmol), 1.0 equiv of $PhSiH_3$ (1.0 mmol), 3.0 mL of toluene, 60 °C, 16 h.

Next, the acyl chloride was varied. The bromobenzoyl chloride **2b** gave the respective furan **9h** in a yield of 70%. Both electron-rich and electron-poor acid chlorides performed similarly. Methoxycarbonylbenzoyl chloride **2c** and methoxybenzoyl chloride **2g** formed furans **9i** and **9j** in yields of 59% and 57%, respectively. The reaction of cyclopropylcarbonyl chloride (**2f**) with ethyl benzoyl acrylate yielded the trisubstituted furan **9k** with 67% yield.

https://doi.org/10.1021/acs.joc.4c00985
J. Org. Chem. 2024, 89, 10729−10735

Additionally, R^2 could be modified. While the benzyl derivative reacted as expected, forming trisubstituted furan **9l** in a slightly lower yield of 63%, with 19% tetrasubstituted furan **10l** as the side product, the altered electronic properties on the double bond when employing an amide derivative led to changed selectivities. Presumably, the diminished mesomeric effect of the amide group in comparison to the ester drastically changes the preferred reaction path. The less electron-deficient morpholine amide **8m** reacted to the trisubstituted furan **9m** in a moderate yield of 49%, but at the same time, a considerable amount of tetrasubstituted furan **10m** was formed with a yield of 46%. In contrast to the formation of tetrasubstituted furan **10a** from acyl acrylate **8a** (Table 2, entry 14) when utilizing the phosphetane catalyst **3a**, unexpectedly high selectivities toward the trisubstituted furan **9m** were observed in a good yield of 78% with only 8% of tetrasubstituted furan **10m** as the side product. A similar effect could be seen in the reaction of diethylamide **8n** under standard reaction conditions, forming the trisubstituted furan **9n** and tetrasubstituted furan **10n** in yields of 61% and 28%, respectively. However, the modified conditions led to yields of 88% and 8%, respectively.

The reaction of acyl acrylates **8** with acyl chlorides **2** and phosphine catalysts **3** also shows multiple plausible reaction pathways (Figure 4). Analogous to the formation of furan **4** from diacylethene **1**, the trisubstituted furan **9** can be either formed by a reaction sequence of Michael addition to the more electron-deficient β-position in relation to the ester group, *C*-acylation, and a ring-closure reaction (reaction path **I-a**) or by a reaction sequence of Michael addition to the less electron-poor α-position, *O*-acylation, deprotonation, and intramolecular Wittig reaction (reaction path **II-a**). The viability of the ring-closure reaction (reaction path **I-a**) was demonstrated in the conversion of diacyl acrylate **11** using phospholene catalyst **3d** in the presence of benzoyl chloride (**2a**) and DIPEA. Both trisubstituted furan **9a** and tetrasubstituted furan **10a** were formed, albeit in lowered selectivity (Figure 5, reaction **1**). Also, the optimization of this reaction demonstrated that the lack of an added base leads to a moderate yield of trisubstituted furan **9a** (53%), indicating that the primary reaction pathway is **I-a**.[37] A lack of base in the intramolecular Wittig reaction of reaction pathway **II-a** is not expected to lead to product formation.

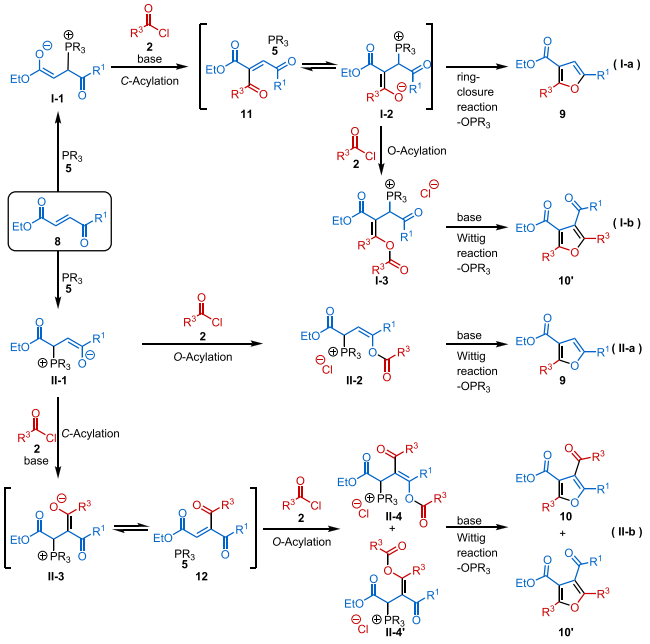

Figure 4. Plausible reaction pathways for the synthesis of tri- and tetrasubstituted furans **9** and **10** from acyl acrylates **8**. The reduction of phosphine oxide **3** using phenylsilane as the terminal reductant was omitted from the scheme.

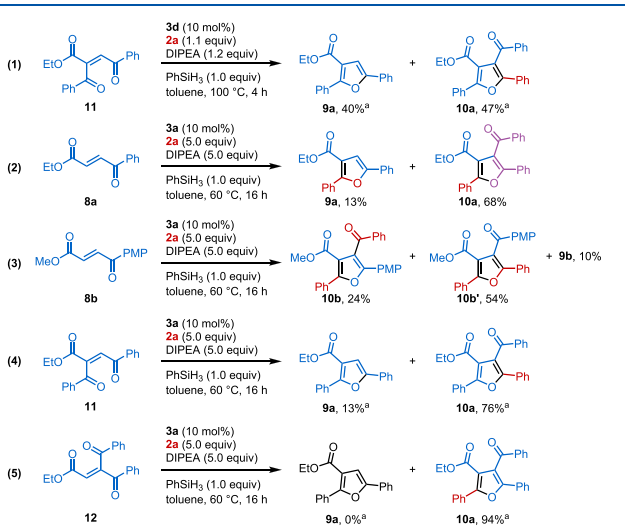

Figure 5. Test reactions for the synthesis of tri- and tetrasubstituted furans **9** and **10** from acyl acrylates **8**. Isolated yields are given. PMP: *p*-methoxyphenyl. [a]Yield determined by GC-FID with hexadecane as the internal standard.

Ethyl benzoyl acrylate (**8a**) was converted with an excess of benzoyl chloride **2a** and DIPEA utilizing phosphetane catalyst **3a**. Here, the tetrasubstituted furan **10a** was isolated in a yield of 68% and the side product **9a** was isolated in a yield of 13% (reaction **2**). When the substituents of acyl acrylate **8** and acyl chloride **2** are distinct, two regioisomers of tetrasubstituted furan **10** are formed. The conversion of methoxy-derivative **8b** led to the formation of the trisubstituted furan **9b** as a side product in 10% yield, while two regioisomers of the tetrasubstituted furans **10b** and **10b′** were isolated in yields of 24% and 54%, respectively (reaction **3**). Also, the formation of tetrasubstituted furan **10** can be described by two viable reaction pathways. In reaction pathway **I-b**, intermediate **I-2** can undergo *O*-acylation, followed by a deprotonation and an intramolecular Wittig reaction to form tetrasubstituted furan **10′**. The viability of this sequence was demonstrated in reaction **4**, although here, the formation of only one regioisomer of furan **10** is expected. The formation of two isomers **10** can be described by the reaction of intermediate **II-1** in *C*-acylation, followed by *O*-acylation, forming two isomers of intermediate **II-3** (reaction path **II-b**). Subsequent deprotonation and intramolecular Wittig reaction led to the formation of two regioisomers of tetrasubstituted furan **10**. Reaction **5** demonstrates the viability of this reaction sequence via the intramolecular Wittig reaction.

An alternate reaction mechanism can be proposed based on the work of Lin and co-workers.[38,39] Here, the diacyl acrylate **11** could be formed in a β-acylation reaction from the intermediates **II-2**, while diacyl acrylate **12** could be formed by *O*-acylation and β-acylation of intermediate **I-1**. This would avoid the proposal of a *C*-acylation reaction. However, diacyl

https://doi.org/10.1021/acs.joc.4c00985
J. Org. Chem. 2024, 89, 10729−10735

acrylates **11** and **12** were never observed in the reaction mixture.

CONCLUSIONS

The reactivity of activated alkenes with acyl chlorides under the P(III)/P(V) redox cycling conditions was investigated. We developed a reaction sequence of Michael addition of the phosphine catalyst and acylation, followed by either an intramolecular Wittig reaction or a ring closure reaction, resulting in the formation of tri- and tetrasubstituted furans. A phosphetane catalyst enabled the synthesis of 12 trisubstituted furans from diacylethenes. The reaction of acyl acrylates resulted in the unexpected formation of not just trisubstituted furans but also tetrasubstituted derivatives, while the product ratio depended on the employed catalyst. Two methods using a phospholene or phosphetane catalyst allowed the synthesis of 14 trisubstituted furans and an additional 6 tetrasubstituted furans. These include 19 novel compounds in this underexplored field of substituted furans.

ASSOCIATED CONTENT

Data Availability Statement

The data underlying this study are available in the published article and its Supporting Information.

Supporting Information

The Supporting Information is available free of charge at https://pubs.acs.org/doi/10.1021/acs.joc.4c00985.

Additional information on reaction optimization, experimental procedures, characterization data, and NMR spectra (PDF)

AUTHOR INFORMATION

Corresponding Author

Thomas Werner − *Leibniz Institute for Catalysis at the University of Rostock (LIKAT Rostock), Rostock D-18059, Germany; Department of Chemistry and Center for Sustainable Systems Design (CSSD), Paderborn University, Paderborn D-33098, Germany;* orcid.org/0000-0001-9025-3244; Email: th.werner@uni-paderborn.de

Authors

Jan Tönjes − *Leibniz Institute for Catalysis at the University of Rostock (LIKAT Rostock), Rostock D-18059, Germany;* orcid.org/0000-0002-3411-9881

Viktorija Medvarić − *Leibniz Institute for Catalysis at the University of Rostock (LIKAT Rostock), Rostock D-18059, Germany; Department of Chemistry and Center for Sustainable Systems Design (CSSD), Paderborn University, Paderborn D-33098, Germany*

Complete contact information is available at: https://pubs.acs.org/10.1021/acs.joc.4c00985

Notes

The authors declare no competing financial interest.

ACKNOWLEDGMENTS

This research project is part of the Leibniz ScienceCampus Phosphorus Research Rostock and is (co-)funded by the funding line strategic networks of the Leibniz Association.

REFERENCES

(1) Delost, M. D.; Smith, D. T.; Anderson, B. J.; Njardarson, J. T. From Oxiranes to Oligomers: Architectures of U.S. FDA Approved Pharmaceuticals Containing Oxygen Heterocycles. *J. Med. Chem.* **2018**, *61* (24), 10996−11020.

(2) Peterson, L. A. Reactive Metabolites in the Biotransformation of Molecules Containing a Furan Ring. *Chem. Res. Toxicol.* **2013**, *26* (1), 6−25.

(3) Hao, H.-D.; Trauner, D. Furans as Versatile Synthons: Total Syntheses of Caribenol A and Caribenol B. *J. Am. Chem. Soc.* **2017**, *139* (11), 4117−4122.

(4) Lipshutz, B. H. Five-membered heteroaromatic rings as intermediates in organic synthesis. *Chem. Rev.* **1986**, *86* (5), 795−819.

(5) Padwa, A.; Flick, A. C. Chapter One - Intramolecular Diels−Alder Cycloaddition of Furans (IMDAF) for Natural Product Synthesis. In *Advances in Heterocyclic Chemistry*, Katritzky, A. R., Ed. Academic Press: 2013; Vol. *110*, pp 1−41.

(6) Makarov, A. S.; Uchuskin, M. G.; Trushkov, I. V. Furan Oxidation Reactions in the Total Synthesis of Natural Products. *Synthesis* **2018**, *50* (16), 3059−3086.

(7) Trushkov, I. V.; Uchuskin, M. G.; Butin, A. V. Furan's Gambit: Electrophile-Attack-Triggered Sacrifice of Furan Rings for the Intramolecular Construction of Azaheterocycles. *Eur. J. Org. Chem.* **2015**, *2015* (14), 2999−3016.

(8) Galkin, K. I.; Ananikov, V. P. When Will 5-Hydroxymethylfurfural, the "Sleeping Giant" of Sustainable Chemistry, Awaken? *ChemSusChem* **2019**, *12* (13), 2976−2982.

(9) Post, C.; Maniar, D.; Voet, V. S. D.; Folkersma, R.; Loos, K. Biobased 2,5-Bis(hydroxymethyl)furan as a Versatile Building Block for Sustainable Polymeric Materials. *ACS Omega* **2023**, *8* (10), 8991−9003.

(10) Eicher, T.; Hauptmann, S.; Speicher, A. *The Chemistry of Heterocycles: Structure, Reactions, Syntheses, and Applications*. 2nd ed.; Wiley-VCH: Weinheim, 2003.

(11) Nejrotti, S.; Prandi, C. Gold Catalysis and Furans: A Powerful Match for Synthetic Connections. *Synthesis* **2021**, *53* (06), 1046−1060.

(12) Blanc, A.; Bénéteau, V.; Weibel, J.-M.; Pale, P. Silver & gold-catalyzed routes to furans and benzofurans. *Org. Biomol. Chem.* **2016**, *14* (39), 9184−9205.

(13) Jin, H.; Fürstner, A. Modular Synthesis of Furans with up to Four Different Substituents by a trans-Carboboration Strategy. *Angew. Chem., Int. Ed.* **2020**, *59* (32), 13618−13622.

(14) Manna, S.; Antonchick, A. P. Copper(I)-Catalyzed Radical Addition of Acetophenones to Alkynes in Furan Synthesis. *Org. Lett.* **2015**, *17* (17), 4300−4303.

(15) Lou, J.; Wang, Q.; Wu, K.; Wu, P.; Yu, Z. Iron-Catalyzed Oxidative C−H Functionalization of Internal Olefins for the Synthesis of Tetrasubstituted Furans. *Org. Lett.* **2017**, *19* (12), 3287−3290.

(16) Gulevich, A. V.; Dudnik, A. S.; Chernyak, N.; Gevorgyan, V. Transition Metal-Mediated Synthesis of Monocyclic Aromatic Heterocycles. *Chem. Rev.* **2013**, *113* (5), 3084−3213.

(17) He, X.; Tang, Y.; Wang, Y.; Chen, J.-B.; Xu, S.; Dou, J.; Li, Y. Phosphine-Catalyzed Activation of Alkylidenecyclopropanes: Rearrangement to Form Polysubstituted Furans and Dienones. *Angew. Chem., Int. Ed.* **2019**, *58* (31), 10698−10702.

(18) Wang, Y.; Luo, Y.-C.; Hu, X.-Q.; Xu, P.-F. A Powerful Cascade Approach for Expeditious Synthesis of Trifluoromethylated Furans. *Org. Lett.* **2011**, *13* (19), 5346−5349.

(19) Ma, Y.-H.; He, X.-Y.; Wang, L.; Yang, Q.-Q. PPh3-Triggered Tandem Synthesis of 2,3-Disubstituted Benzofuran Derivatives from o-Quinone Methides with Acyl Chlorides. *J. Org. Chem.* **2022**, *87* (17), 11852−11856.

(20) Wang, J.; Zhou, R.; He, Z.-R.; He, Z. Phosphane-Mediated Domino Synthesis of Tetrasubstituted Furans from Simple Terminal Activated Olefins. *Eur. J. Org. Chem.* **2012**, *2012* (30), 6033−6041.

(21) Kao, T.-T.; Syu, S. -e.; Jhang, Y.-W.; Lin, W. Preparation of Tetrasubstituted Furans via Intramolecular Wittig Reactions with

Phosphorus Ylides as Intermediates. *Org. Lett.* **2010**, *12* (13), 3066−3069.
(22) O'Brien, C. J.; Tellez, J. L.; Nixon, Z. S.; Kang, L. J.; Carter, A. L.; Kunkel, S. R.; Przeworski, K. C.; Chass, G. A. Recycling the Waste: The Development of a Catalytic Wittig Reaction. *Angew. Chem., Int. Ed.* **2009**, *48* (37), 6836−6839.
(23) Li, G.; Kanda, Y.; Hong, S. Y.; Radosevich, A. T. Enabling Reductive C−N Cross-Coupling of Nitroalkanes and Boronic Acids by Steric Design of P(III)/P(V)═O Catalysts. *J. Am. Chem. Soc.* **2022**, *144* (18), 8242−8248.
(24) Zheng, Y.; Wang, Z.-W.; Cheng, W.-S.; Xie, Z.-Z.; He, X.-C.; Chen, Y.-S.; Chen, K.; Xiang, H.-Y.; Chen, X.-Q.; Yang, H. Phosphine-Mediated Morita−Baylis−Hillman-Type/Wittig Cascade: Access to E-Configured 3-Styryl- and 3-(Benzopyrrole/furan-2-yl) Quinolinones. *J. Org. Chem.* **2022**, *87* (2), 974−984.
(25) Xue, J.; Zhang, Y.-S.; Huan, Z.; Yang, J.-D.; Cheng, J.-P. Catalytic Vilsmeier−Haack Reactions for C1-Deuterated Formylation of Indoles. *J. Org. Chem.* **2022**, *87* (22), 15539−15546.
(26) Xie, C.; Kim, J.; Mai, B. K.; Cao, S.; Ye, R.; Wang, X.-Y.; Liu, P.; Kwon, O. Enantioselective Synthesis of Quaternary Oxindoles: Desymmetrizing Staudinger−Aza-Wittig Reaction Enabled by a Bespoke HypPhos Oxide Catalyst. *J. Am. Chem. Soc.* **2022**, *144* (46), 21318−21327.
(27) Tönjes, J.; Longwitz, L.; Werner, T. Poly(methylhydrosiloxane) as a reductant in the catalytic base-free Wittig reaction. *Green Chem.* **2021**, *23* (13), 4852−4857.
(28) Longwitz, L.; Werner, T. Reduction of Activated Alkenes by P(III) /P(V) Redox Cycling Catalysis. *Angew. Chem., Int. Ed.* **2020**, *59* (7), 2760−2763.
(29) Lee, C.-J.; Chang, T.-H.; Yu, J.-K.; Madhusudhan Reddy, G.; Hsiao, M.-Y.; Lin, W. Synthesis of Functionalized Furans via Chemoselective Reduction/Wittig Reaction Using Catalytic Triethylamine and Phosphine. *Org. Lett.* **2016**, *18* (15), 3758−3761.
(30) Fan, X.; Chen, R.; Han, J.; He, Z. Convergent Synthesis of Polysubstituted Furans via Catalytic Phosphine Mediated Multicomponent Reactions. *Molecules* **2019**, *24* (24), 4595.
(31) Chien, P.-C.; Chen, Y.-R.; Chen, Y.-J.; Chang, C.-F.; Marri, G.; Lin, W. Synthesis of Furo[2,3-f]dibenzotropones via Intramolecular Wittig Reaction of Alkylidene Dibenzo-β-tropolones. *Adv. Synth. Catal.* **2024**, *366* (3), 420−425.
(32) Chen, K.-W.; Syu, S. -e.; Jang, Y.-J.; Lin, W. A facile approach to highly functional trisubstituted furansvia intramolecular Wittig reactions. *Org. Biomol. Chem.* **2011**, *9* (7), 2098−2106.
(33) Handoko; Panigrahi, N. R.; Arora, P. S. Two-Component Redox Organocatalyst for Peptide Bond Formation. *J. Am. Chem. Soc.* **2022**, *144* (8), 3637−3643.
(34) Li, G.; Miller, S. P.; Radosevich, A. T. PIII/PV═O-Catalyzed Intermolecular N−N Bond Formation: Cross-Selective Reductive Coupling of Nitroarenes and Anilines. *J. Am. Chem. Soc.* **2021**, *143* (36), 14464−14469.
(35) Tönjes, J.; Kell, L.; Werner, T. Organocatalytic Stereospecific Appel Reaction. *Org. Lett.* **2023**, *25* (51), 9114−9118.
(36) Hong, S. Y.; Radosevich, A. T. Chemoselective Primary Amination of Aryl Boronic Acids by PIII/PV═O-Catalysis: Synthetic Capture of the Transient Nef Intermediate HNO. *J. Am. Chem. Soc.* **2022**, *144* (20), 8902−8907.
(37) For additional information see the Supporting Information.
(38) Liou, Y.-C.; Su, Y.-H.; Ku, K.-C.; Edukondalu, A.; Lin, C.-K.; Ke, Y.-S.; Karanam, P.; Lee, C.-J.; Lin, W. Organophosphane-Promoted Synthesis of Functionalized α,β-Unsaturated Alkenes and Furanones via Direct β-Acylation. *Org. Lett.* **2019**, *21* (20), 8339−8343.
(39) Lee, C.-J.; Sheu, C.-N.; Tsai, C.-C.; Wu, Z.-Z.; Lin, W. Direct β-acylation of 2-arylidene-1,3-indandiones with acyl chlorides catalyzed by organophosphanes. *Chem. Commun.* **2014**, *50* (40), 5304−5306.

https://doi.org/10.1021/acs.joc.4c00985
J. Org. Chem. 2024, 89, 10729−10735

7.4 Metal-free reduction of nitrous oxide via P^{III}/P^{V}=O cycling: mechanistic insights and catalytic performance

R. Zhou, V. Medvarić, T. Werner, J. Paradies, *J. Am. Chem. Soc.* **2025**, *147*, 37879.

DOI: 10.1021/jacs.5c06190

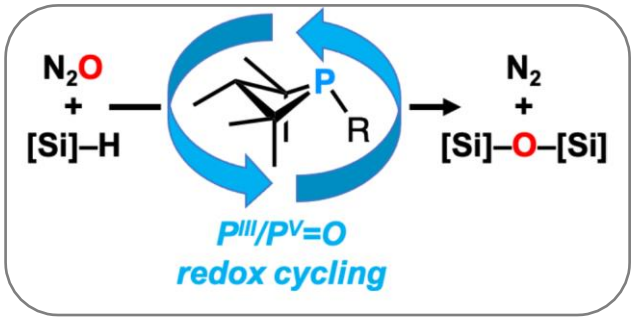

Abstract:

The catalytic reduction of nitrous oxide (N_2O) has been achieved through a metal-free P^{III}/P^{V}=O catalysis. Kinetic analysis revealed that the oxygen transfer reaction to the phosphetane is rate determining. Computational investigations support a reaction mechanism in which the phosphetane catalyst preferentially interacts with the nitrogen terminus of N_2O, leading to the formation of a P–N=N–O intermediate in the cis configuration. Natural population analysis indicates stabilizing interactions between the occupied non-bonding oxygen orbitals and the anti-bonding orbitals of the phosphetane backbone, facilitating the oxygen atom transfer. Following nitrogen extrusion, the active phosphetane species is regenerated via silane-mediated reduction. The catalytic activity was quantitatively assessed by monitoring nitrogen evolution through gas chromatography (GC) analysis.

JACS
JOURNAL OF THE AMERICAN CHEMICAL SOCIETY
pubs.acs.org/JACS
Communication

Metal-Free Reduction of Nitrous Oxide via P^{III}/P^{V}=O Cycling: Mechanistic Insights and Catalytic Performance

Rundong Zhou, Viktorija Medvarić, Thomas Werner, and Jan Paradies*

Cite This: J. Am. Chem. Soc. 2025, 147, 37879−37884
Read Online
ACCESS | Metrics & More | Article Recommendations | Supporting Information

ABSTRACT: The catalytic reduction of nitrous oxide (N_2O) has been achieved through metal-free P^{III}/P^{V}=O catalysis. Kinetic analysis revealed that the oxygen transfer reaction to the phosphetane is rate determining. Computational investigations support a reaction mechanism in which the phosphetane catalyst preferentially interacts with the nitrogen terminus of N_2O, leading to the formation of a P−N=N−O intermediate in the *cis* configuration. Natural population analysis indicates stabilizing interactions between the occupied nonbonding oxygen orbitals and the antibonding orbitals of the phosphetane backbone, facilitating the oxygen atom transfer. Following nitrogen extrusion, the active phosphetane species is regenerated via silane-mediated reduction. The catalytic activity was quantitatively assessed by monitoring the nitrogen evolution through gas chromatography (GC) analysis.

Nitrous oxide (N_2O) is a potent greenhouse gas and dominant ozone depleting substance.[1] It accounts for 6% of global warming contribution,[2,3] and exhibits a global warming potential that is 265 times higher than that of carbon dioxide.[4] The emissions from crop production or industrial processes have led to a 20% increase in atmospheric N_2O concentrations over the past three centuries.[2,5] Given the environmental impact of N_2O, efficient strategies for its chemical utilization[6−11] and catalytic decomposition are urgently needed.[12−16] Typical heterogeneous (transition) metal based oxides operate at elevated temperatures above 300 °C for effective N_2O reduction.[12−14] Several molecular transition metal based systems were developed in order to mitigate these harsh reaction conditions.[17−26] Despite these significant advances, the interest in alternative N_2O activation mechanisms is the focus of current research. The direct reduction of N_2O by triphenylphosphine proceeds under supercritical conditions (100−140 bar) at 100 °C within 3 h (Scheme 1 a).[27]

The fixation and decomposition of N_2O under milder conditions was achieved by phosphane/borane derived frustrated Lewis pairs,[28−31] though catalytic conversions were not realized (Scheme 1b).[32−38] The catalytic decomposition at room temperature was achieved by Cantat and co-workers through the activation of disilane by fluoride or alkoxides (Scheme 1c).[39] Catalysis of group 15 element compounds has emerged as powerful strategy for organic synthesis.[40−42] Particularly, P^{III}/P^{V}=O catalysis proved as highly versatile when coupled with silanes as mild reducing agents.[43−54] Given that phosphetane oxides readily undergo reduction by silanes to the corresponding phosphetanes,[55−57] we envisioned the application in the catalytic reduction of N_2O under mild conditions (Scheme 1d).

To compare the reactivity of phosphetanes toward N_2O with the ones reported by Stephan,[38] we subjected **1a** and **1b** as Lewis base to the reaction with 1 equiv. $B(C_6F_5)_3$ (**2a**) and ca. 2 equiv. N_2O at room temperature. The sole observed products were P−B adducts, exhibiting ^{31}P NMR chemical shifts of $\delta(^{31}P)$= 41.9 and 53.7/52.8 ppm for **1a•2a** (*trans*) and **1b•2a** (*cis*/*trans* isomers), without formation of N_2 (Scheme 2a).

Heating the mixture to 70 °C did not alter the NMR spectra. However, when **2a** was replaced with $B(2,6\text{-}F_2\text{−}C_6H_3)_3$[58] (**2b**) (Scheme 2b), N_2 formation was observed in the ^{14}N NMR spectra ($\delta(^{14}N)$= 310 ppm), along with the formation of the phosphetane oxides ($\delta(^{31}P)$ = 74.2 (*trans*) and 74.1/65.9 ppm

Scheme 1. Metal-Free N_2O Decomposition

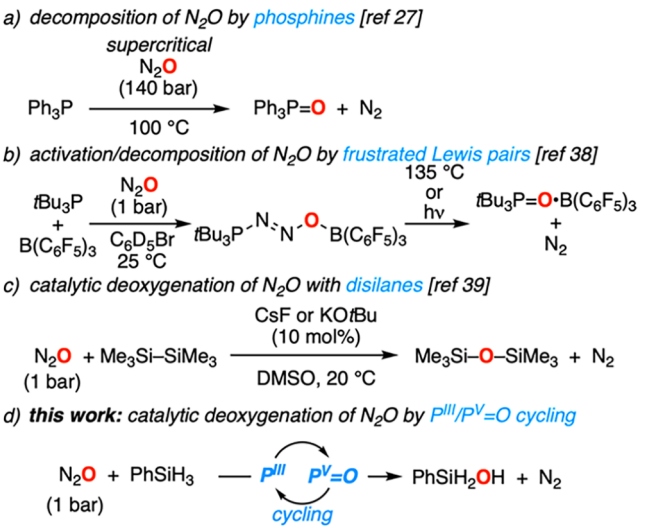

Received: April 16, 2025
Revised: September 8, 2025
Accepted: September 9, 2025
Published: September 15, 2025

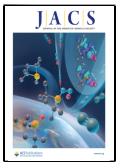

Scheme 2. Reaction of Phosphetane Derived Lewis Pairs with N_2O

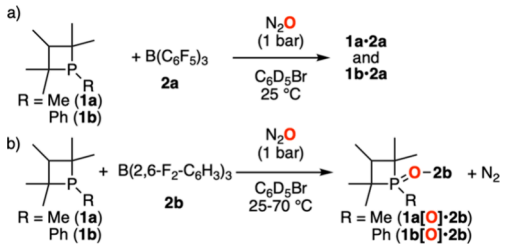

for **1a**[**O**] and **1b**[**O**] (*cis*/*trans* isomers)) as adducts with **2b**. To explore the catalytic potential of this transformation, 10 equiv of $PhSiH_3$ was added to the reaction mixture of **1a**[**O**]/**2b** (1:1) and 2 equiv. of N_2O (Figure 1a).

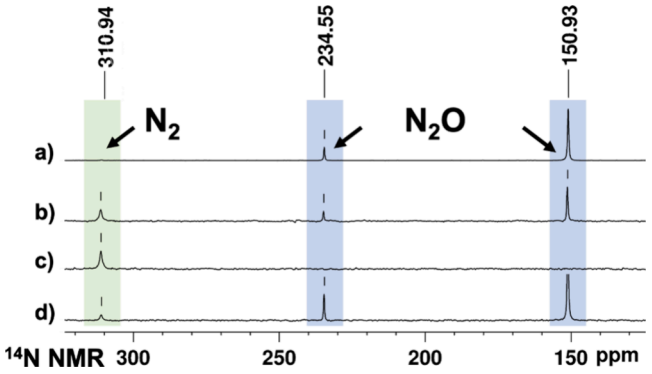

Figure 1. ^{14}N NMR spectra (36 MHz) of **1a**[**O**]/**2b** (1:1), 10 equiv. of $PhSiH_3$ (0.1 M C_6D_5Br) (a) after addition of 2 equiv. of N_2O at room temperature; (b) after 18 h at 70 °C and (c) after 48 h at 70 °C; (d) only **1a**/**2b** (1:1), N_2O (1 bar) after 18 h at 70 °C.

The reaction was maintained at 70 °C for 18 h. The resulting ^{14}N NMR spectra (Figure 1b) revealed a new resonance at $\delta(^{14}N)$ = 310 ppm. After 48 h, the original N_2O signals (δ = 150, 234 ppm) disappeared, indicating complete conversion to N_2 (Figure 1c). Trapping of the presumed **1a**−N═N−O−**2b** intermediate was unsuccessful at low temperatures (−20 °C). However, the direct formation of **1a**[**O**]•**2b** and N_2 was observed at 70 °C (Figure 1d, Table S2). Notably, a control experiment without **2b** provided comparable results, suggesting that the phosphetanes alone are sufficient for catalytic N_2O reduction.[59] This was confirmed by heating a 0.1 M solution of **1a** under 1 bar of N_2O to 70 °C for 18 h (Figure 2).

Indeed, **1a** is cleanly converted into **1a**[**O**] (Figure 2a-b) and can be recycled by the addition of $PhSiH_3$ (Figure 2c). Analogous potential for P^{III}/P^{V}═O cycling was observed for **1b** (Figures S26−29). Among the tested reducing reagents, $PhSiH_3$ proved to be the most effective (see Table S1). To demonstrate the catalytic reduction of N_2O, we followed the reaction by gas chromatography (GC) (Figure 3a).

Both phosphetanes catalyze the reduction of N_2O, but with differing reaction kinetics (TOF = 0.4 h^{-1} (**1a**), 0.1 h^{-1} (**1b**), Table 1 entries 1 and 2). Elevating the reaction temperature to 100 °C enhanced the catalytic activity (Figure 3b; Table 1, entries 2 and 3). Under these conditions, PPh_3 also exhibited catalytic activity, albeit with a markedly lower efficiency (entry 5). Both phosphetanes retained catalytic function when the environmentally benign polymethylhydrosiloxane (PMHS)[60]

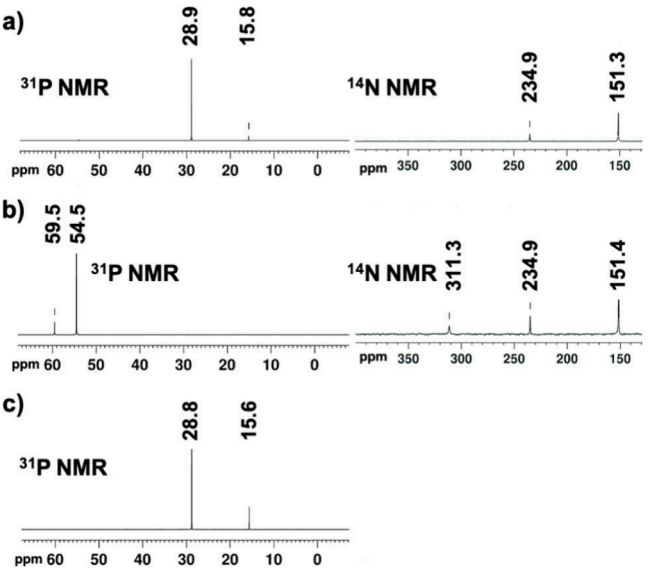

Figure 2. ^{31}P NMR (left, 202 MHz) and ^{14}N NMR (36 MHz, right) spectra of **1a** (0.1 M C_6D_5Br) (a) after addition of N_2O (1 bar) at 25 °C, (b) after 18 h at 70 °C, (c) after removal of N_2O/N_2, addition of 10 equiv. of $PhSiH_3$ and heating to 70 °C for 18 h.

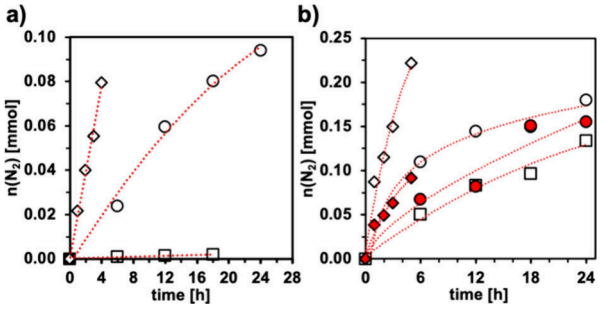

Figure 3. Quantification of N_2 gas evolution vs time: 9.5 mL N_2O (0.42 mmol), 0.5 mmol phenyl silane in 0.5 mL C_6H_5Br: (a) 0.050 mmol catalyst, 70 °C; (b) 0.025 mmol for **1a** and **1b**; 0.050 for PPh_3, 100 °C; (◇ **1a**; ○ **1b**; □ PPh_3; (solid red tilted square) **1a**; (solid red circle) **1b** with PMHS instead of phenyl silane).

Table 1. Catalytic Evaluation of Phosphetanes and PPh_3 in the N_2O Reduction[§]

entry	cat./silane	Temp [°C]	TON	TOF [h^{-1}]
1	**1a**(0.050)/$PhSiH_3$	70	1.6[a]	0.4[b]
2	**1b**(0.050)/$PhSiH_3$	70	0.5[c]	0.1[c]
3	**1a**(0.025)/$PhSiH_3$	100	9.0[d]	3.3[b]
4	**1b**(0.025)/$PhSiH_3$	100	4.2[c]	0.7[c]
5	PPh_3(0.05)/$PhSiH_3$	100	0.9[c]	0.1[c]
6	**1a**(0.025)/PMHS	100	3.5[d]	1.2[b]
7	**1b**(0.025)/PMHS	100	1.2[c]	0.2[c]

[§]Conditions: 9.5 mL N_2O (0.42 mmol), 0.5 mmol silane in 0.5 mL C_6H_5Br, values in parentheses correspond to catalyst loading; N_2 concentrations were determined by gas chromatography (GC); [a]4 h; [b]1 h; [c]6 h; [d]5h.

was employed as the terminal reductant (entries 6 and 7). Nevertheless, the overall activity of these P^{III}/P^{V}═O systems remains lower compared to the low-valent bismuth catalysts recently reported by Cornella and co-workers.[17]

To gain insight into the catalytic mechanism, we determined the reaction orders of the individual components. The oxygen

https://doi.org/10.1021/jacs.5c06190
J. Am. Chem. Soc. 2025, 147, 37879−37884

transfer from N_2O to the phosphetanes (in the absence of $PhSiH_3$) exhibits a first-order dependence for both **1a** and **1b** (Figure S38). Similarly, the reduction of the corresponding phosphetane oxides (**1a**[**O**] and **1b**[**O**]) by $PhSiH_3$ proceeds with first-order kinetics in both the phosphetane oxide and the silane. The activation energies (E_a) for the oxygen transfer step were determined to be 11.5 ± 3 kcal/mol for **1a** and 18.1 ± 2 kcal/mol for **1b**. In comparison, the reduction of the phosphetane oxides requires slightly lower E_a of 10.6 ± 1 kcal/mol for **1a**[**O**] and 10.3 ± 2 kcal/mol for **1b**[**O**], indicating that N_2O activation constitutes the rate-determining step. The order of the phosphetane catalysts in the full catalytic reaction was determined to be of first-order.[61] Based on these kinetic data, control experiments and earlier reports a catalytic cycle is proposed in which initially the P atom adds to the N-terminus of N_2O (Scheme 3).[33,35−38]

Scheme 3. Proposed Catalytic Cycle of the Phosphetane-Catalyzed N_2O Reduction

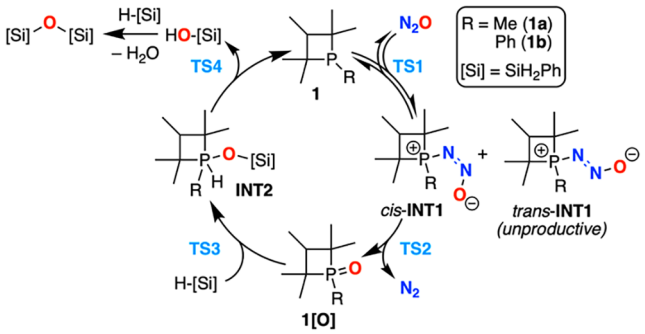

This generates the *cis* and *trans* configured zwitterionic species *cis*-**INT1** and *trans*-**INT1** as transient high energy intermediates. The *cis*-configured diastereomer extrudes N_2 through an intramolecular reaction, generating phosphetane oxide **1**[**O**]. The reduction of **1**[**O**] by silanes proceed through the intermediate **INT2** followed by HO−[Si] elimination, as discussed in the literature.[55,57] In support of this mechanistic picture, we performed quantum-chemical calculations at the DLPNO−CCSD(T)/cc-pVTZ//PBEh-3c/def2-mTZVP//openCOSMO-RS level of theory. Given that the methyl group in 3-position in the phosphetane is spatially distant from the reactive phosphorus center and is unlikely to influence catalysis, the computational study focused on the simplified 2,2,4,4-tetramethyl derivatives **1′a** and **1′b**.

To explain the different kinetics of the Me- and Ph-substituted derivatives, we analyzed their structural and electronic features. The Me-derivative **1′a** shows a slightly higher pyramidalization than the Ph-derivative **1′b** (sum of C−P−C angles: 78.2° (**1′a**); 64.3° (**1′b**): Figure S90. This aligns with experimental data suggesting increased lone pair s-character in **1′b**, inferred from its larger $^{31}P-^{77}Se$ coupling constant.[62] Natural population analysis (NPA)[63] also shows a slightly lower partial charge on phosphorus in **1′b** (+0.789e) than in **1′a** (+0.748e). The reaction of **1′a** with N_2O's N-terminus is endergonic by 12.5 kcal/mol and proceeds via *cis*-$\mathbf{TS1}_{1'a}$ with a 28.7 kcal/mol barrier to form *cis*-$\mathbf{INT1}_{1'a}$ (Figure 4a).

The *trans*-isomer is 3.7 kcal/mol less stable and forms via a high barrier of 59.7 kcal/mol (*trans*-$\mathbf{TS1}_{1'a}$), rendering its formation kinetically unfavorable. This aligns with the absence of detectable phosphetane−N_2O adducts in the NMR spectra.

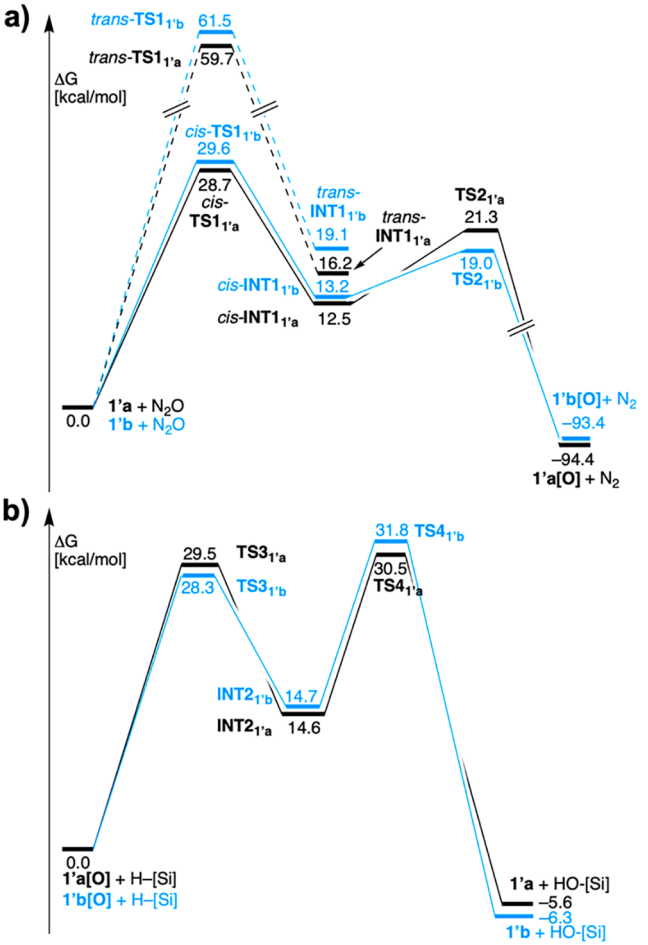

Figure 4. Calculated profile of free energy at 343 K (ΔG_{343}) of (a) phosphetane catalyzed N_2O reduction and (b) phosphetane oxide reduction by $PhSiH_3$ (H−[Si]).

The intramolecular O-atom transfer to form **1′a**[**O**] has a 7.4 kcal/mol lower barrier than the initial addition, making $\mathbf{TS1}_{1a'}$ rate-determining. For **1′b**, the N_2O addition barrier (*cis*-$\mathbf{TS1}_{1'b}$) is only 0.9 kcal/mol higher than that for **1′a**. Although absolute computed barriers exceed experimental values by 11−17 kcal/mol, the trend is consistent. Oxide formation via $\mathbf{TS2}_{1'b}$ proceeds with a barrier 2.3 kcal/mol lower than that of $\mathbf{TS2}_{1'a}$. The free energy of oxide formation is similar for both (**1′a**: −94.4 kcal/mol; **1′b**: −93.4 kcal/mol). Direct conversion of **1′a** or **1′b** to oxides via a single TS is hindered by high barriers (42.3 and 43.3 kcal/mol; Table S32). Silane reduction of **1′a**[**O**] and **1′b**[**O**] requires energy comparable to N_2O addition (Figure 4b), and aligns with known calculated barriers for strained cyclic phosphine oxides.[55,57] While the computed activation barriers exceed experimental values by ca. 10 kcal/mol, the relative trend is preserved, with oxide transfer consistently requiring slightly higher energy than the reduction pathway.

To gain insight into the electronic structure governing N_2O binding, we performed natural population analysis (NPA) on the transition states leading to the *cis* and *trans* adducts of **1′a** and **1′b**. In *cis*-$\mathbf{TS1}_{1'a}$ (Figure 5, top), activation of N_2O is facilitated by electron donation from LP_P into the unoccupied π^*_{N-N}, σ^*_{N-O} and σ^*_{N-N} orbitals.

Back-donation from LP_N and LP_O into the σ^*_{C-P} orbitals stabilizes the transition state. These donor−acceptor inter-

https://doi.org/10.1021/jacs.5c06190
J. Am. Chem. Soc. 2025, 147, 37879−37884

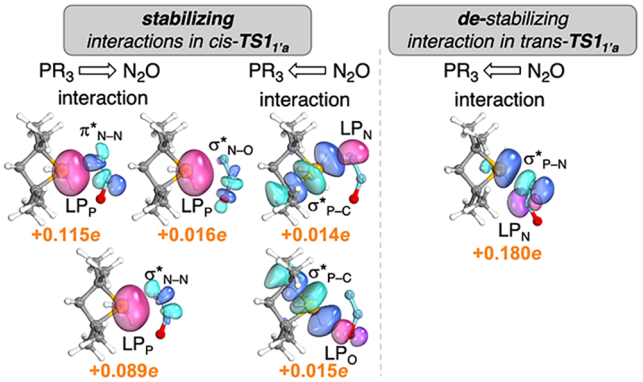

Figure 5. Donor (red/purple)/acceptor (blue/cyan) orbitals in *cis*-**TS1**$_{1'a}$ (left) and *trans*-**TS1**$_{1'a}$ (right) including charge transfer values (orange); LP = lone pair.[64]

actions are absent in *trans*-**TS1**$_{1'a}$ (Figure 5, bottom), where destabilization arises from $LP_N \rightarrow \sigma^*_{P-N}$ charge transfer. A similar pattern is observed for **1′b** (Figure S91). Local energy decomposition analysis (LED) revealed that the interaction energies with N_2O (**1′a**: −9.5 kcal/mol; **1′b**: −10.6 kcal/mol) are outweighed by the deformation energy required to bend N_2O from its linear geometry (**1′a**: 30.6 kcal/mol; **1′b**: 31.9 kcal/mol), while the deformation energy for the phosphetanes is minimal (1.5 kcal/mol). The transition states leading to the *trans*-adducts (*trans*-**INT1**$_{1'a}$ and *trans*-**INT1**$_{1'b}$) exhibit considerably higher activation energies due to a positive interaction energy of 17.5 kcal/mol and deformation energy of ca. 38 kcal/mol. The bonding situation in *cis*-**INT1**$_{1'a}$ and *cis*-**INT1**$_{1'b}$ can be described as zwitterionic, featuring a *cis*-configured azonyl (−N=N−O) group and a weak LP_{O-P} interaction due to the partial positive polarization of phosphorus (Figure 6).

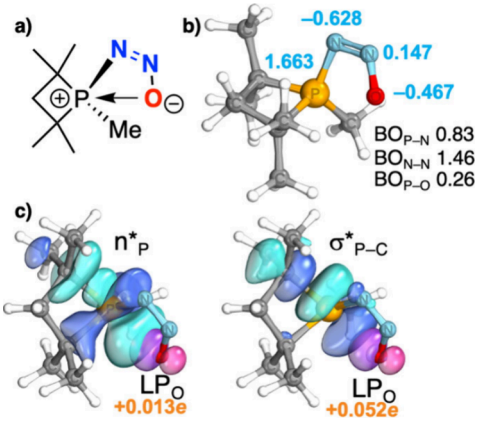

Figure 6. (a) Lewis structure of *cis*-**INT1**$_{1'a}$; (b) computed structure of *cis*-**INT1**$_{1'a}$ with NPA charges (blue) and Wiberg-Meyer bond orders (BO); c) donor (red/purple)/acceptor (blue/cyan) orbitals of *cis*-**INT1**$_{1'a}$ (charge transfer values in orange).

This P−O interaction primes the system for O atom transfer from the N_2O-fragment to the P-center. In **TS2**$_{1'a}$ and **TS2**$_{1'b}$ the P−O distances are 1.73 Å and 1.87 Å respectively, which is 0.51 Å and 0.38 Å shorter than in the N_2O adducts. According to LED, the greater stabilization of **TS2**$_{1'b}$ compared to **TS2**$_{1'a}$ arises from the higher electrostatic interaction between the N_2O and the P-center (see Tables S33, S34). The distortion energy of the N_2O fragment is for both transition states 2.9 kcal/mol which is compensated by a structural relaxation of the phosphetanes by −4.1 kcal/mol (**1′a**) and −3.4 kcal/mol (**1′b**).

Strain release has been identified as the principal factor for the difference in reactivity between phosphetanes and acyclic congeners.[65] Thus, the low reactivity of PPh_3 is attributed to the higher barrier of *cis*-**TS2**$_{PPh3}$ of 24.1 kcal/mol, resulting from significant N_2O-distortion and positive deformation energy (Table S35, Figures S92 and S95).

In summary, we developed a mild $P^{III}/P^{V}{=}O$ catalyzed decomposition of nitrous oxide (N_2O) using phenyl silane as a reductant. Kinetic and computational studies identified the addition of the phosphetane to the N-terminus of N_2O as rate-determining step in the catalytic N_2O reduction. The determined activation barriers for the regeneration of the phosphetane through silane-reduction of the phosphetane oxide were found to be by 0.9 to 3.8 kcal/mol lower as the N_2O activation.

■ ASSOCIATED CONTENT

Supporting Information

The Supporting Information is available free of charge at https://pubs.acs.org/doi/10.1021/jacs.5c06190.

General methods; synthetic procedures; ^{1}H, ^{13}C, ^{14}N, ^{31}P NMR spectra; kinetic data; computational results (PDF)

Atomic coordinates of computational study (XYZ)

■ AUTHOR INFORMATION

Corresponding Author

Jan Paradies − *Chemistry Department, Center for Sustainable Systems Design, Paderborn University, 33098 Paderborn, Germany*; orcid.org/0000-0002-3698-668X; Email: jan.paradies@uni-paderborn.de

Authors

Rundong Zhou − *Chemistry Department, Center for Sustainable Systems Design, Paderborn University, 33098 Paderborn, Germany*

Viktorija Medvarić − *Chemistry Department, Center for Sustainable Systems Design, Paderborn University, 33098 Paderborn, Germany; Leibniz Institute for Catalysis at the University of Rostock (LIKAT Rostock), D-18059 Rostock, Germany*

Thomas Werner − *Chemistry Department, Center for Sustainable Systems Design, Paderborn University, 33098 Paderborn, Germany; Leibniz Institute for Catalysis at the University of Rostock (LIKAT Rostock), D-18059 Rostock, Germany*; orcid.org/0000-0001-9025-3244

Complete contact information is available at: https://pubs.acs.org/10.1021/jacs.5c06190

Author Contributions

The manuscript was written through contributions of all authors. All authors have given approval to the final version of the manuscript.

Funding

The German science foundation (DFG) is gratefully acknowledged for financial support (PA 1562/18−1). R. Z. thanks the Paderborn University for a graduate fellowship.

Notes

The authors declare no competing financial interest.

■ ACKNOWLEDGMENTS

The authors gratefully acknowledge the computing time made available to them on the high-performance computer Noctua2 at the NHR Center for Parallel Computing (PC2). This center is jointly supported by the Federal Ministry of Research, Technology and Space and the state governments participating in the National High-Performance Computing (NHR) joint funding program (www.nhr-verein.de/en/our-partners).

■ REFERENCES

(1) Ravishankara, A. R.; Daniel, J. S.; Portmann, R. W. Nitrous Oxide (N_2O): The Dominant Ozone-Depleting Substance Emitted in the 21st Century. *Science* **2009**, *326* (5949), 123−125.
(2) Intergovernmental Panel On Climate Change (Ipcc). *Climate Change 2021 − The Physical Science Basis: Working Group I Contribution to the Sixth Assessment Report of the Intergovernmental Panel on Climate Change*, 1st ed.; Cambridge University Press, 2023.
(3) Rao, S.; Riahi, K. The Role of Non-CO_2 Greenhouse Gases in Climate Change Mitigation: Long-Term Scenarios for the 21st Century. *Energy Journal* **2006**, *27* (3_suppl), 177−200.
(4) Global-Warming-Potential-Values (Feb 16 2016).
(5) Christensen, S.; Rousk, K. Global N_2O Emissions from Our Planet: Which Fluxes Are Affected by Man, and Can We Reduce These? *iScience* **2024**, *27* (2), No. 109042.
(6) Severin, K. Synthetic Chemistry with Nitrous Oxide. *Chem. Soc. Rev.* **2015**, *44* (17), 6375−6386.
(7) Genoux, A.; Severin, K. Nitrous Oxide as Diazo Transfer Reagent. *Chem. Sci.* **2024**, *15*, 13605.
(8) Severin, K. Homogeneous Catalysis with Nitrous Oxide. *Trends in Chem.* **2023**, *5* (8), 574−576.
(9) Landman, I. R.; Fadaei-Tirani, F.; Severin, K. Nitrous Oxide as a Diazo Transfer Reagent: The Synthesis of Triazolopyridines. *Chem. Commun.* **2021**, *57* (87), 11537−11540.
(10) Suleymanov, A. A.; Le D u, E.; Dong, Z.; Muriel, B.; Scopelliti, R.; Fadaei-Tirani, F.; Waser, J.; Severin, K. Triazene-Activated Donor−Acceptor Cyclopropanes: Ring-Opening and (3 + 2) Annulation Reactions. *Org. Lett.* **2020**, *22* (11), 4517−4522.
(11) Banert, K.; Plefka, O. Synthesis with Perfect Atom Economy: Generation of Diazo Ketones by 1,3-Dipolar Cycloaddition of Nitrous Oxide at Cyclic Alkynes under Mild Conditions. *Angew. Chem., Int. Ed.* **2011**, *50* (27), 6171−6174.
(12) Zhuang, Z.; Guan, B.; Chen, J.; Zheng, C.; Zhou, J.; Su, T.; Chen, Y.; Zhu, C.; Hu, X.; Zhao, S.; Guo, J.; Dang, H.; Zhang, Y.; Yuan, Y.; Yi, C.; Xu, C.; Xu, B.; Zeng, W.; Li, Y.; Shi, K.; He, Y.; Wei, Z.; Huang, Z. Review of Nitrous Oxide Direct Catalytic Decomposition and Selective Catalytic Reduction Catalysts. *Chem. Eng. J.* **2024**, *486*, No. 150374.
(13) Wu, X.; Du, J.; Gao, Y.; Wang, H.; Zhang, C.; Zhang, R.; He, H.; Lu, G.; Wu, Z. Progress and Challenges in Nitrous Oxide Decomposition and Valorization. *Chem. Soc. Rev.* **2024**, *53* (16), 8379−8423.
(14) Zhang, Y.; Tian, Z.; Huang, L.; Fan, H.; Hou, Q.; Cui, P.; Wang, W. Advances in Catalytic Decomposition of N_2O by Noble Metal Catalysts. *Catalysts* **2023**, *13* (6), 943.
(15) Hinokuma, S.; Iwasa, T.; Kon, Y.; Taketsugu, T.; Sato, K. N_2O Decomposition Properties of Ru Catalysts Supported on Various Oxide Materials and SnO_2. *Sci. Rep.* **2020**, *10* (1), No. 21605.
(16) Konsolakis, M. Recent Advances on Nitrous Oxide (N_2O) Decomposition over Non-Noble-Metal Oxide Catalysts: Catalytic Performance, Mechanistic Considerations, and Surface Chemistry Aspects. *ACS Catal.* **2015**, *5* (11), 6397−6421.
(17) Pang, Y.; Leutzsch, M.; Nöthling, N.; Cornella, J. Catalytic Activation of N_2O at a Low-Valent Bismuth Redox Platform. *J. Am. Chem. Soc.* **2020**, *142* (46), 19473−19479.
(18) Pauleta, S. R.; Carepo, M. S. P.; Moura, I. Source and Reduction of Nitrous Oxide. *Coord. Chem. Rev.* **2019**, *387*, 436−449.
(19) Martinez, J. L.; Schneider, J. E.; Anferov, S. W.; Anderson, J. S. Electrochemical Reduction of N_2O with a Molecular Copper Catalyst. *ACS Catal.* **2023**, *13* (19), 12673−12680.
(20) Deeba, R.; Chardon-Noblat, S.; Costentin, C. Importance of Ligand Exchange in the Modulation of Molecular Catalysis: Mechanism of the Electrochemical Reduction of Nitrous Oxide with Rhenium Bipyridyl Carbonyl Complexes. *ACS Catal.* **2023**, *13* (12), 8262−8272.
(21) Bösken, J.; Rodríguez-Lugo, R. E.; Nappen, S.; Trincado, M.; Grützmacher, H. Reduction of Nitrous Oxide by Light Alcohols Catalysed by a Low-Valent Ruthenium Diazadiene Complex. *Chem.—Eur. J.* **2023**, *29* (20), No. e202203632.
(22) Ortega-Lepe, I.; Sánchez, P.; Santos, L. L.; Lara, P.; Rendón, N.; López-Serrano, J.; Salazar-Pereda, V.; Álvarez, E.; Paneque, M.; Suárez, A. Catalytic Nitrous Oxide Reduction with H2Mediated by Pincer Ir Complexes. *Inorg. Chem.* **2022**, *61* (46), 18590−18600.
(23) Molinillo, P.; Lacroix, B.; Vattier, F.; Rendón, N.; Suárez, A.; Lara, P. Reduction of N_2O with Hydrosilanes Catalysed by RuSNS Nanoparticles. *Chem. Commun.* **2022**, *58* (51), 7176−7179.
(24) Chen, X.; Wang, H.; Du, S.; Driess, M.; Mo, Z. Deoxygenation of Nitrous Oxide and Nitro Compounds Using Bis(N-Heterocyclic Silylene)Amido Iron Complexes as Catalysts. *Angew. Chem., Int. Ed.* **2022**, *61* (7), No. e202114598.
(25) Jurt, P.; Abels, A. S.; Gamboa-Carballo, J. J.; Fernández, I.; Le Corre, G.; Aebli, M.; Baker, M. G.; Eiler, F.; Müller, F.; Wörle, M.; Verel, R.; Gauthier, S.; Trincado, M.; Gianetti, T. L.; Grützmacher, H. Reduction of Nitrogen Oxides by Hydrogen with Rhodium(I)−Platinum(II) Olefin Complexes as Catalysts. *Angew. Chem., Int. Ed.* **2021**, *60* (48), 25372−25380.
(26) Zeng, R.; Feller, M.; Ben-David, Y.; Milstein, D. Hydrogenation and Hydrosilylation of Nitrous Oxide Homogeneously Catalyzed by a Metal Complex. *J. Am. Chem. Soc.* **2017**, *139* (16), 5720−5723.
(27) Poh, S.; Hernandez, R.; Inagaki, M.; Jessop, P. G. Oxidation of Phosphines by Supercritical Nitrous Oxide. *Org. Lett.* **1999**, *1* (4), 583−586.
(28) Welch, G. C.; Juan, R. R. S.; Masuda, J. D.; Stephan, D. W. Reversible, Metal-Free Hydrogen Activation. *Science* **2006**, *314* (5802), 1124−1126.
(29) Stephan, D. W. Diverse Uses of the Reaction of Frustrated Lewis Pair (FLP) with Hydrogen. *J. Am. Chem. Soc.* **2021**, *143* (48), 20002−20014.
(30) Stephan, D. W. Catalysis, FLPs, and Beyond. *Chem.* **2020**, *6* (7), 1520−1526.
(31) Lam, J.; Szkop, K. M.; Mosaferi, E.; Stephan, D. W. FLP Catalysis: Main Group Hydrogenations of Organic Unsaturated Substrates. *Chem. Soc. Rev.* **2019**, *48* (13), 3592−3612.
(32) Stephan, D. W.; Erker, G. Frustrated Lewis Pair Chemistry of Carbon, Nitrogen and Sulfur Oxides. *Chem. Sci.* **2014**, *5* (7), 2625−2641.
(33) Mo, Z.; Kolychev, E. L.; Rit, A.; Campos, J.; Niu, H.; Aldridge, S. Facile Reversibility by Design: Tuning Small Molecule Capture and Activation by Single Component Frustrated Lewis Pairs. *J. Am. Chem. Soc.* **2015**, *137* (38), 12227−12230.
(34) Xu, X.; Kehr, G.; Daniliuc, C. G.; Erker, G. Formation of Unsaturated Vicinal Zr+/P Frustrated Lewis Pairs by the Unique 1,1-Carbozirconation Reactions. *J. Am. Chem. Soc.* **2014**, *136* (35), 12431−12443.
(35) Kelly, M. J.; Gilbert, J.; Tirfoin, R.; Aldridge, S. Frustrated Lewis Pairs as Molecular Receptors: Colorimetric and Electrochemical Detection of Nitrous Oxide. *Angew. Chem., Int. Ed.* **2013**, *52* (52), 14094−14097.
(36) Gilbert, T. M. Computational Studies of Complexation of Nitrous Oxide by Borane−Phosphine Frustrated Lewis Pairs. *Dalton Trans.* **2012**, *41* (30), 9046−9055.
(37) Neu, R. C.; Otten, E.; Lough, A.; Stephan, D. W. The Synthesis and Exchange Chemistry of Frustrated Lewis Pair−Nitrous Oxide Complexes. *Chem. Sci.* **2011**, *2* (1), 170−176.

(38) Otten, E.; Neu, R. C.; Stephan, D. W. Complexation of Nitrous Oxide by Frustrated Lewis Pairs. *J. Am. Chem. Soc.* **2009**, *131* (29), 9918−9919.
(39) Anthore-Dalion, L.; Nicolas, E.; Cantat, T. Catalytic Metal-Free Deoxygenation of Nitrous Oxide with Disilanes. *ACS Catal.* **2019**, *9* (12), 11563−11567.
(40) Lipshultz, J. M.; Li, G.; Radosevich, A. T. Main Group Redox Catalysis of Organopnictogens: Vertical Periodic Trends and Emerging Opportunities in Group 15. *J. Am. Chem. Soc.* **2021**, *143* (4), 1699−1721.
(41) Dunn, N. L.; Ha, M.; Radosevich, A. T. Main Group Redox Catalysis: Reversible PIII/PV Redox Cycling at a Phosphorus Platform. *J. Am. Chem. Soc.* **2012**, *134* (28), 11330−11333.
(42) Moon, H. W.; Cornella, J. Bismuth Redox Catalysis: An Emerging Main-Group Platform for Organic Synthesis. *ACS Catal.* **2022**, *12* (2), 1382−1393.
(43) Xie, C.; Chen, G.; Feng, C.-G.; Lin, G.-Q.; Hong, R. Recent Advances in Asymmetric P(III)/P(V)═O Redox Catalysis. *Tetrahedron Lett.* **2024**, *152*, No. 155337.
(44) Tönjes, J.; Medvarić, V.; Werner, T. Synthesis of Trisubstituted Furans from Activated Alkenes by P(III)/P(V) Redox Cycling Catalysis. *J. Org. Chem.* **2024**, *89* (15), 10729−10735.
(45) Tönjes, J.; Kell, L.; Werner, T. Organocatalytic Stereospecific Appel Reaction. *Org. Lett.* **2023**, *25* (51), 9114−9118.
(46) Li, G.; Lavagnino, M. N.; Ali, S. Z.; Hu, S.; Radosevich, A. T. Tandem C/N-Difunctionalization of Nitroarenes: Reductive Amination and Annulation by a Ring Expansion/Contraction Sequence. *J. Am. Chem. Soc.* **2023**, *145* (1), 41−46.
(47) Li, G.; Kanda, Y.; Hong, S. Y.; Radosevich, A. T. Enabling Reductive C−N Cross-Coupling of Nitroalkanes and Boronic Acids by Steric Design of P(III)/P(V)═O Catalysts. *J. Am. Chem. Soc.* **2022**, *144* (18), 8242−8248.
(48) Hong, S. Y.; Radosevich, A. T. Chemoselective Primary Amination of Aryl Boronic Acids by P(III)/P(V)═O-Catalysis: Synthetic Capture of the Transient Nef Intermediate HNO. *J. Am. Chem. Soc.* **2022**, *144* (20), 8902−8907.
(49) Li, G.; Miller, S. P.; Radosevich, A. T. PIII/PV═O-Catalyzed Intermolecular N−N Bond Formation: Cross-Selective Reductive Coupling of Nitroarenes and Anilines. *J. Am. Chem. Soc.* **2021**, *143* (36), 14464−14469.
(50) Longwitz, L.; Werner, T. Reduction of Activated Alkenes by PIII/PV Redox Cycling Catalysis. *Angew. Chem., Int. Ed.* **2020**, *59* (7), 2760−2763.
(51) Li, G.; Qin, Z.; Radosevich, A. T. P(III)/P(V)-Catalyzed Methylamination of Arylboronic Acids and Esters: Reductive C−N Coupling with Nitromethane as a Methylamine Surrogate. *J. Am. Chem. Soc.* **2020**, *142* (38), 16205−16210.
(52) Li, G.; Nykaza, T. V.; Cooper, J. C.; Ramirez, A.; Luzung, M. R.; Radosevich, A. T. An Improved P(III)/P(V)═O-Catalyzed Reductive C−N Coupling of Nitroaromatics and Boronic Acids by Mechanistic Differentiation of Rate- and Product-Determining Steps. *J. Am. Chem. Soc.* **2020**, *142* (14), 6786−6799.
(53) Longwitz, L.; Spannenberg, A.; Werner, T. Phosphetane Oxides as Redox Cycling Catalysts in the Catalytic Wittig Reaction at Room Temperature. *ACS Catal.* **2019**, *9* (10), 9237−9244.
(54) Longwitz, L.; Jopp, S.; Werner, T. Organocatalytic Chlorination of Alcohols by P(III)/P(V) Redox Cycling. *J. Org. Chem.* **2019**, *84* (12), 7863−7870.
(55) Zhang, J.; Kong, W.-Y.; Guo, W.; Tantillo, D. J.; Tang, Y. Combined Computational and Experimental Study Reveals Complex Mechanistic Landscape of Brønsted Acid-Catalyzed Silane-Dependent P═O Reduction. *J. Am. Chem. Soc.* **2024**, *146* (20), 13983−13999.
(56) Kirk, A. M.; O'Brien, C. J.; Krenske, E. H. Why Do Silanes Reduce Electron-Rich Phosphine Oxides Faster than Electron-Poor Phosphine Oxides? *Chem. Commun.* **2020**, *56* (8), 1227−1230.
(57) Fianchini, M.; O'Brien, C. J.; Chass, G. A. Reduction Rate of 1-Phenyl Phospholane 1-Oxide Enhanced by Silanol Byproducts: Comprehensive DFT Study and Kinetic Modeling Linked to Reagent Design. *J. Org. Chem.* **2019**, *84* (17), 10579−10592.
(58) Sitte, N. A.; Bursch, M.; Grimme, S.; Paradies, J. Frustrated Lewis Pair Catalyzed Hydrogenation of Amides: Halides as Active Lewis Base in the Metal-Free Hydrogen Activation. *J. Am. Chem. Soc.* **2019**, *141* (1), 159−162.
(59) **2b** alone did not induce N_2O reduction.
(60) van Kalkeren, H. A.; Blom, A. L.; Rutjes, F. P. J. T.; Huijbregts, M. A. J. On the Usefulness of Life Cycle Assessment in Early Chemical Methodology Development: The Case of Organophosphorus-Catalyzed Appel and Wittig Reactions. *Green Chem.* **2013**, *15* (5), 1255−1263.
(61) Bures, J. A Simple Graphical Method to Determine the Order in Catalyst. *Angew.Chem. Int. Ed.* **2016**, *55*, 2028−2031.
(62) $^1J_{P\text{-}Se}$: 734 Hz (**1a**[**Se**]); 724/753 Hz (*cis*/*trans*-**1b**[**Se**]) compared to noncyclic analogues Me_3PSe ($^1J_{P\text{-}Se}$ = 684 Hz) and Me_2PhPSe ($^1J_{P\text{-}Se}$ = 710 Hz).
(63) Nikolaienko, T. Y.; Bulavin, L. A.; Hovorun, D. M. JANPA: An Open Source Cross-Platform Implementation of the Natural Population Analysis on the Java Platform. *Comput. Theor. Chem.* **2014**, *1050*, 15−22.
(64) Representation created with IBOView. https://www.iboview.org.
(65) Cremer, S.; Trivedi, B.; Weitl, F. Rates of Hydroxide Decomposition of Cyclic Phosphonium Salts. *J. Org. Chem.* **1971**, *36* (21), 3226−3231.

https://doi.org/10.1021/jacs.5c06190
J. Am. Chem. Soc. 2025, 147, 37879−37884